WATER AND SOIL REDISTRIBUTION IN A CULTIVATED SASKATCHEWAN LANDSCAPE

A Thesis Submitted to the
College of Graduate Studies and Research
in Partial Fulfillment of the Requirements
for the Degree of Doctor of Philosophy
in the Department of Soil Science
University of Saskatchewan
Saskatoon

By
Jeffrey Thomas Braidek

PERMISSION TO USE

In presenting this thesis in partial fulfillment of the requirements for a Postgraduate degree from the University of Saskatchewan, I agree that the Libraries of this University may make it freely available for inspection. I further agree that permission for copying of this thesis in any manner, in whole or in part, for scholarly purposes may be granted by the professor or professors who supervised my thesis work or, in their absence, by the Head of the Department or the Dean of the College in which my thesis work was done. It is understood that any copying or publication or use of this thesis or parts thereof for financial gain shall not be allowed without my written permission. It is also understood that due recognition shall be given to me and to the University of Saskatchewan in any scholarly use which may be made of any material in my thesis.

Requests for permission to copy or to make other use of material in this thesis in whole or part should be addressed to:

Head of the Department of Soil Science
University of Saskatchewan
Saskatoon, Saskatchewan S7H 5A8

ABSTRACT

The concept of topographically controlled moisture redistribution underlies the conceptual model of soil development used by most researchers in the semi-arid northern Great Plains. The first part of this study explores the variability in the process of soil moisture redistribution, and its spatial distribution as it may be linked to topographic or pedogenic attributes. Recent advances in tillage research have shown that within cultivated landscapes tillage-induced redistribution of soils is the dominant erosion mechanism. The second part of this study attempts to validate the new model of tillage redistribution under Saskatchewan conditions.

The redistribution of soil moisture was monitored on three occasions between June 1997 and October 1998 using the redistribution of a chloride tracer as a surrogate for moisture redistribution. The results of the chloride tracer provided clear evidence for the direction and magnitude of water flow during the study period. The results confirm the distinction in the moisture redistribution process between depression-centred soils and upland soils. The primary control on the movement of the tracer at depression-centred soils was spring flooding in early 1998. Subsequent redistribution of the remaining tracer was dominated by discharge phenomena. Subsurface flow in upland soils is clearly anisotropic, with observed differences in the degree of lateral and vertical redistribution of the chloride mass between landform elements and between soil profile classes.

Two tillage experiments were conducted to evaluate the tillage process under Saskatchewan field conditions. The results of the tillage experiments were compared with the medium to long-term soil redistribution history as derived from cesium-137 redistribution. The cesium-137 results clearly show that the field-scale pattern of erosion at this Saskatchewan site corresponds to the characteristic pattern for tillage-induced erosion. Experimentally determined erosion values largely match or exceed those derived from the cesium-137 redistribution.

Cesium-137 derived erosion rates for divergent shoulders, divergent backslopes and convergent backslopes were 42.3, 32.4, and 10.8 Mg ha^{-1} y^{-1}, respectively. Experimentally determined values for net tillage erosion in these landform elements using a surface applied granular tracer and the median slope gradient for each category were 44, 74, and 86 Mg ha^{-1} y^{-1}, respectively. Net erosion values determined using an aqueous tracer applied to the soil surface had values of 16, 28, and 32 Mg ha^{-1} y^{-1} for divergent shoulders, divergent backslopes and convergent backslopes respectively. The comparatively low net erosion value for the divergent shoulder landform elements in the second experiment reflects the lack of a slope curvature factor in the erosion calculation.

These results confirm that the redistribution of water and the redistribution of soil materials by tillage are the basic controls on the distribution of soil taxa in this landscape.

ACKNOWLEDGEMENTS

I owe a great deal to my primary supervisor Dr. Dan Pennock who has been extraordinarily generous with his time and resources, thank you very much. I am equally indebted to my co-supervisor Dr. Eeltje de Jong for his patience and experience.

I would like to thank my committee members for their input at different stages of the project: Drs. Ken Van Rees, Darwin Anderson, Lawrence Martz, and especially Gary Kachanoski for his help with the tillage section. In addition I would like to thank Dr. Jim Richardson, the external examiner, for his insightful comments.

Many others have supplied help in the field and with the data analysis. I would like to acknowledge the contributions of Dr. Bing Si, Mike Solohub, Barry Goetz, Bob Anderson and Kirk Elliot among these.

I would like to specially thank Claude Labrecque and family of St. Denis, Saskatchewan for access to their property and their assistance in the field.

Lastly, a special thank you is owed to Dr. Lynne Bell for helping me keep it all together.

TABLE OF CONTENTS

LIST OF TABLES

LIST OF FIGURES

LIST OF ABBREVIATIONS

Landform Elements

DSH	Divergent Shoulder
CHS	Convergent Shoulder
DBS	Divergent Backslope
CBS	Convergent Backslope
DFS	Divergent Footslope
CFS	Convergent Footslope
LEV	Level

Soil Subgroups

O.R	Orthic Regosol
R.DBC	Rego Dark Brown Chernozem
CA.DBC	Calcareous Dark Brown Chernozem
O.DBC	Orthic Dark Brown Chernozem
E.DBC	Eluviated Dark Brown Chernozem
GLR.DBC	Gleyed Rego Dark Brown Chernozem
GL.DBC	Gleyed Dark Brown Chernozem
R.HG	Rego Humic Gleysol
O.HG	Orthic Humic Gleysol
HU.LG	Humic Luvic Gleysol

Soil Profile Class

REGO	Includes O.R. and R.DBC soil subgroups
CALC	Includes CA.DBC soil subgroup
ORTHIC	Includes O.DBC and E.DBC soil subgroups
GLEYED-REGO	Includes GLR.DBC and R.HG soil subgroups
GLEYED	Includes GL.DBC, O.HG, and HU.LG soil subgroups

...continued next page

Equation variables

SWE	Snow water equivalent (mm)
d_s	Depth of snow pack (cm)
ρ_s	Bulk density of the snow (kg m^{-3})
ρ_b	Bulk density of the soil
h	Height at a given point on the hillslope
t	Time
x	Distance in the horizontal direction
Qs	Flux of soil in the x direction
Q_{SNET}	The net soil transport rate for a given slope gradient given one tillage pass upslope and one downslope (kg m^{-1})
D	Depth of tillage (m)
k	Tillage transport coefficient (kg m^{-1})
$\overline{d}$	Mean tillage displacement distance (m)
$\overline{d}_{up}$	The mean tracer displacement following one tillage operation upslope (m)
$\overline{d}_{down}$	The mean tracer displacement following one tillage operation downslope (m)
$\overline{d}_{NET}$	Net tillage displacement (m) following one tillage pass upslope and one downslope
A	The y intercept of a linear regression equation
B	The slope of a linear regression equation
G	The tangent of the slope gradient
T_M	The unit soil transport rate for a single tillage pass (kg m^{-1})
T_{MNET}	The net soil transport rate for a landscape, with a range of slope gradients, in which there is one tillage pass upslope and one tillage pass downslope (kg m^{-1})

1. INTRODUCTION

Landscape-scale research in soil science seeks to understand soil phenomena within the context of their environmental surroundings. Research in soil genesis in the first third of the 20th century established the link between landscape position and soil formation (and the taxonomic units that resulted from distinctive soil forming regimes). Milne's (1936) concept of the catena is regarded as the first major expression of this linkage, but the underlying concepts had been applied in the Canadian Prairies by J. H. Ellis, culminating in his major work "The Soils of Manitoba" (Ellis, 1938). He recognized the occurrence of a genetically linked series of soils in undulating landscapes, and that hydrological processes were the key control:

> "Local variations in topographical position ... such as knolls, slopes, and depressions, will result in soil climates which differ from the normal regional soils. For example, if the precipitation on a given section of land is 18 inches per year, the soil on the knolls will receive 18 inches less the amount which runs off. Hence the soils on the knolls will have a locally arid climate in comparison with the normal soils. ... On the other hand, the soils of the depressions ... will receive 18 inches of precipitation plus the amount of water which runs off the adjacent higher land" (Ellis, 1938, p. 26)

Ellis goes on to explain the occurrence of locally thinner soils on knolls, and thicker soils with evidence of gleying in the depressions due to this redistribution of runoff. This model was further developed by many mid-20th Century soil scientists and underlies the soil association concept used for mapping throughout the province of Saskatchewan and other Northern Great Plain locales.

The interactions between soil formation and groundwater movement that are responsible for Gleysolic and related soils were established by the end of the last century (reviewed in Richardson et al., 2001). The role of water redistribution processes on soil formation in non-groundwater influenced soils is much less clear. Although a repetitive catenary pattern of soil development has been observed many times, the magnitude and

direction of moisture redistribution responsible for the pattern has not been directly documented. Schematic diagrams of three-dimensional patterns of water flow such as those of Pennock et al. (1987) are based on anisotropic or lateral flows of water within the soil column, but these hypothesized flow patterns have not been demonstrated experimentally in Prairie soils. Anisotropy in moisture flow is defined here as relative differences in vertical flow versus lateral flow.

The first objective of my dissertation research was to determine the direction and magnitude of water flow in a typical hummocky glacial till landscape. This would allow the relative balance between runoff redistribution, groundwater interactions, and lateral flow to be established and then related to stable pedological and topographical units of the landscape. The need for massive amounts of data to account for variability in soil properties, topographic attributes and antecedent soil moisture conditions has restricted the development of mathematic models that can be used to predict moisture redistribution within landscapes (Chappell and Ternan, 1992; Seyfried and Wilcox, 1995). An alternative method that can be used to identify and quantify landscape components with different patterns of moisture redistribution, and that taken in this study, is to use surrogate variables as indicators of the hydrological regime (Speight, 1974; Chappell and Ternan, 1992; Seyfried and Wilcox, 1995). The quantitative results can then be extended to other portions of the landscape showing a similar pattern among the surrogate variables. In my study the relationship between the magnitude and redistribution of water flow and topographic and pedogenic attributes was assessed to determine if these attributes were effective surrogates variables that could be used to extend the results.

Ellis' (1938) work also identifies a second major soil landscape characteristic – the changes in soil morphology caused by erosion.

> "A further effect of relief on soils is brought about by run-off. During times of heavy rains and during run-off from the melting snows, surface soil may be removed by water erosion from the higher positions and deposited in the lower positions. In the higher positions the knolls tend to become more shallow by the removal of the surface material, and the soils at the foot of the slopes become deeper through the accumulation of the material eroded from the higher levels. Under cultivation, wind is also a powerful factor in removing soil.... These

forces, causing the removal of surface soil, develop what is known as truncated soil profiles." (Ellis, 1938, p.27).

Prior to the mid-1990's, researchers in soil erosion focused on water and wind as the dominant erosion processes. However, recent research has shown that the observed field-scale pattern of erosion and deposition in cultivated landscapes does not match the expected pattern for water or wind erosion. Instead, the observed pattern of soil redistribution matches that expected for tillage dominated erosion (Govers et al., 1994; Govers et al., 1999). The research into tillage displacement using small plot trials (e.g., Lindstrom et al., 1992; Lobb et al., 1995; Poesen et al., 1997), has shown that tillage erosion is of sufficient magnitude to account for the observed pattern of field-scale redistribution. Thus, tillage is now considered the dominant mechanism of erosion on many cultivated sites.

The second objective of my study was to assess the direction and magnitude of soil redistribution due to tillage under Saskatchewan conditions. Direct measurements of tillage translocation were made with a tracer and the results were compared against the medium-term erosion pattern established by the cesium-137 technique (Martz and de Jong, 1987; Pennock and de Jong, 1990b; Govers et al., 1996). Again, I related the rates of redistribution to readily mappable topographic and pedogenic attributes as surrogate indicators of the redistribution regime. Although researchers have identified several factors which effect tillage displacement and redistribution (Guiresse and Revel, 1995; Lobb et al., 1995; Lobb et al., 1999), it is topography that offers the greatest opportunity to act as a surrogate indicator of tillage translocation

Although the primary focus of this work is on the link between the water and soil redistribution processes and readily mappable soil/topographical attributes, the establishment of this relationship is central to other, more applied issues. For example, in southern Saskatchewan the growing season rainfall is normally exceeded by the potential evapotranspiration, and resulting water deficits can severely limit plant growth (de Jong and Kachanoski, 1987). As such, the redistribution and storage of soil moisture are critical factors affecting crop development at the landscape-scale and has been shown to greatly limit the applicability of precision farming techniques in this region.

As well, the redistribution of soil nutrients and agricultural chemicals by water is of concern as a potential source of environmental pollution (Eghball et al., 1996). Hence this basic process research is essential for the development of spatially distributed process models in the Prairie landscape.

The dissertation is divided into four main chapters. The first chapter establishes the pedology of the research site and presents data on the medium-term (i.e., 30 to 40 year) spatial pattern of soil redistribution as measured with cesium-137. This chapter provides the context for evaluating the process-based results in the subsequent chapters.

The next two chapters on water redistribution and soil redistribution by tillage are presented in a self-contained research paper format. Each chapter has a complete Materials and Methods and Literature Review section. Chapter 3 focuses on the results of a tracer study to assess within-soil water redistribution. The magnitude and direction of water movement are evaluated over three time periods and related to pedological and topographical attributes at the site. The evaluation of tillage translocation using a surface tracer is completed in Chapter 4, and the results for the observed translocation are compared to topographical controls evaluated in other research studies. In Chapter 5 the importance of the two processes are evaluated and their effects on soil formation synthesized.

2. SOIL DISTRIBUTION AND MEDIUM-TERM SOIL REDISTRIBUTION AT THE STUDY SITE

2.1. Introduction

My research was conducted in order to examine the link between redistribution processes and soil topographical and pedological attributes. In this chapter the pedological and parent material characteristics of the study landscape are presented to establish the framework for the subsequent analysis and to establish the comparability of the research site to other studies. Previous studies in these landscapes have also established that the pedological characteristics of the surficial soil horizon in cultivated landscapes are strongly influenced by soil redistribution. The influence of redistribution is examined by assessing the spatial pattern of ^{137}Cs redistribution at the study site. Both the long-term pedological attributes and the medium-term soil redistribution results provide the context for examining the results of the process studies in the subsequent sections of the dissertation.

2.2. Literature Review

2.2.1. Controls on Landscape-scale Soil Distribution

Since the onset of research on soil distribution in the Canadian Prairies, the role of water redistribution in soil formation has been recognized. As discussed in Chapter 1, Ellis (1938) attributes the differences in soil formation to redistribution of runoff followed by vertical infiltration of water. In the mid-20th Century considerable effort was spent on understanding the interactions between groundwater and soil formation. By the 1970's and 1980's it was clear these interactions between groundwater and surface soil formation could explain a range of pedological features, primarily those associated with soluble components such as salinity and solonetz formation (St. Arnaud, 1976). The hydrological pathways associated with groundwater provided another lateral moisture redistribution mechanism besides runoff. A review of some of the groundwater

literature is given in Section 3.2.1

These groundwater interactions also affect soils immediately adjacent to the depressions. Various authors working in Saskatchewan and in adjacent Northern Great Plains locales have observed unsaturated flow outward from a depression-centred wetland towards the surrounding upland (Miller et al., 1985; Zebarth, 1988; Knuteson et al., 1989; Richardson et al. 1992; Hayashi et al., 1998). Evaporative discharge from this laterally moving water causes the build-up of solutes in a ring around the depression and this mechanism has been well established in the literature (reviewed by Richardson et al., 2001).

These processes result in a continuum of groundwater-influenced soils associated with these depressions. In the centre of the depressions, soils of the Gleysolic order are typically found; these soils exhibit mottled soil matrices from periodic water saturation. Where strong vertical water movement occurs without the onset of reducing conditions Eluviated Chernozemic soils occur. Gleyed Rego Chernozemic and Rego Gleysolic soils may occur at the edge of recharge-dominated depressions, where they are formed by lateral groundwater movement away from the depression centre, capillary rise of the groundwater, and deposition of calcium carbonate by a combination of evaporative and transpiration water loss (Knuteson et al., 1989; Steinwand and Richardson, 1989; Fuller et al., 1999). Note that within the Canadian System of Soil Classification, the Gleyed Rego Chernozemic and Rego Gleysolic soils are fundamentally composed of an A horizon over a C-horizon (Soil Classification Working Group, 1998). Secondary accumulation of carbonates in the C-horizon is indicated as a Cca. However, this notation does not explicitly acknowledge that the carbonate accumulation is pedogenic in nature. Pedogenic activity within a section of the parent material should by definition require that section to be classified as a B-horizon. Within the American soil classification system, Soil Taxonomy, this distinction is noted through the use of the Bk designation (Soil Survey Staff, 1988).

The characteristic progressive thickening of soils downslope in many Prairie landscapes cannot be as readily explained by groundwater interactions. In a typical catena in hummocky till landscapes in the Prairies, the convex shoulder areas are

occupied by thin Orthic Regosolic or Rego and Calcareous Chernozemic soils (St. Arnaud, 1976). The backslope and footslopes are dominantly Orthic Chernozemic soils, and the thickness of the solum typically increases downslope. The transition zone with the groundwater-influenced soils commonly has Eluviated or Gleyed subgroups of the Chernozemic order.

Soil profile development in these non-groundwater influenced locations is believed to be are largely controlled by differences in slope- induced moisture redistribution at the small catchment and hillslope scales (Miller et al., 1985; Zebarth and de Jong, 1989a). As greater amounts of soil moisture accumulate, there is greater potential for lateral and vertical redistribution of materials, which leads to enhanced profile development. This model implies that differences in profile development reflect long-term differences in the post-glacial soil moisture regime (St. Arnaud, 1976; Pennock and de Jong, 1990a).

In a hummocky Saskatchewan landscape, Zebarth and de Jong (1989a) observed a distinct pattern of spatially variable soil moisture, increasing in the sequence shoulders < backslopes < footslopes. This pattern was stable over time, with the landscape elements maintaining a similar rank order. They suggest that topography tends to maintain temporal stability of water distribution in the landscape by the redistribution of water as snow, runoff and interflow. Their work builds on that of authors such as Huggett (1975) and O'Loughlin (1986) who suggested that systematic lateral changes in moisture redistribution within a landscape are due to the development of lateral subsurface flow and the convergence or divergence of flow (both surface and subsurface) in response to surface topography.

In Saskatchewan, surface flows are periodic phenomena, primarily occurring during the spring melt and in association with torrential rainfall events during the growing season, when the rate of water applied to the surface will exceed the infiltration rate. Subsurface redistribution in both the vertical and lateral dimensions is believed to be an ongoing phenomenon; and by implication, this most likely continues to occur when the soil is in an unsaturated condition. However, little is known about the landscape variability in lateral unsaturated subsurface flow in Saskatchewan. Field

studies by McCord and Stephens (1987) and McCord et al. (1991) suggest that lateral flow may be an important redistribution mechanism in unsaturated conditions, but little direct hydrological field evidence on lateral flows has been produced since their work.

2.2.2. Estimating Medium–term Soil Redistribution Using Cesium-137

The pedological attributes such as B-horizon thickness and depth to calcium carbonate that are central to soil classification typically reflect the operation of long-term soil forming processes. The attributes of the surficial soil horizon were initially controlled by similar factors, but since the onset of cultivation soil erosion and deposition has had a major effect on these horizons.

Soil redistribution within a landscape, i.e., erosion and deposition, occurs because of wind, water and tillage action. Recent studies in erosion processes, conducted primarily under European conditions, suggest that erosion in cultivated fields in temperate environments is dominated by tillage processes rather than water- or wind-driven processes (Lindstrom et al., 1990; Lindstrom et al., 1992; Govers et al., 1994; Govers et al., 1996). It has been demonstrated that the field-scale pattern of net soil redistribution can be assessed using the distribution of cesium-137 as a surrogate indicator of soil redistribution (Govers et al., 1996; Govers et al., 1999).

The basis for the use of cesium-137 in soil redistribution studies has been well established. Atmospheric testing of nuclear weapons from 1952 until the Nuclear Test Ban treaty in 1963 released cesium-137 (^{137}Cs) into circulation in the upper atmosphere (Ritchie and McHenry, 1990; Walling and He, 1999). Subsequently the cesium returned to the earth with precipitation and created a layer of cesium-enriched topsoil. Detectable input of ^{137}Cs to soils has been observed since 1954, with the peak year of deposition in 1963 (Ritchie and McHenry, 1990; Walling and He, 1999). In the Northern Hemisphere atmospheric input stopped with the Nuclear Test Ban Treaty (Ritchie and McHenry, 1990). Since the late 1970's direct atmospheric deposition of ^{137}Cs due to nuclear explosions has been insignificant (Walling and He, 1999).

Cesium is rapidly and strongly adsorbed in the upper few centimetres of an uncultivated soil (Ritchie and McHenry, 1973), especially to the clay and organic matter components (Davis, 1963; Walling and He, 1999). The adsorbed cesium is essentially non-exchangeable and there is little vertical movement or leaching as a result. In a review of earlier studies, Davis (1963) reports that ^{137}Cs applied to soil columns in the laboratory remained in the upper 5 centimetres. De Jong et al. (1983) found that the majority of cesium had remained in the upper 10 cm at three uncultivated sites in Saskatchewan. The distribution of cesium within an uncultivated profile shows an exponential decrease with soil depth (Ritchie and McHenry, 1990). In cultivated landscapes, the cesium is uniformly distributed through the plough layer (Ritchie and McHenry, 1973; Ritchie and McHenry, 1990; Walling and He, 1999).

Cesium-137 is a relatively long-lived isotope with a half-life of 30.2 years (Martz and de Jong, 1987; Walling and He, 1999). This long half-life plus the strong bond to soil particles in the upper portion of the profile make ^{137}Cs an excellent indicator of soil redistribution over the medium to long term (40 to 50 years). After ^{137}Cs arrives at the soil surface, its subsequent redistribution within the landscape will reflect the redistribution of the soil particles.

The use of ^{137}Cs redistribution as a surrogate measure of soil redistribution has been a well established technique for nearly two decades (Pennock et al., 1994a; Quine et al., 1994; Quine, 1999). Ritchie and McHenry (1990) provide an extensive bibliography with their review of the method, as do Walling and He (1999). Early work in developing the method included investigations by Davis (1963), Ritchie et al. (1974), Rogowski and Tamura (1965), Rogowski and Tamura (1970).

When using ^{137}Cs to assess soil redistribution within a cultivated site, the cesium measured at positions within the cultivated site is compared against cesium levels determined at a non-cultivated reference site. Cesium values less than the reference value will indicate net erosion of soil at that sample point, while cesium values greater than the reference value will indicate a position with net deposition of soil materials (Martz and de Jong, 1987; Quine, 1999). The reference site should be a near as possible to the cultivated site to ensure similar precipitation history (the delivery mechanism for

cesium from the atmosphere).

In Saskatchewan, de Jong et al. (1983) found no variation in ^{137}Cs concentration associated with subjectively defined lower-, mid-, and upper-slope positions at non-cultivated sites. Similarly, Pennock et al. (1994a) found that variability of ^{137}Cs about the mean at non-cultivated sites was not associated with landform shape as defined in the landform element classification of Pennock et al. (1987) that is used in this paper.

The important advantages of using the cesium method in soil erosion investigations are the method's ability to provide (i) spatially distributed data, (ii) data representative of the net effect of all erosion processes, and (iii) data that shows the net effect of erosion processes over the medium to longer term (40 to 50 years) (Govers et al., 1996).

2.3. Materials and Methods

2.3.1. Description of the Research Site

The research site was established on the west side of the SE 24-37-2-W3 approximately 40 km east of Saskatoon, Saskatchewan near the hamlet of St. Denis. The site was mapped by Acton and Ellis (1978) as a loam-textured soil on glacial till parent material with gently to moderately rolling topography (slopes of 6-9%) (Figure 2.1). The site is in the Dark Brown Soil Zone and the soils are classified as the Weyburn association; with >40% of the area occupied by Orthic Dark Brown Chernozemic profiles, >15% of the area occupied by combinations of Calcareous and Rego Dark Brown Chernozemic and Orthic Regosolic profiles, and > 15% of the area occupied by Gleysolic soils.

The quarter section had initially been cultivated 50 to 60 years ago (C. Labrecque, landowner, pers. comm.). Air photos of the site indicate that all but the topographic depression in the centre of the site was cultivated by 1956. This depression was cultivated between 1978 and 1985 (C. Labrecque, pers. comm.). The soils in the depression are strongly gleyed, suggesting that historically these soils were saturated at least on a temporary or seasonal basis. Following the classification scheme of Stewart

and Kantrud (1971) this depression will be referred to as a tillage pond. The site is typical of the most common combination of parent material, texture, and topography within Saskatchewan. The complex topography at the site offers a good opportunity to study the effects of slope on material redistribution in this environment.

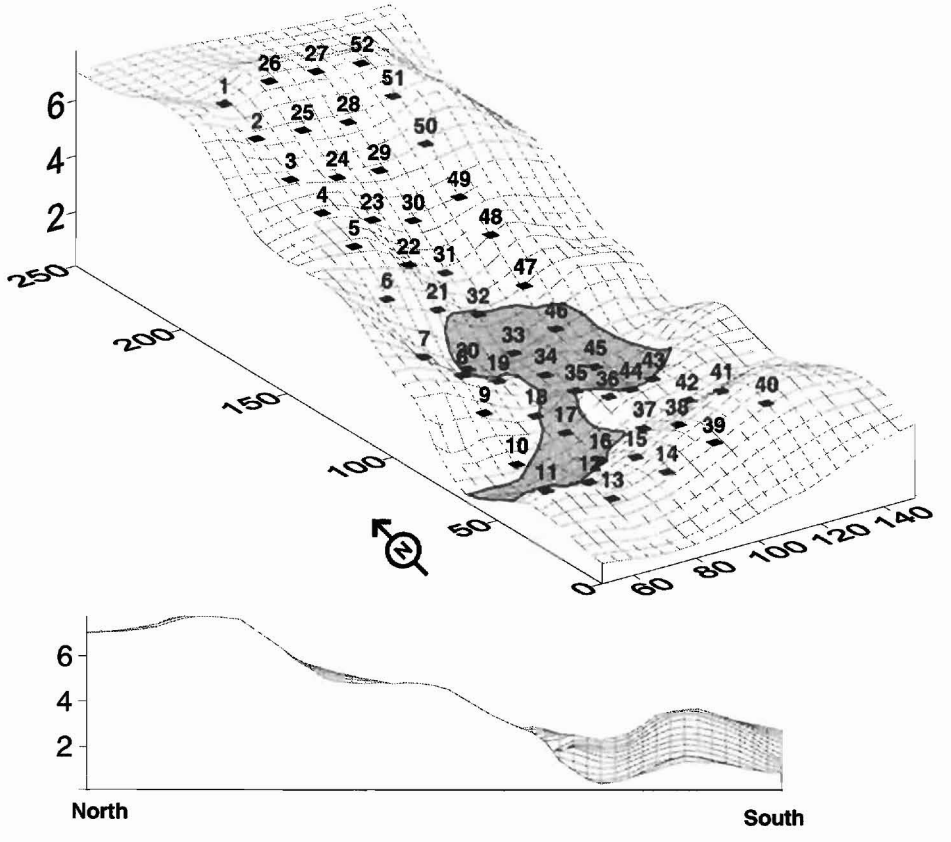

Figure 2.1 The wireframe image of the primary study site with the 52 point grid. The grey toned area in the middle of the site is a topographic depression that was observed to be saturated in the spring of 1998 and is dominated by gleyed soils. The lower image shows the site in cross-section looking from west to east. Axes units are in meters.

Based on the 1:50,000 scale topographic map sheet (73B/1) the median elevation at the site is approximately 549 m above mean sea level. The Saskatchewan Water Corporation Water Well Data Base shows that the water table was located at 9.8 m below ground surface in a well set at approximately the same surface elevation on the quarter section immediately east of the study site (SW19-37-1-W3).

2.3.2. Climate of the Study Site

The study site is within the moist mixed grassland ecoregion, which has an annual total precipitation of 380 mm and an annual snowfall of 110 cm (Padbury and Acton, 1994). Approximately 30% of the annual precipitation arrives as snow (de Jong and Kachanoski, 1987; Padbury and Acton, 1994; Pomeroy and Gray, 1995). The 30-year normal snowfall is equivalent to 110 mm of rainfall annually (Environment Canada, 1992). Snowfall depth is converted to snow water equivalent (SWE) using equation 2.1 (Pomeroy and Gray, 1995). For new snowfall, snow density is estimated at 100 kg m^{-3} (Pomeroy and Gray, 1995).

$$SWE = 0.01 * d_s * \rho_s \quad (2.1)$$

where, SWE is the snow water equivalent in mm, d_s is the depth of snow in cm, and ρ_s is snow density in kg m^{-3}.

Up to 85% of the annual runoff from agricultural watersheds comes from snowmelt (Nicholaichuk, 1967), whereas the summer growing season moisture will only account for 1% of the run off (de Jong and Kachanoski, 1987).

Rainfall during the growing season is of variable duration and intensity and the majority arrives in the early summer. Ninety-eight percent of the annual rainfall is received between the months of April and October (Table 2.1). The 30-year normal annual rainfall recorded at the Saskatoon SRC climate station is 250.7 mm, snowfall is 110.1 cm, and total annual mean precipitation is 360.6 mm (Environment Canada, 1992).

Table 2.1 The percent of annual rainfall received in each month of the growing season, based on the thirty year average from 1961 to 1990.

Percent of Annual Rainfall						
April	May	June	July	August	September	October
4.2	16.6	25.4	22.2	14.1	12.4	3.1

2.3.3. Topographical Survey and Development of the Digital Elevation Model

Pennock et al. (1987, 1994b) demonstrated that hummocky Saskatchewan landscapes can be quantitatively classified into topographically defined landform elements that have distinctive hydrological and pedological regimes. The classification uses a Digital Elevation Model (DEM) of the study site, and assigns a landform element classification to each grid cell of the DEM based on the calculated gradient, profile curvature and plan curvature for each cell. Thus each segment within the landscape is classified according to its three-dimensional form.

For this project, elevation data was collected at 759 points across the study area using a total station and single prism. Approximately 600 points were within a 2.5-ha area that enclosed the primary study site. The remaining 159 points were scattered over a 5-ha area to quantify the surrounding contributing watershed. The data points were not collected in a regular grid pattern; instead, the distance between points was adjusted to capture as much topographic variation as possible.

The field data was then used in the Surfer 7.0 (Golden Data Software, Inc.) suite of programs to construct the DEM. The elevation for each grid node of the DEM is interpolated from the set of elevation data collected in the field.

The accuracy of the interpolation affects the form of the DEM and the resulting landform classification. Although the inverse distance weighted function has been used to construct DEMs of similar Saskatchewan landscapes (Pennock et al., 1987; Pennock and de Jong, 1990b; Pennock et al., 1994b), in this study it gave a surface with considerable local elevation differences, which was contrary to the appearance of the site in the field. This "bulls-eye" appearance of DEMs constructed using inverse distance weighted interpolators is typical of this technique (Golden Software, 1999).

The Surfer 7.0 User's Guide (Golden Software Inc., 1999) recommends kriging because it generates an accurate map for most data sets. Interpolation of the topographic data was conducted using kriging with a fitted non-linear Gaussian function (Figure 2.2) and a grid cell size of 5 x 5 m. Burrough and McDonnell (1998) suggest that elevation data will often produce a smoothly varying pattern in the variogram, which can be fit

with a Gaussian model. For this project the fitted Gaussian function was selected.

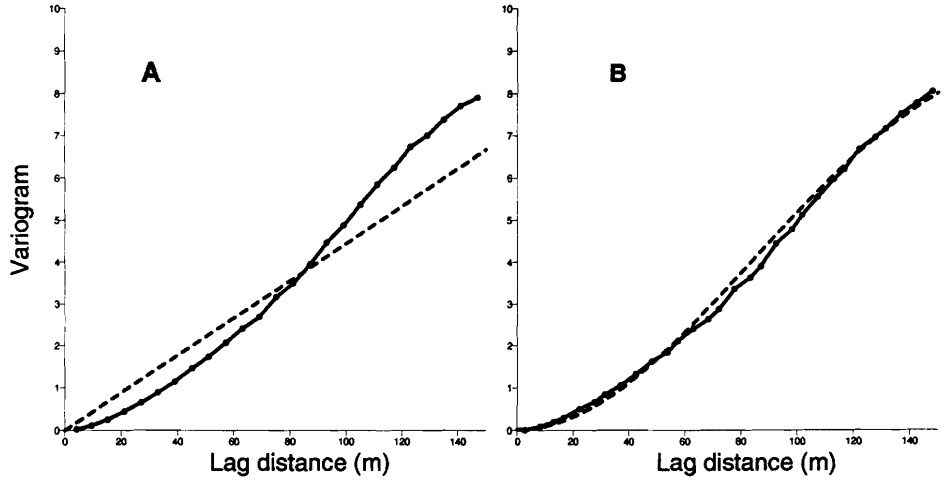

Figure 2.2 The variogram of the elevation data (solid line) with: (A) the default linear kriging function (dashed line), and (B) the fitted Gaussian function (dashed line).

Following the development of a DEM, landform elements were determined based on slope gradient, plan curvature, and profile curvature (Pennock et al., 1987; Pennock et al., 1994b). The specific contributing area and specific dispersal area for each grid cell (Costa-Cabral and Burges, 1994) were also determined. The initial landform classification is done using profile curvature; slope segments are classified into shoulders, footslopes, backslopes or levels depending on the degree of profile curvature. The criteria used in the classification is taken from Young (1972). Profile curvatures of $< -0.1\ ^{\circ}m^{-1}$ and $> +0.1\ ^{\circ}m^{-1}$ define footslope and shoulder elements respectively. Linear (or level) slope segments are defined as having a profile curvature $>-0.1\ ^{\circ}m^{-1}$ and $< +0.1\ ^{\circ}m^{-1}$. Linear profile segments are differentiated using gradient: a grid cell with a gradient of $>3.0^{\circ}$ is classified as a backslope, a gradient of $<3.0^{\circ}$ defines a level segment. Plan curvature is then used to divide shoulders, footslopes, and backslopes into convergent elements (concave plan curvature, i.e. negative values, those $< 0.0\ ^{\circ}m^{-1}$) and divergent elements (convex plan curvature, i.e. positive values, those $>0.0\ ^{\circ}m^{-1}$). The abbreviations used throughout the thesis for these elements are shown in Table 2.2.

Table 2.2 Abbreviations for landform elements.

Abbreviation	Landform Element
DSH	Divergent Shoulder
CSH	Convergent Shoulder
DBS	Divergent Backslope
CBS	Convergent Backslope
DFS	Divergent Footslope
CFS	Convergent Footslope
LEV	Level

2.3.4. Field and Laboratory Measurements

To assess the pattern of soil distribution at this site, profile descriptions were collected at all points that were monitored for chloride redistribution. Ninety-six soil profile descriptions were collected at three different sampling times between the fall of 1997 and the fall of 1998. Profile descriptions were used to classify the soils at the site (Soil Classification Working Group, 1998) (Table 2.3).

The parent material of the Weyburn soils mapped at the study site is described as loamy glacial till (Acton and Ellis, 1978). Loamy glacial sediments associated with hummocky terrain typically have inclusions of other textures, and the range in textures may cause considerable variation is soil hydraulic properties. The particle size of the soils and sediments at the site were sampled and analyzed to ensure that systematic variation in soil texture was not a factor at the site. Fifteen of the fifty-two locations sampled for chloride redistribution in the fall of 1997 were analyzed for particle size distribution using standard pipette analysis.

Table 2.3 Abbreviations for soil subgroups arranged from driest to wettest landscape position. a) Soil Classification Working Group, 1998; b) Soil Survey Staff, 1998.

Abbreviation	Soil Subgroup [a]	Soil Taxonomy [b]
O.R	Orthic Regosol	Typic Cryorthent
R.DBC	Rego Dark Brown Chernozem	Calcareous Typic Haplocryoll
CA.DBC	Calcareous Dark Brown Chernozem	Calcareous Typic Haplocryoll
O.DBC	Orthic Dark Brown Chernozem	Typic Haplocryoll
E.DBC	Eluviated Dark Brown Chernozem	Typic Argicryoll
GLR.DBC	Gleyed Rego Dark Brown Chernozem	Calcic Cryaquoll
GL.DBC	Gleyed Dark Brown Chernozem	Typic Cryaquoll
R.HG	Rego Humic Gleysol	Calcareous Histic Cryaquoll
O.HG	Orthic Humic Gleysol	Typic Cryaquoll
HU.LG	Humic Luvic Gleysol	Argic Cryaquoll

During the Fall 1998 sampling at the St. Denis site, cores were taken at 29 locations to determine ^{137}Cs concentration to 0.45 m. These locations correspond to those at which chloride redistribution was evaluated as a surrogate measure of moisture redistribution. The cesium concentrations were measured using gamma spectroscopy techniques following the method of de Jong et al. (1983). The measured cesium values were compared against a value of 1638 Bq m^{-2} determined at an uncultivated site less than 4 km away at legal location NE 10-37-2-W3 (unpublished data from the Master's thesis project of N. Slobodian, 2001). The reference site has never been cultivated and has a glacial till landscape similar to that at the St. Denis site. Cesium values above 1638 Bq m^{-2} at the St. Denis site will indicate local accumulation of cesium-enriched topsoil, and values below 1638 Bq m^{-2} will indicate a loss of topsoil material, i.e. erosion.

Historic air photos show that the upland portion of the study site has been under cultivation since at least 1956, and that the depression-centred tillage pond at the site was cultivated some time between 1978 and 1985. The time of cultivation for the upland soils, from the cessation of ^{137}Cs deposition until sampling was estimated at approximately 35 years.

2.3.5. Data Presentation

In much of the thesis data are presented graphically using box and whisker plots. These plots readily show the median value and range of data within individual classes or categories. A description of the box and whisker plots is given in Figure 2.3.

2.4. Landscape-scale Soil Distribution Model

The site is dominated by Chernozemic soils, which occur at all landscape positions (Table 2.4). There are fewer Gleysolic soils and these occur primarily in the footslope and level positions. The majority of Regosolic soils are found on the divergent shoulders, and, to a lesser extent, at other divergent positions in the landscape.

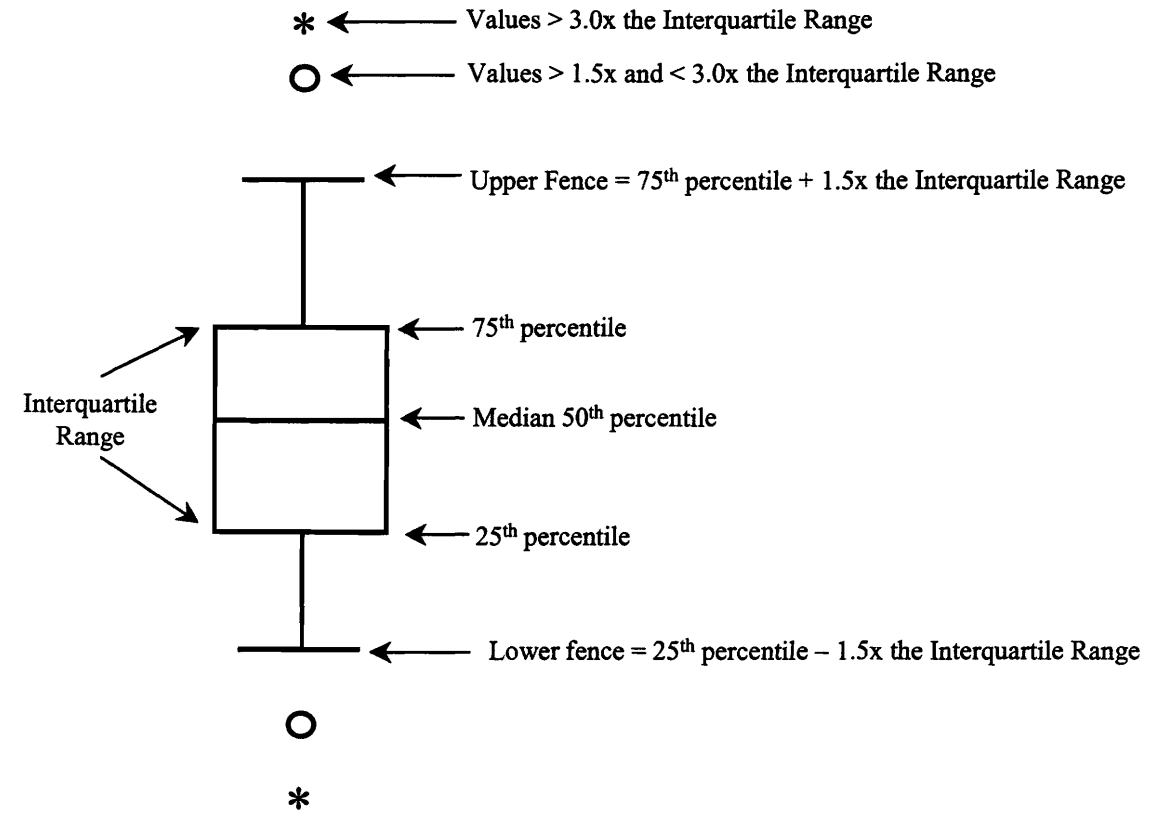

Figure 2.3 Diagram of a box and whisker plot.

Table 2.4 The distribution of 96 soil profiles by landform element. Profiles were sampled in the Fall of 1997, the Spring of 1998 and the Fall of 1998 in conjunction with sampling of the chloride tracer experiment.

				Landform Element							
Soil Order	Soil Subgroup	Class Criteria	New Soil Profile Class	DSH	CSH	DBS	CBS	DFS	CFS	LEV	Total
Regosol	O.R	calcareous non-gleyed	REGO	9		7		1			17
Chernozem	R.DBC			2		1	1	1			5
Chernozem	CA.DBC		CALC	3		6	3	1	2	5	20
Chernozem	O.DBC	non-calcareous non-gleyed	ORTHIC		1	4	20		5	6	36
Chernozem	E.DBC				1					1	2
Chernozem	GLR.DBC	gleyed calcareous	GLEYED-REGO					1			1
Gleysol	R.HG							1		2	3
Chernozem	GL.DBC	gleyed non-calcareous	GLEYED						2		2
Gleysol	O.HG					1			3	1	5
Gleysol	HU.LG								5		5
Total				14	2	19	24	5	17	15	96

Thin profiles such as O.R and R.DBC dominate the divergent positions in the landscape and Gleysols and gleyed subgroups of Chernozemic soils dominate the footslopes and level depressional complexes. Representatives of CA.DBC and O.DBC profiles are widely dispersed across a range of landform elements. Soils with O.DBC profiles clearly dominate the CBS landform elements.

The ten soil subgroups presented in Table 2.4 can be grouped into five soil profile classes that are believed to broadly reflect differences in the long-term soil moisture regime and the degree of profile development (Bedard-Haughn and Pennock, 2002). The REGO soil profile class includes soils with no or minimal B-horizon formation and $CaCO_3$ presence in the surface A-horizon. The CALC soil profile class includes the Calcareous Dark Brown Chernozemic soils, which have incomplete removal of the $CaCO_3$ from the B-horizons, and which are a common soil in the study landscape. The ORTHIC soil profile class includes the O.DBC and E.DBC subgroups, which have complete removal of carbonate from the B and evidence for translocation of clay. The GLEYED-REGO soil profile class includes the GLR.DBC and R.HG subgroups, which are the soils with deposition of $CaCO_3$ from laterally flowing groundwater. Finally the GLEYED soil profile class includes the GL.DBC, O.HG, and HU.LG subgroups all of which have complete removal of carbonate from the solum and evidence of mottling.

The degree of soil formation can be quantified using readily mappable soil characteristics such as the depth of the A-horizon, the depth to C-horizon, thickness of the B-horizon, and depth to calcium carbonate. There is surprisingly little differentiation in the depth of the A-horizon among soil profile classes (Figure 2.4). Only the GLEYED class has a greater depth of A-horizon than the other soil profile classes. Profile development as indicated by the depth to the C-horizon (Figure 2.5), the depth to calcium carbonate (Figure 2.6), and the thickness of the B-horizon (Figure 2.7) generally increases in the expected catenary sequence REGO<CALC<ORTHIC<GLEYED (Zebarth and de Jong, 1989a).

The soils in the GLEYED-REGO class do not fit with the general landscape model of soil development predicated on the concept of downward moisture flux. The

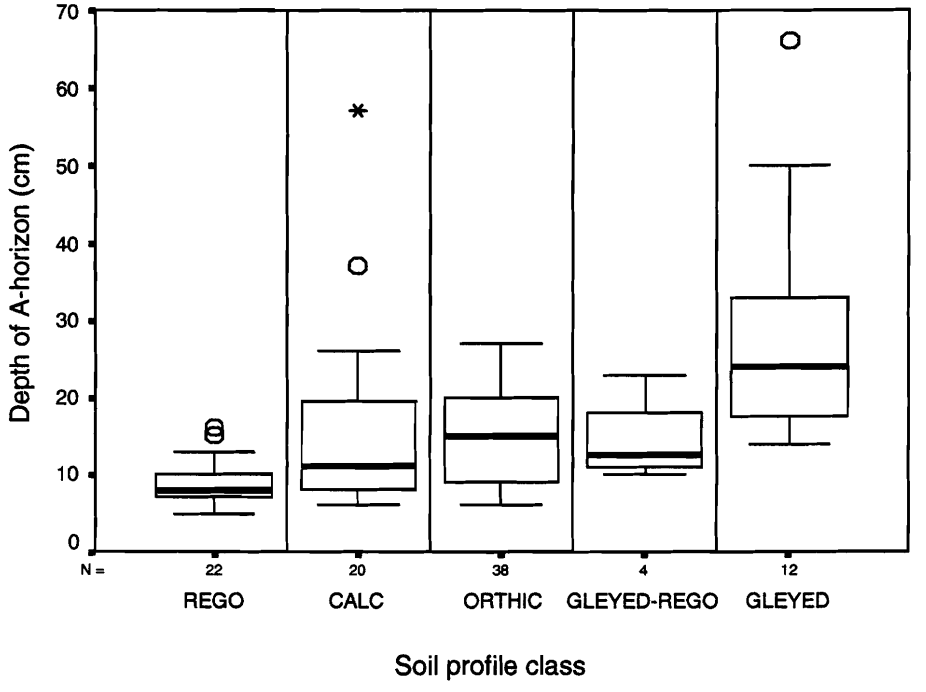

Figure 2.4 Depth of the A-horizon (cm) by soil profile class.

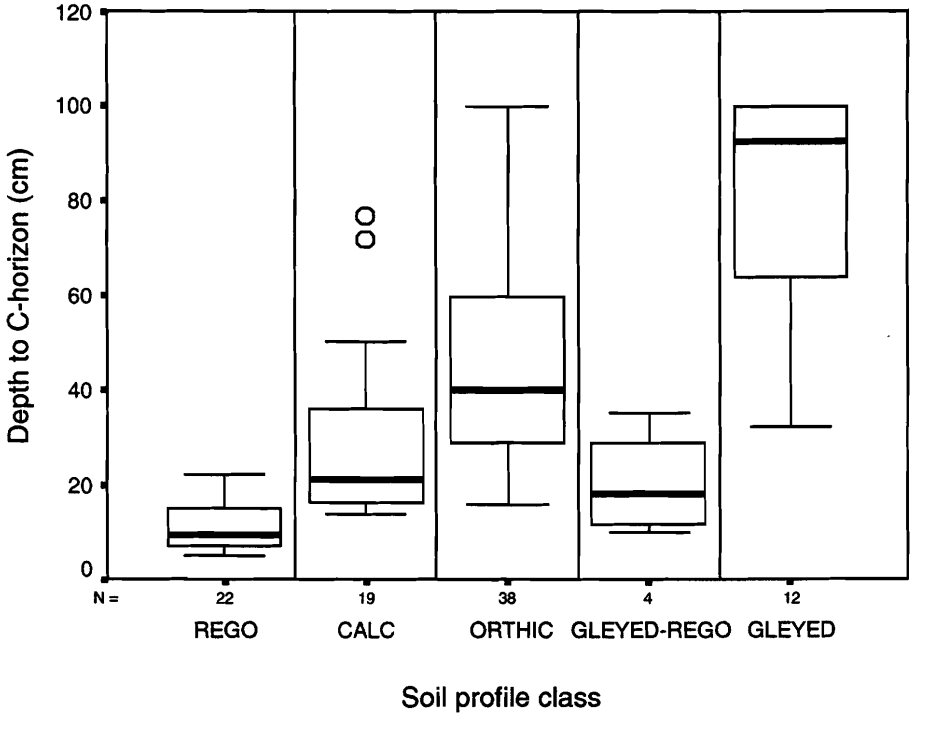

Figure 2.5 Depth to the C-horizon (cm) by soil profile class.

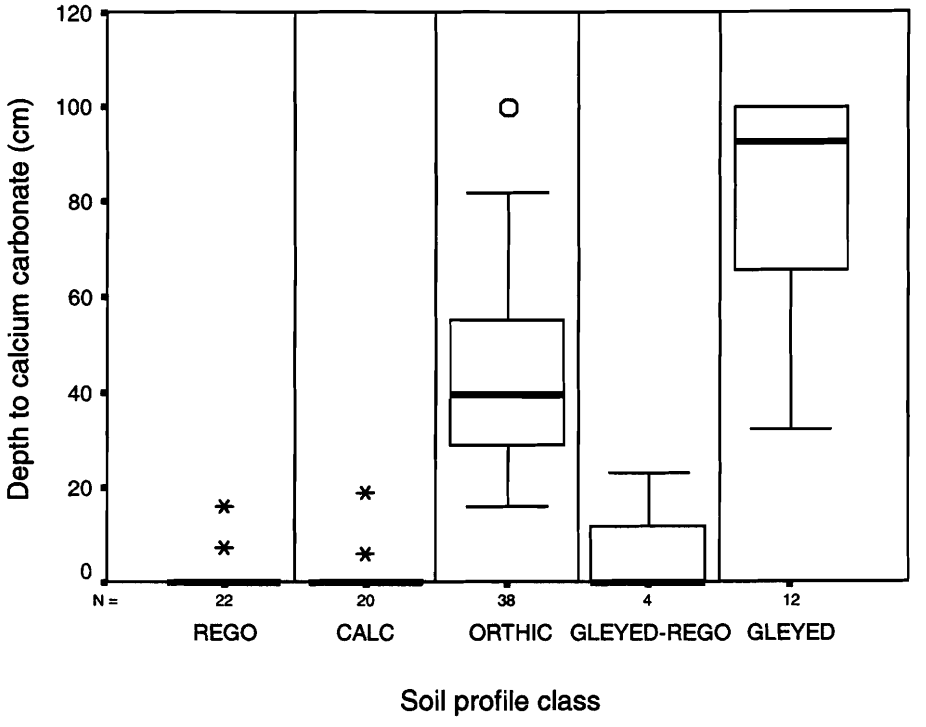

Figure 2.6 Depth to calcium carbonate by soil profile class.

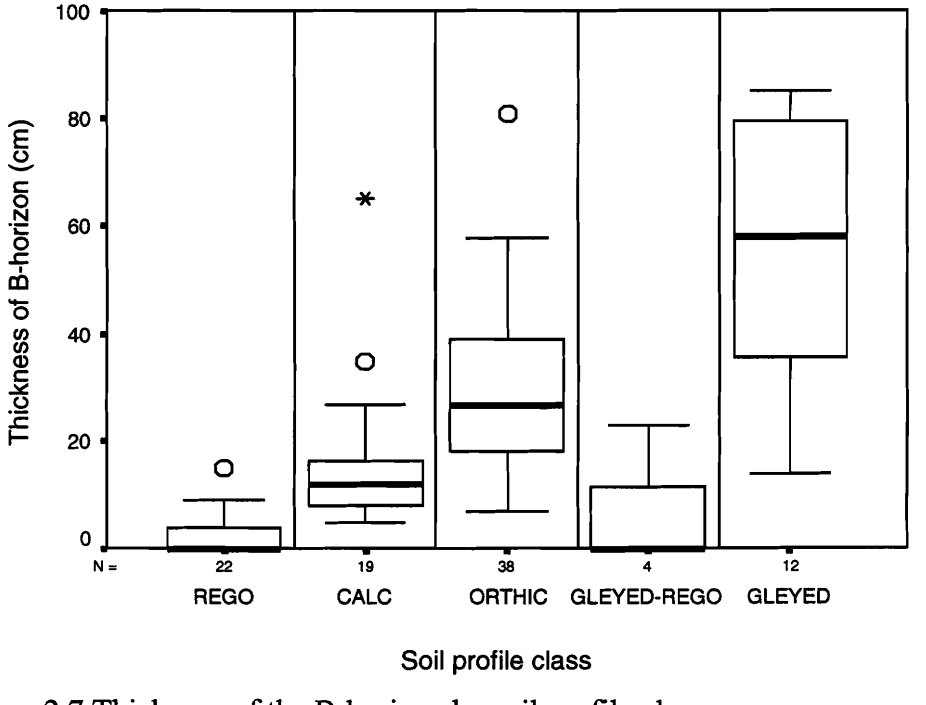

Figure 2.7 Thickness of the B-horizon by soil profile class.

presence of GLEYED-REGO profiles in DFS and LEV elements associated with the depression-centred tillage pond is consistent with the development of these profiles from laterally flowing groundwater (Mills and Zwarich, 1986; Knuteson et al., 1989; Fuller et al., 1999). The gley characteristics imply occasional saturation of the soil profile, and a deep profile would be expected, not the comparatively shallow depth to $CaCO_3$ that is observed. Bedard-Haughn and Pennock (2002) suggest that carbonated profiles that also have gley characteristics (e.g., the GLEYED-REGO class) may reflect periodic changes in the dominant direction of water flow, as it is unlikely that the conditions required for gleying and carbonate deposition will develop simultaneously. In the field these soils were identified as having secondary carbonate accumulation in the C-horizon by vigorous effervescence of carbon dioxide following the application of dilute hydrochloric acid. Had the depth of secondary carbonate accumulation in the C-horizon been acknowledged as a B horizon (as it is in Soil Taxonomy), specifically identifying it as a horizon of pedogenic activity, the depth to the C-horizon and thickness of B-horizon, Figures 2.5 and 2.7 respectively, would show a smooth continuum of increasing depth of pedogenic activity from the REGO soil class to the GLEYED soil class.

The association between soil taxa and landform element assumes that the terrain attributes used to define the landform elements strongly influence water redistribution (and hence the soils that form in the elements). It is readily apparent that the convergent landform elements consistently have a greater depth of profile development than divergent landform elements. This distinction is especially clear for the depth to C-horizon (Figure 2.8), the depth to calcium carbonate (Figure 2.9) and the thickness of the B-horizon (Figure 2.10). Soil profile development among level landform elements tends to span the range between the convergent and divergent landform elements.

There is little difference in depth of the A-horizon between the DSH, DBS, CBS, DFS and LEV landform elements (Figure 2.11). All of these horizons are comparable in thickness to the plough layer at the site. Only the CSH and CFS landform elements clearly show a greater depth of A-horizon than the plough layer thickness.

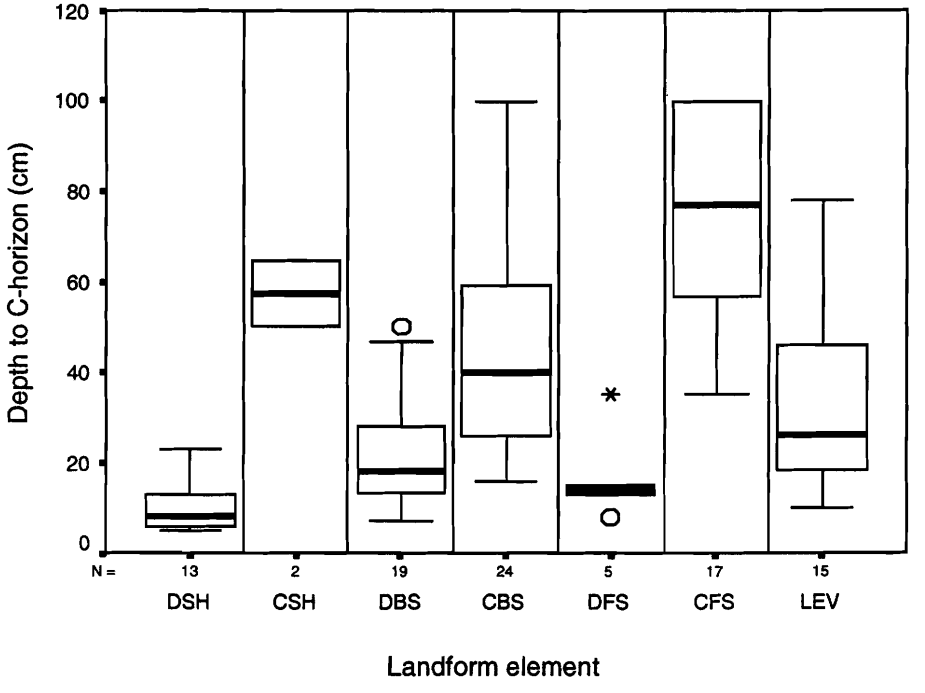

Figure 2.8 Depth to the C-horizon by landform element.

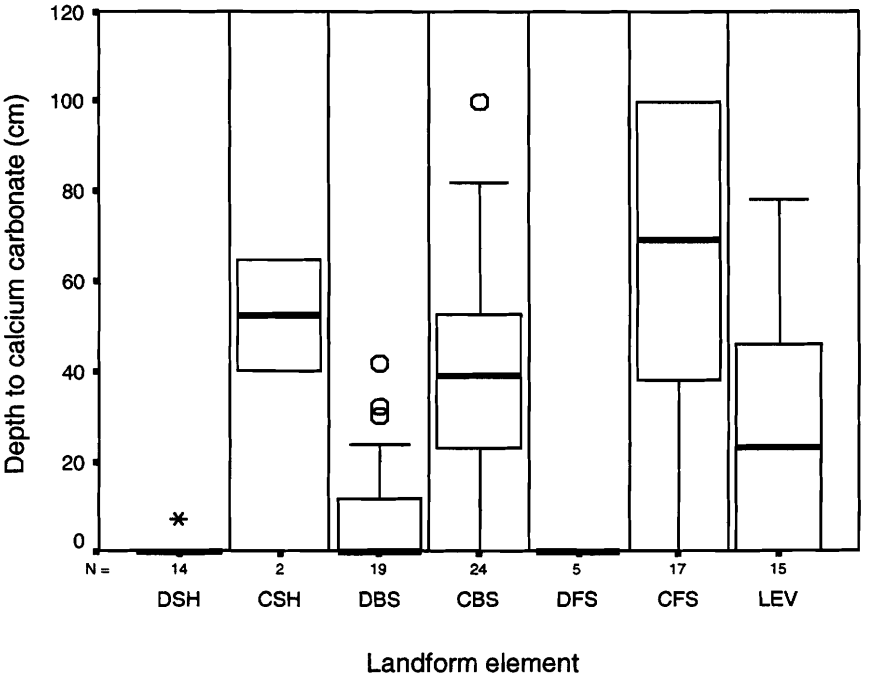

Figure 2.9 Depth to calcium carbonate by landform element.

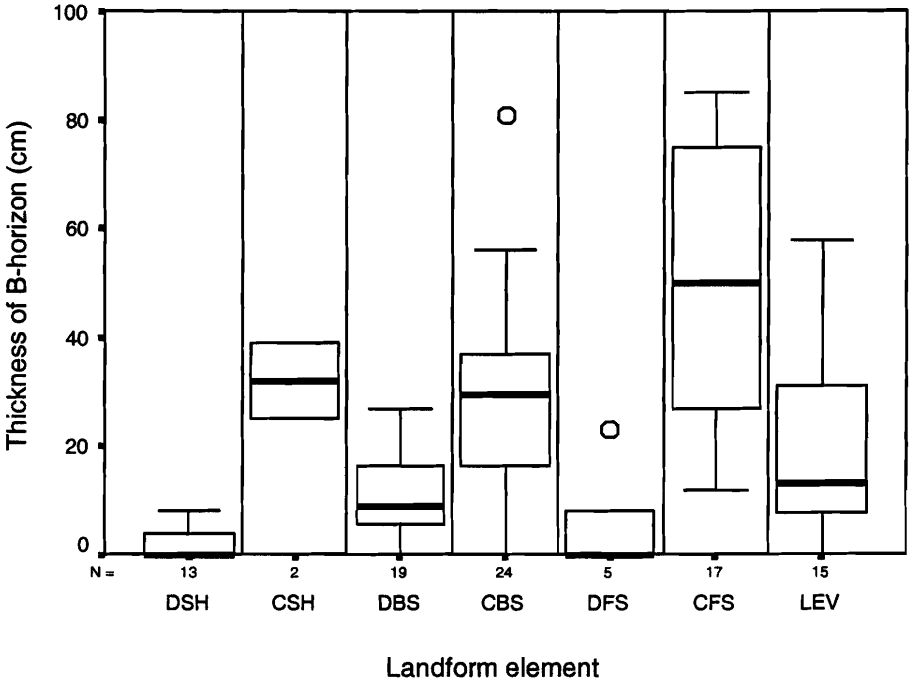

Figure 2.10 Thickness of the B-horizon (cm) by landform element.

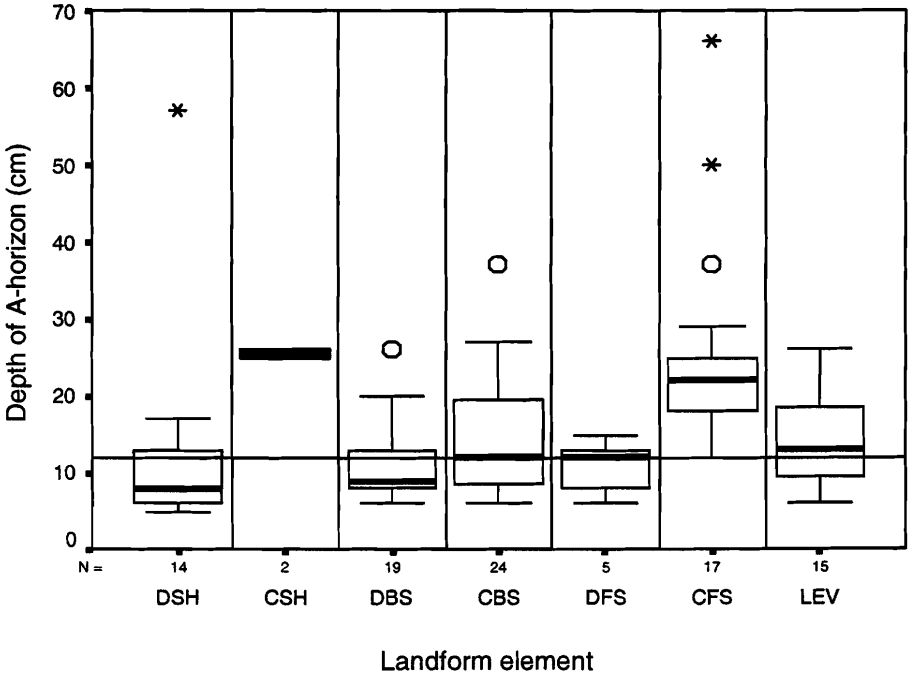

Figure 2.11 Depth of the A-horizon by landform element. The reference line at 12 cm depth indicates the deepest plough depth observed at the site.

2.4.1. Particle Size Distribution

The combined mean sand, silt and clay content for all locations and all depths (0 to 0.50 m) were 39, 41 and 20 % (Figure 2.12). Although there is considerable variability in sand and silt content at all depths of all landform elements, there is no obvious systematic difference among the landform elements. The exception may be in two of three convergent footslope elements that had a decrease in sand content and a corresponding increase in silt content in the 0.35- to 0.50-m sampling increment. Clay content shows little change across landform elements and sampling depths.

2.4.2. Cesium-137 Redistribution Results

The majority of locations at the site have lost ^{137}Cs over time (Figure 2.13). The DBS and DSH positions have lost the greatest amount of cesium, and the low dispersion of values indicates a very consistent response in these elements. The CBS and Level elements have median ^{137}Cs levels close to the reference site. Only convergent footslope positions are dominantly depositional, and a wide range of ^{137}Cs levels are associated with these depositional positions.

The erosion rate was calculated using two methods; the power equation from Kachanoski (1993) and the proportional method employed by Pennock and de Jong (1987). Both methods produce similar results until the erosion rate approaches 40 Mg ha^{-1} y^{-1}; beyond this point the results from the two methods diverge, with the power method of Kachanoski (1993) calculating greater rates of erosion (Figure 2.14). Erosion rates range from near zero to 51.1 Mg ha^{-1} y^{-1} using the proportional method, and from near zero to 70.0 Mg $ha^{-1}y^{-1}$ using the power method.

Studies by de Jong et al. (1983) and de Jong and Kachanoski (1988) determined erosion rates ranging from approximately 8 to 26 Mg $ha^{-1}y^{-1}$ for medium textured soils in the Dark Brown soil zone. The work by Pennock et al. (1994b) established a similar range of erosion rates, from 7 to 23 Mg $ha^{-1}y^{-1}$, for a site in the Black soil zone. Regardless of the method of calculation, the site under study near St. Denis clearly has greater extremes of erosion than those identified in the earlier work for similar landscapes.

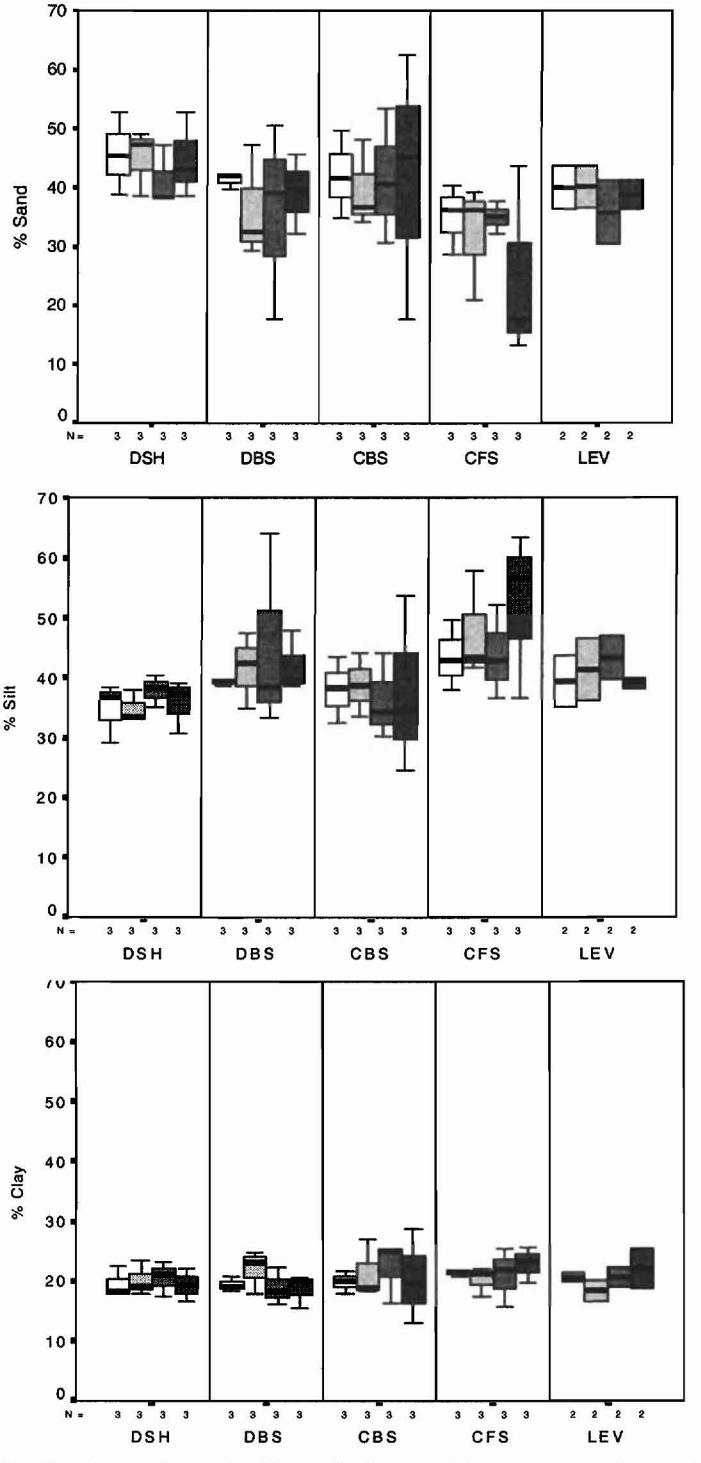

Figure 2.12 The distribution of sand, silt and clay in fifteen cores from the fall 1997 sampling. Within each landform element category the data are grouped by sampling depth, from left to right; 0 to 0.10, 0.10 to 0.20, 0.20 to 0.35 and 0.35 to 0.50 m.

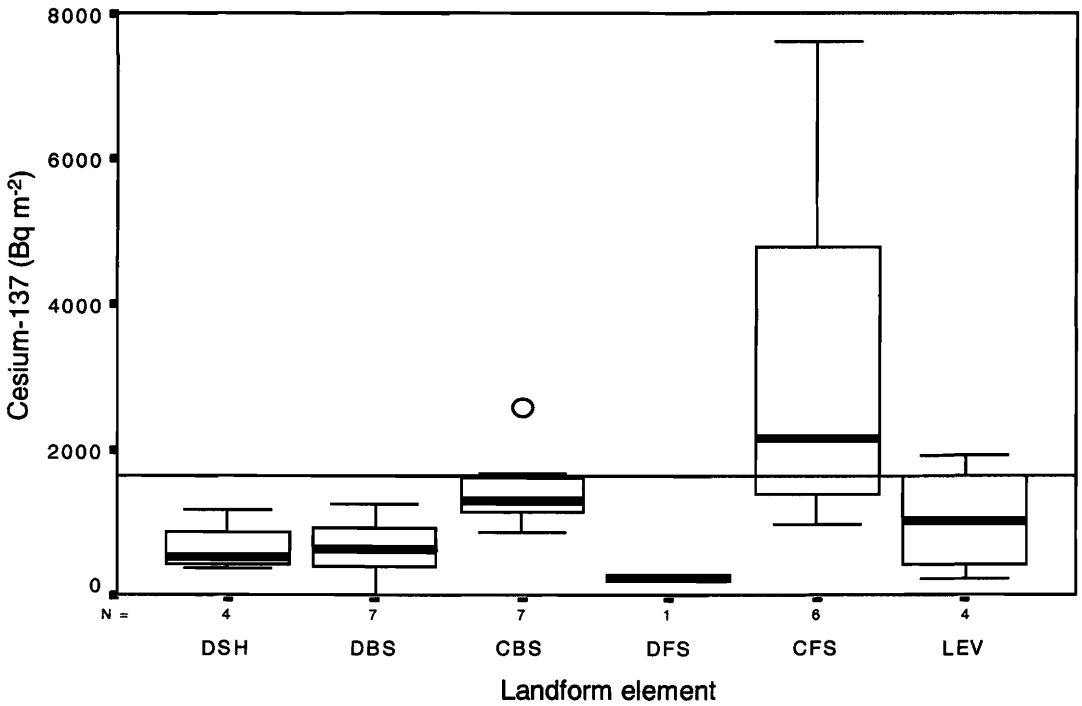

Figure 2.13 The distribution of cesium-137 in the 0- to 45-cm depth at the St. Denis study site. Reference line indicates 1638 Bq m^{-2} cesium.

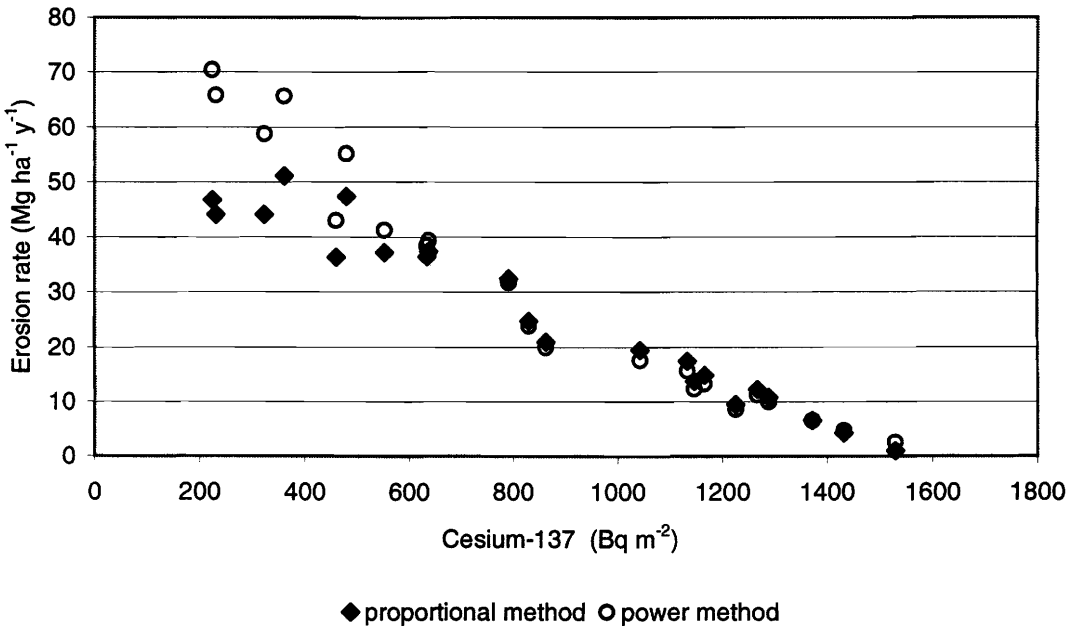

Figure 2.14 Erosion rate (Mg ha^{-1} y^{-1}) vs. cesium-137 concentration (Bq m^{-2}). Only locations showing a soil loss are included.

Efforts to graph the Cs^{137} derived erosion rates from this study against profile curvature (the rate of change in the slope) or other individual topographic variables provided no clear relationship. Pennock and de Jong (1990b) also found a weak relationship between erosion and individual slope variables. They suggest that the spatial pattern of soil loss or gain is best understood by using classifications that group the landscape into three dimensional landform elements. By stratifying erosion rate according landform element, which is defined by curvature both in the profile and plan directions, we see that there is spatial pattern apparent for the medium-term erosion at the St. Denis site.

Convergent footslopes are dominantly depositional whereas the other landform elements are dominantly erosional (Figure 2.15). The eroded landform elements show a decrease in median erosion rate from the divergent shoulder to divergent backslope to convergent backslope. Level landform elements have a range of values for soil loss.

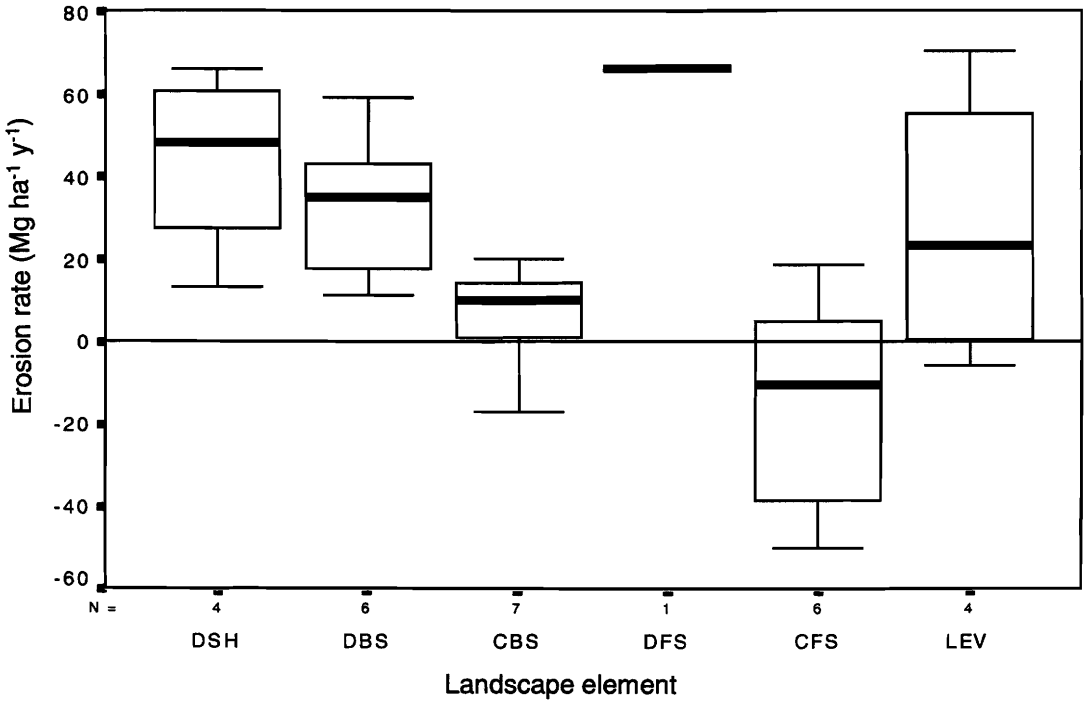

Figure 2.15 Cesium-137 based erosion rates (Mg ha^{-1} y^{-1}) by landform element. All locations included.

The pattern of decreasing erosion rate from DSH to DBS to CBS at the St. Denis site follows that identified by Pennock and de Jong (1990b). The St. Denis results differ in the behaviour of the DFS and Level elements. Pennock and de Jong (1990b) report that level and divergent footslope elements were dominated by soil deposition, but this was not observed at the St. Denis site. This difference in behaviour may be explained by the difference in mean plan curvature between the two sites. Pennock and de Jong (1990b) report that their level elements had a concave mean plan curvature. The level elements with soil loss at the St. Denis site all have a convex plan curvature and the single level element that is receiving soil at St. Denis has a concave plan curvature.

Thus it appears that divergent landform elements, including level elements with convex plan curvature, tend to have higher rates of soil loss and more variability in the erosion rate than concave positions. This fits fully with the literature, which acknowledges that convex landforms will show greater soil loss.

2.5. Summary

The research site has a suite of sediments and soils that is very comparable to other hummocky glacial till sites examined in Saskatchewan. Overall there is clear association between soil taxa and the three-dimensional landform elements, and soil thickness and degree of development increases from DSH elements to the CFS elements. The small range of A-horizon thickness and the results of the ^{137}Cs analysis strongly suggest that this landscape has been more severely eroded over the past four decades than other landscapes examined in Saskatchewan.

3. MOISTURE REDISTRIBUTION

3.1. Introduction

Within cultivated landscapes, soil components are largely redistributed by tillage and by moisture flows. Spatial variation in the physical and chemical controls on hydrological processes, and temporal variation in moisture inputs limit our ability to predict within-field differences in moisture redistribution using numerical models (Bloschl and Sivapalan, 1995; Seyfried and Wilcox, 1995). In order to further our understanding of within field variation in moisture redistribution, and in order to more effectively manage sites with differing patterns of redistribution, we must be able to identify and locate these differences in the field. My research was undertaken to address the hypothesis that distinct patterns of moisture and particle redistribution can be identified at the field scale by using readily mappable topographic and pedogenic properties as surrogate indicators of the redistribution regime.

3.2. Literature Review

3.2.1. Landscape-scale Redistribution

There is a long history of soil scientists surrogate indicators, such as topographic and pedogenic attributes, as a time and cost effective way to identify portions of a landscape with similar soils or soil process (Moore et al., 1993). There is an equally long recognized association between soil development and landscape position (Huggett, 1975; Hall and Olson, 1991; Hudson, 1992). The current conceptual model used to explain spatial differences in soil formation developed from the catena concept as introduced by Milne (1936), which attributed differences in soils along a catena to differences in drainage conditions and the differential transport, deposition, leaching and translocation of soil materials. This concept has evolved into the toposequence model of soil development largely in use today, which recognizes that changes in topography

influence the local expression of the soil forming factors by their control on the redistribution of moisture. Implicit in this model of soil formation is the understanding that soil-forming processes operate in three dimensions, having lateral as well as vertical differentiation (Huggett, 1975; Burt and Trudgill, 1985; Hall and Olson, 1991).

Given that slope-induced moisture redistribution is believed to have dominated the process of soil formation, it may be possible to utilize either slope properties or soil morphology as surrogate variables to identify differences in the pattern of moisture redistribution across the field. It is believed that much of the variability in hydrological response across a landscape is deterministic in nature and can be attributed to the interaction between ecosystem components such as topography, vegetation and geology (Phillip, 1980; Seyfried and Wilcox, 1995). From a geomorphic perspective, it has been suggested that locations with similar topographic form would show similar hydrologic behaviour, providing the form was defined in terms of a relevant hydrologic parameter, and assuming a relatively constant climate (Speight, 1974).

In a review of hydrological modeling in small catchments, Chappell and Ternan (1992) note the importance of subsurface flow for moisture redistribution and identify the need for a hydromorphic soil classification, based on hydrologically related soil catena and soil horizon properties. They suggest that such a classification would enable researchers to reduce the number of sampling points required to characterize the variation within a catchment. Park and Burt (1999) found a close association between Fe oxide distribution and lateral flow, and note that extension of their results across a landscape will require a similar classification system linking slope configuration, soil properties and hydrologic process.

Other researchers have focused on topographic characteristics largely to identify areas of potential saturation in order to model runoff. As outlined by Hall and Olson (1991) this body of research has evolved from qualitative description of landform morphology to quantitative description of slope attributes including aspect, gradient, profile curvature, and plan curvature. Using quantitatively defined slope attributes and indices derived from these attributes, researchers have attempted to predict soil moisture distribution within a landscape (Burt and Butcher, 1985; O'Loughlin, 1986; Moore et al.,

1988).

In Saskatchewan, Pennock et al. (1987) classified a hummocky till landscape into seven quantitatively defined landforms based on slope gradient, profile curvature and plan curvature. Each landform classification was dominated by soils with distinct combinations of soil profile development and A-horizon depth, which are indicators of different hydrological processes. Similar systematic variation in soil morphology and chemical characteristics, in association with landscape position, has been observed in other glacial till landscapes in Saskatchewan and North Dakota (Miller et al., 1985; Zebarth, 1988; Richardson et al., 1992).

Zebarth and de Jong (1989a), working in a hummocky till landscape in Saskatchewan, observed a distinct pattern of spatially variable soil moisture, increasing in the sequence shoulders < backslopes < footslopes. This pattern was stable over time, with the landscape elements maintaining a similar rank order. They suggest that topography tends to maintain temporal stability of water distribution in the landscape by the redistribution of water as snow, runoff and interflow.

Systematic lateral changes in moisture redistribution within a landscape are due to two primary phenomena, the development of lateral subsurface flow and the convergence or divergence of flow (both surface and subsurface) in response to surface topography (O'Loughlin, 1986). It has been demonstrated theoretically that when water infiltrates a sloping soil lateral flows will result if the hydraulic conductivity parallel to the surface is less than that normal to the surface (Zaslavsky and Rogowski, 1969; Burt and Trudgill, 1985; Miyazaki, 1993). As the hydraulic conductivity parallel to the surface increases (relative to the hydraulic conductivity normal to the surface), flows will be increasingly deflected laterally. Two mechanisms contribute to the effective anisotropy of hydraulic conductivity within the soil profile: i) variation induced by physical changes to the soil matrix including changes due to texture, root development, horizonation, compaction, freeze and thaw cycles, and dessication and ii) variation in the soil water content which determines the matric forces at work within the profile. The latter phenomenon is known as 'state dependent anisotropy' (McCord and Stephens, 1987; McCord et al., 1991; Jackson, 1992).

Lateral flows can occur either as saturated or unsaturated flows. Some hydrological researchers (Freeze, 1980) believe that lateral flow occurs dominantly as saturated flow, however, Zaslavsky and Sinai (1981) have suggested that in theory lateral flows will develop whenever there is a sloping soil surface whether flow is saturated or not. Unsaturated lateral flow was observed by McCord and Stephens (1987) and McCord et al.(1991) in a homogenous sandy profile. However, little is known about unsaturated flow in semi-arid environments like Saskatchewan (Zebarth, 1988), where the soil moisture regime is dominated by unsaturated conditions.

The topographic form of the landscape not only affects the redistribution of surface flow but also impacts upon subsurface flow. Surface and subsurface flow lines will converge at concave positions and diverge from convex positions (Zaslavsky and Rogowski, 1969; Huggett, 1975). Zaslavsky and Rogowski (1969) show, in theory that soil moisture will accumulate at points with a concave slope, and will diverge from a position with a convex slope. Under nearly level topography, the soil moisture flow lines are expected to converge at a point deep beneath the surface. Where curvature increases and slopes become steeper, the zones of convergence will appear at shallower depths.

Surface runoff is generated under two conditions: i) the precipitation rate exceeds the infiltration rate (Hortonian runoff), and ii) the soil is saturated from below because of a rising transient water table causing return flow or saturation overland flow to occur when no further soil moisture storage is available. Hortonian runoff is more common on upslope areas, and saturation overland flow is more common in near-channel wetlands or localized depressions (Freeze, 1980). In sloping landscapes the dominant downslope movement of flow will tend to contain zones of saturation resulting from fluctuating groundwater levels to areas at the base of the slope (O'Loughlin, 1981).

Burt and Trudgill (1985) suggest that the zones of maximum subsurface flow will occur in areas of flow line convergence, zones at the base of a slope, and areas with reduced soil moisture storage capacity. At a convergent slope position there is a greater potential for the volume of flow to exceed the ability of the soil profile to transmit it downslope, potentially leading to the development of local saturation and the generation

of return overland flow. Concave sites, i.e., topographic depressions, notably at the bottom of a hillslope, will collect runoff from upslope positions, and may become either temporarily or permanently saturated. Winter (1992) has suggested that the sites of surface water and soil water convergence, i.e., depressions, are sites for an enhanced interaction between these flows and groundwater.

Studies of near surface groundwater movement have significantly added to our understanding of water redistribution within hummocky landscapes in the northern plains environment. Toth (1963) theorized that well defined local relief will give rise to local flow patterns, and that these local flow patterns my overlay and interact with regional flow patterns. Toth (1963) further theorized that local flow systems would be dominated by recharge beneath the upper portions of the landscape and discharge flow in the lower elevations. Water infiltrating the soil and moving downwards to recharge the aquifer is identified as recharge flow. Water moving from the groundwater towards the surface is identified as discharge flow. Meyboom (1963, 1966) working in Saskatchewan observed local flow systems in association with depressions and noted that there was a seasonal reversal of flow direction with the depressions acting as sites of groundwater recharge during the spring and as groundwater discharge sites later in the season. Toth (1963) has suggested that in complex flow systems differences in soil attributes can evolve over short lateral distances in response to differences in the flow system and in the solute load of the soil water. Meyboom (1966) observed that discharge flow from a depression led to the development of a ring of soils around the depression that was high in secondary carbonates. Meyboom (1966) speculated that this discharge flow was driven by the uptake of moisture by willows surrounding the depressions. Several other authors (Miller, 1983; Mills and Zwarich, 1986; Richardson et al., 1992; Hayashi et al., 1998) have noted evidence of seasonal reversal of flow direction and have observed moisture transfer from a depression to the soils of the surrounding upland. This flow, called "evaporative discharge" by Richardson et al. (1992), brings moisture and solutes to the surface and is the mechanism responsible for the ring of regosolic-carbonated soil profiles surrounding the sloughs that are similar to the soils underlying the willow rings of Meyboom (1966).

Studies by (Lissey, 1968)revised Toth's earlier theory (1963) about recharge and discharge zones in northern plains landscapes. Lissey determined that in the northern plains environment recharge and discharge are primarily depression centred events. Recharge events are dominated by the spring runoff and associated throughflow. Little of the water infiltrating the uplands during the remainder of the year percolates sufficiently deep to recharge the groundwater. It is believed that much of the soil water infiltrating the uplands returns to the atmosphere by evapotranspiration before the next recharge event occurs (Richardson et al., 2001).

3.2.2. Redistribution Within the Soil Profile

The ability of the soil to infiltrate and transmit water through the profile will change over time largely in response to changing soil moisture conditions and corresponding changes in matric suction (Angulo-Jaramillo et al., 1996). The infiltration rate is a function of the morphology of the pore system, which is controlled by the texture and structure of the soil, its continuity to the soil surface, and the potential forces applied to the water, i.e., gravity, matric suction, and any pressure head at the surface (usually minimal under upland conditions in the field) (Hillel, 1998). As water enters the soil, matric suction at the surface will decrease rapidly thus lowering the subsequent rate of infiltration. Water arriving at the surface will continue to infiltrate the soil until the rate at which the water is supplied exceeds the rate of infiltration. Excess water will then move as Hortonian overland flow.

Infiltrating water will utilize macropores as preferential flow paths, rapidly moving into the soil profile while by passing the soil matrix (Beven and Germann, 1982; Espeby, 1990; Chen et al., 1999). Roth et al. (1991) observed that a chloride tracer uniformly applied to the soil surface broke up into several disconnected plumes of differing solute concentration as the tracer was leached downward. They suggest that the initial solute pulse appeared to split into many pulses of varying velocities, with rapidly moving pulses moving some of the tracer deeply into the soil following relatively little precipitation. Some tracer was found at a depth of 2.2 m after only 0.15 m of water had been applied.

It has been shown that cultivation will destroy the macropore continuity to the soil surface thus changing the soil infiltrability and near surface redistribution pattern. Andreini and Steenhuis (1990) observed that only the top 0.01 m was saturated by rainfall before preferential flow pathways were utilized at no-till plots, whereas on cultivated plots the entire plough depth (0.15 m) was saturated before preferential flow paths were utilized.

Several authors have noted a high degree of spatial variability in infiltration and subsequent redistribution when measured over a range of scales from <1 to 20 m (Schulin et al., 1987; Butters et al., 1989; van Wesenbeeck and Kachanoski, 1994; Chen et al., 1999; Olson and Cassel, 1999). This variability in infiltration is largely attributed to the influence of macropores that behave as preferential flow paths. Macropore flow is principally a function of soil structure (Lin et al., 1999), and the variability in solute travel time over small lateral distances is closely related to the dimensions of the pedon (Kachanoski et al., 1990; van Wesenbeeck and Kachanoski, 1991; van Wesenbeeck and Kachanoski, 1994).

Following infiltration, soil moisture and solutes will move out of the transporting macropores and into the soil matrix. Chen et al. (1999) observed that, over time, the upper portion of the profile showed a uniform redistribution of a bromide tracer, while redistribution at depth continued to show a much greater variability. Timing and total volume of water applied to the soil in subsequent precipitation events were important factors influencing the redistribution pattern.

3.2.3. The Use of Tracers to Monitor Moisture Redistribution

Tracers have long been used to follow the movement of soil water in both laboratory and field studies. In field studies, tracers can be either applied by the researcher or can be naturally occurring in the environment. An ideal tracer should move freely with the soil water, should not be significantly adsorbed by the soil, should have a naturally low background concentration in the soil, should not be degraded or consumed by organisms during the experiment, and should be inexpensive and environmentally safe (Davis et al., 1980; Bowman, 1984).

There are many potential tracers for monitoring water redistribution; however, field studies using applied tracers have extensively used bromide (Br^-) and chloride (Cl^-). Occasionally these are used sequentially to label waters applied at different times, enabling the researcher to monitor the impact of subsequent precipitation on the pattern of redistribution (Schulin et al., 1987; Chen et al., 1999). Although the background levels of Br^- in the soil are generally considered to be only 0.01x that of Cl^- (Bowman, 1984) many researchers still choose to use Cl^- due to the higher cost of Br^- salts.

Field studies using applied tracers have been conducted under irrigated (Butters et al., 1989; van Wesenbeeck and Kachanoski, 1994; Chen et al., 1999) and natural rainfall conditions (Schulin et al., 1987; McCord et al., 1991; Roth et al., 1991; Afyuni et al., 1994; Olson and Cassel, 1999). Butters et al. (1989) suggest that prior to 1989 there were only a limited number of transport studies conducted under unsaturated field conditions.

One group of researchers, using applied tracers to monitor soil water behaviour has emphasized the mathematical modeling of vertical infiltration and the groundwater recharge flux (Schulin et al., 1987; Butters and Jury, 1989; Butters et al., 1989; Roth et al., 1991). Reports of this work are largely found within the hydrology literature. Although field variation in transport properties is acknowledged by these authors, the emphasis is on area averaging of infiltration data and there is little exploration of the physical basis for spatial variation in moisture redistribution.

McCord and Stephens (1987) and McCord et al. (1991) used a Br^- tracer to track lateral flow in a uniform sandy soil, and to subsequently identify moisture dependant anisotropy (state dependent anisotropy) in the hydraulic conductivity of the profile as the mechanism driving lateral redistribution.

The majority of field studies using applied tracers to explore spatial variability in the redistribution of soil moisture are found within the soil science literature. Many papers report on studies at the very small scale (<1.0 m) that effectively explore differences in redistribution as related to variation in soil structure and porosity (e.g., Chen et al., 1999).

At larger scales of interest, there are fewer studies. Van Wesenbeeck and Kachanoski (1994) report on a study at which the scale of observation extended to 5.0 m. At their site, moisture redistribution was related to differences in profile depth. Deeper movement of soil moisture coincided with a deeper B-horizon. Afyuni et al. (1994) and Olson and Cassel (1999), exploring differences in moisture redistribution associated with landscape position, found that a Br^- tracer moved deeper into the soil profile at a footslope position than at either a linear slope or a shoulder position.

Applied tracers are generally employed to observed moisture redistribution over a relatively short time span, from a few days to less than two years. One exception to this is the recent work in Saskatchewan by Dyck (2001) who monitored the deep movement of a chloride pulse that had been initiated approximately 40 years earlier (Ballantyne, 1974).

Naturally occurring tracers used to monitor moisture redistribution are used to look at redistribution over the much longer term, i.e. several decades, usually with intent to measure ground water recharge. Allison et al. (1994) review several tracers used to estimate ground water recharge over the long term.

In most of southern Saskatchewan, soils are formed on calcareous parent material. During soil formation the carbonate minerals are dissolved and leached from the upper profile. The depth of carbonate-free profile above the C/Cca horizon is considered the long-term average depth of leaching (Pennock and de Jong, 1990a; St. Arnaud, 1976). Thus, the carbonates can be considered a tracer that shows the long-term mean depth of water movement. However, this relationship between the historic depth to carbonates, and the current pattern of moisture redistribution has not been documented for the conditions encountered in central Saskatchewan. The relationship may be complicated by the impact of several decades of tillage-induced soil redistribution.

3.2.4. Summary

The pattern of soil moisture distribution in the landscape has a temporal stability that is associated with distinct topographic forms. It is believed that redistribution of

surface and subsurface flows is primarily controlled by topographic form and this control maintains the stability of this pattern of moisture distribution. There is a strong theoretical basis for the development of lateral subsurface flows under sloping topography. Tracer experiments over the past 20 years have confirmed lateral flow even under unsaturated conditions with a soil lacking clear horizon development. Lateral flow will be enhanced when vertical flow is relatively restricted in comparison to flow parallel to the surface. Changes to hydraulic conductivity with depth can result from changes in soil texture, the development of soil horizons, soil compaction, the influence of plant roots, or soil moisture gradients among other reasons.

Moisture flows will diverge from positions with a convex slope curvature and moisture will converge at positions with a concave slope curvature. Our conceptual model of soil development suggests that sites receiving more water will have a greater degree of profile development than sites receiving less water. The conceptual model of profile development matches the generally observed distribution of soils in Saskatchewan, with thicker profiles developing at concave landscape positions and thinner profile development at positions with convex surface curvature (Pennock and de Jong, 1987; Zebarth and de Jong, 1989a).

Given i) the acknowledged influence of topography on moisture redistribution, and ii) the belief that soil profile development reflects the long-term hydrological processes at a site, and iii) that profile attributes can themselves influence both lateral and vertical redistribution, then clearly topography and soil profile characteristics have the potential for delineating landscape areas with distinct hydrological behaviour.

3.3. Materials and Methods

3.3.1. Introduction

Soil moisture redistribution was determined by following the movement of a chloride tracer applied to small plots at multiple grid points over a 0.8-ha area. To account for variations in surface conditions due to farm practice, and seasonal variation

in precipitation, sampling was conducted over two growing seasons during a 16-month period from June 1997 to October 1998. Cultivation and management of the site followed common practice for the study area and field operations were performed using field scale tillage equipment. During the first season the field was left fallow and in the second season the field was seeded to canola and then tilled following the fall harvest. The research site has been described in Section 2.3.1.

3.3.2. Experimental Design

At the study site a fifty-two point sampling grid was established. The grid had four rows and a spacing of 15 m between rows and 15 m between each of the 13 points in each row (Figure 3.1). At each grid point three 1-m^2 micro-plots were established with 2 m spacing between adjacent plots (Figure 3.2). The micro-plots were arranged so that they were approximately perpendicular to the dominant slope at each grid point. Chloride was applied to the surface of each micro-plot to act as a tracer of moisture redistribution. The chloride was surface-applied to all micro-plots as a fine granular KCl (known as Standard Product) at the rate of 675 g KCl m^{-2} (32.09 mg Cl^- cm^{-2}) on June 24 and 25, 1997. The KCl was lightly worked into the surface of the soil (to a depth of approximately 0.02 m) using a hand held garden cultivator. At the study site background chloride levels were found to be < 25 ug g^{-1} (see Section 3.4.2).

The three micro-plots were established at each grid point to allow for destructive sampling of one micro-plot at each of three different times: Fall 1997 (October 1997), Spring 1998 (May 1998), and Fall 1998 (September 1998). The assumption was that the three micro-plots would show similar behaviour given the small relative distance between them.

From June 1997 to September 1997 the field was left fallow and untilled. In May 1998 the site was sampled following the spring melt and (at most locations) before seeding. From May 1998 to September 1998 the site was planted to canola, harvested and then tilled once in the fall prior to sampling. Cultivation and management of the site followed common practice for the study area and field operations were performed using field scale tillage equipment.

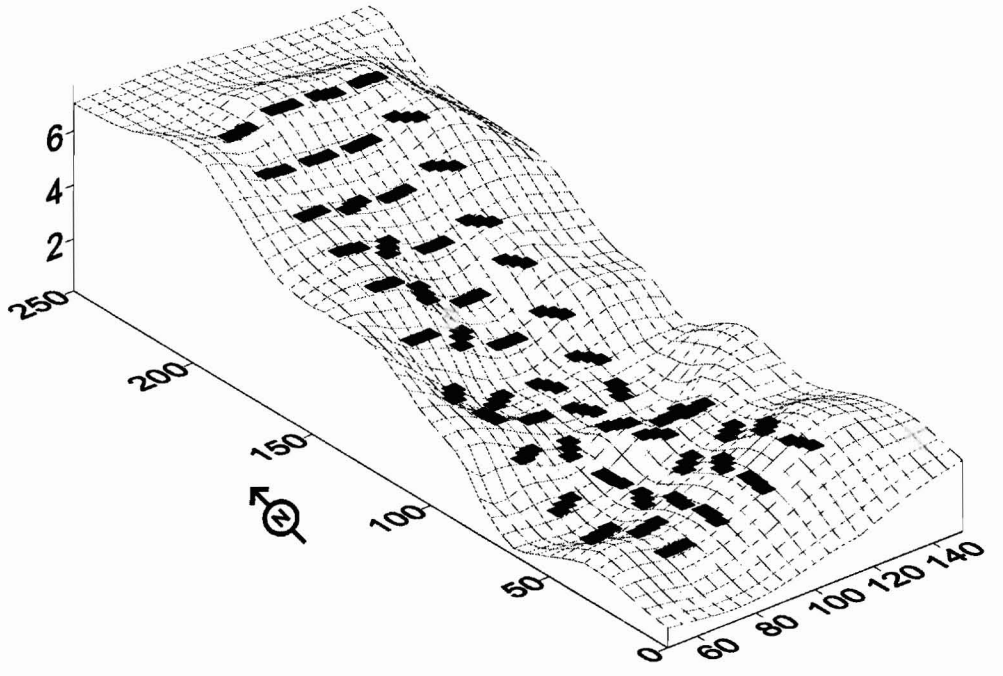

Figure 3.1 The study site with the 52-point sampling grid. At each grid point there are three 1-m^2 micro-plots aligned perpendicular to the dominant slope direction.

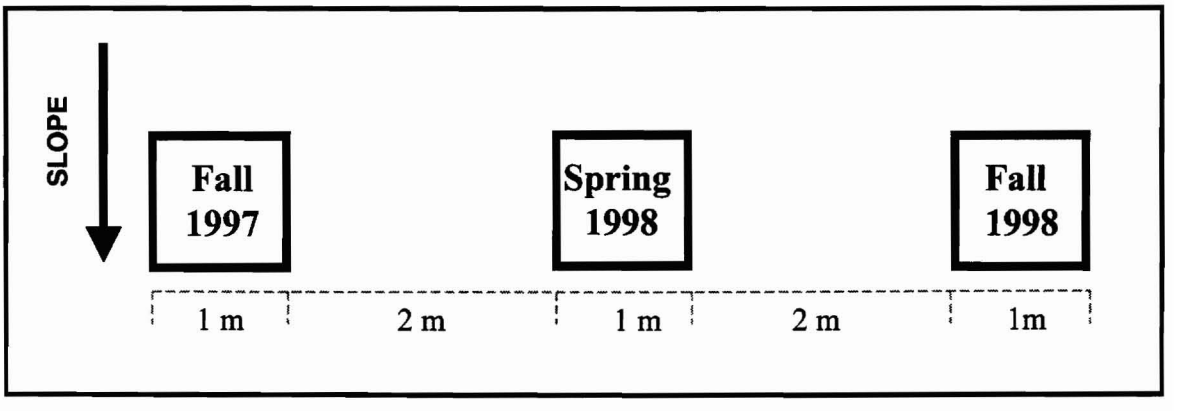

Figure 3.2 Arrangement of the three micro-plots at each grid point, with plots labelled by their time of sampling.

Data from a topographic survey of the study site was used to construct a digital elevation model with a 5 by 5 m grid cell size (discussed in Section 2.4). Each grid cell was classified into one of seven landform elements based on slope gradient and curvature following the procedure of Pennock et al. (1987). Each micro-plot was then

assigned a set of topographic parameters and a landform element classification based on the grid cell in which it was located. To compare chloride redistribution, sites were grouped by landform element and to ensure that the landform classification for each location was comparable across time the three micro-plots at each location were all given the same landform element classification using the computer generated classification for the centre (Spring 1998) micro-plot.

Location 32 (Figure 2.1) was the only location classified as a convergent shoulder landform element. This location was manually reclassified as a convergent backslope element, based on the landform element complex that identifies the dominant landform element classification of the surrounding grid cells (Pennock et al., 1994b).

Rainfall over the two growing seasons was measured on site using a tipping bucket mechanism. There was 178 mm of rain received in the first growing season from June 24 to October 22. Based on the long-term normal precipitation (Environment Canada, 1992) we would expect approximately 57% of the annual rainfall during this time or approximately 143 mm. Hence precipitation in this period was slightly above normal levels.

During the second growing season there was 150 mm of rain received from April 8 to September 29. This is approximately 68% of the long-term normal rainfall for this period.

During the winter of 1997-98, a snow survey was conducted on February 5, 1998. Snow depth and density were measured at each of the 52 grid locations. Density measurements were obtained gravimetrically using a 0.08-m diameter core sampler. The snow water equivalent was calculated using equation 3.1 (Pomeroy and Gray, 1995):

$$SWE = 0.01 * d_s * \rho_s \qquad (3.1)$$

where
SWE = the snow water equivalent in mm
d_s = the depth of the snow pack in cm
ρ_s = the bulk density of the snow in kg m^{-3}

3.3.3. Sampling Procedures

On each sampling date samples were collected using a truck mounted punch with a 0.053-m diameter core following the sampling pattern shown in Figure 3.3.

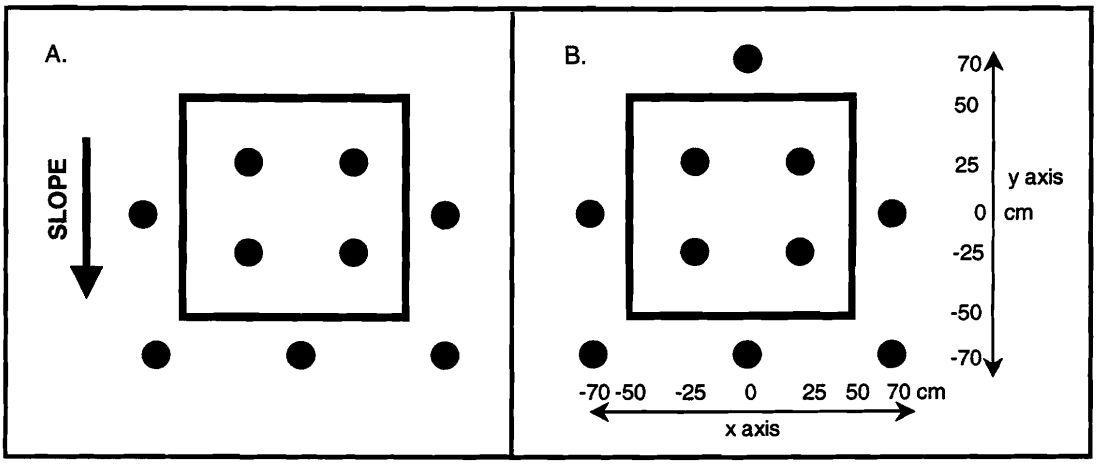

Figure 3.3 Standard pattern of sampling cores at one micro-plot for A.) Fall 1997, and B.) Spring 1998 and Fall 1998

At each sampling point a single core was taken to 0.50-m depth and then the core was split into increments of 0.0 to 0.10, 0.10 to 0.20, 0.20 to 0.35, and 0.35 to 0.50 m. A decision was taken to limit the depth of sampling and the number of cores at each site in order to maximize the number of locations under observation. Even so, the time required for the laboratory analysis of all samples collected from the 52 grid locations in the Fall 1997 sampling was found to be too great, and the number of locations sampled was reduced in the Spring 1998 sampling to 15 and in the Fall 1998 sampling to 29. In order to compare results across time, the data presented below is composed only of those twenty-nine locations sampled in both the Fall of 1997 and the Fall of 1998. Of these twenty-nine, fifteen were also sampled in the Spring of 1998 and this data is also presented.

At each micro-plot a single core was taken to approximately 1-m depth to describe the soil profile (discussed in Section 2.5).

3.3.4. Laboratory Analysis

Samples were air dried, weighed and ground to pass through a 2 mm sieve. Soil

bulk density was calculated on an air-dry basis.

Samples collected during the fall of 1997 were analyzed for chloride using an Orion ® Model 96-17B combination chloride selective electrode. The method of Janzen (1993) was followed to extract the soluble salts from a 2:1 water:soil suspension. Twenty-five grams of soil was mixed with 50 ml of distilled water and shaken for 1hour. The mixture was then gravity filtered through Number 2 filter paper. Seventeen ml of the filtrate was captured and to this was added 0.34 ml of $NaNO_3$ as an ionic buffer following the instructions with the chloride electrode. The electrode was inserted into the filtrate and readings were compared against standards of known concentration.

Gravity filtration of the 2:1 suspension proved to be a time-consuming process and produced a filtrate containing large amounts of suspended materials. Subsequently it was learned that high levels of suspended organic materials may give an elevated false reading of chloride concentration, especially where the true chloride concentration was very low (Sikora and Stevenson, 1987).

To remove the influence of suspended materials on the analysis, and in an effort to speed the sample handling process the Spring 1998 and Fall 1998 samples were determined colorimetrically using a Technicon® AutoAnalyzer®. Samples used for colorimetric analysis were extracted using the same method noted above. After shaking, the solution was vacuum filtered to remove solids and then the filtrate was compared against known standards for chloride content using the colorimeter. No ionic buffer was added to the filtrate for this procedure.

3.3.5. Data Analysis

3.3.5.1. Chloride Recovery

The measured chloride concentration for each sample (ug g^{-1}) was reduced by the background threshold value of 25 ug g^{-1} (Section 3.4.2). The results were then converted to a mass per area basis (ug cm^{-2}) using the depth of the sampling increment and the mean soil bulk density for each increment at each location.

For each location, the chloride distribution between sampling points was

interpolated over the x and y axes using the Surfer 7.0 software (Golden Software Inc., 1999). This provided an estimate of the total chloride mass recovered within the sampling area for each sampling depth at each location. Recovered chloride was determined for each depth increment at each location and then summed to give total recovery to 0.50-m depth.

Interpolation and gridding of the chloride data (ug cm^{-2}) was done using a *thin plate spline* as the interpolation algorithm and a grid cell size of 1 by 1 cm. The thin plate spline was chosen as the interpolation method because the limited number of sampling points at each location precluded the use of kriging. Kriging should have a minimum of 50 to 100 points to construct the semi-variogram (Burrough and McDonnell, 1998; Utset et al., 2000). The Surfer 7.0 Users Guide (Golden Software Inc., 1999) suggests radial basis function methods in cases where there are limited numbers of points. The thin plate spline is one of a suite of methods known as radial basis function methods. Several authors support the use of thin plate splines (Laslett et al., 1987; Hutchinson and Gessler, 1994; McCauley and Engel, 1997), suggesting that their results are comparable with kriging while at the same time not being subject to the restrictions of the semi-variogram, nor lending themselves to errors by inexperienced users.

3.3.5.2. Fitting Known Functions to Recovered Chloride

An effort was made to fit known mathematic functions derived from a physical basis to the recovered chloride concentration data. It was felt that if successful, the fitted function would offer better estimates of the total recovered mass, the centre of mass and the variance.

A log-normal curve was found to closely approximate the vertical redistribution of chloride along the z-axis (i.e., vertical infiltration). This form of redistribution in the vertical axis has been observed by several researchers (Ellsworth and Jury, 1991; Van de Pol et al., 1977). Approximately half of the Spring 1998 and the Fall 1998 sampling locations were fit to a log-normal distribution; in nearly all of these cases a good fit was obtained regardless of the total chloride recovered.

Taylor's Equation (Taylor, 1953), a solution to the Convection Dispersion Equation, which offers a symmetrical distribution around the mean (i.e., a normal distribution) was applied to the recovered chloride data in the x and y axes. Taylor's equation did not provide a good fit to all data sets. It was apparent that the recovered chloride was not moving symmetrically and thus could not be adequately represented by Taylor's equation. Taylor's equation presupposes equal diffusive redistribution in all directions. In this experiment recovery downslope from the area of application tended to be greater than recovery upslope.

Further issues arose surrounding the representation of the spatial data and its input format into the curve fitting Mathcad program. The validity of such a curve fitting exercise was questionable given the limited data set determined at each micro-plot. Because we attempt to fit a curve in a single dimension, we sum the measurements found at individual sampling points by either the x, y or z coordinate. The result is only 4 or 5 points on which to construct a curve. While this limited data set may be adequate to fit a symmetrical distribution, it appears insufficient for describing the tail of a non-symmetrical distribution (as with the lateral movement of the tracer).

3.3.5.3. The Chloride Weighted Centre of Mass

The weighted centre of mass for chloride was calculated for each depth increment and for the full 0- to 0.50-m sampling depth using the method as outlined by Stewart (1987). The shift in the centre of mass provides an indication of the direction of movement (x, y, and z coordinates), and an indication of the magnitude of movement (the distance of displacement). The initial position of the chloride centre of mass is at the soil surface in the middle of the 1-m^2 micro-plot where the x, y and z coordinate values all equal zero.

The magnitude of the vector running from the initial centre of mass position to the new centre of mass provides a measure of the magnitude of the displacement of the centre of mass. The magnitude of the vector can be considered to be either 1) the length of the vector (i.e., the distance that the centre of mass has moved, or 2) the weighting factor used to calculate the centre of mass coordinates (Stewart, 1995). The weighting

factor used in this case is the sum of the chloride (ug cm^{-2}) from all cores for each sampling depth at each location, this gives an indication of the mass of chloride moving from the initial position through the new centre of mass.

3.4. Fall 1997 Results and Discussion

3.4.1. Introduction

In the 1996 crop year the study site had been planted to wheat and the site had been left in stubble over the winter of 1996 to 1997. On June 18, 1997 the site was tilled from the north to the south and then from the east to the west by the cooperating landowner using a 15.2 m wide cultivator that had 0.40-m wide V-shaped shovels on 0.35-m centres and a spring loaded tine harrow with tines on 0.15-m centres. Tillage speed averaged at 10.5 km h^{-1}. Tillage depth varied from 0.08 to 0.10 m. Herbicide was applied on two occasions over the summer months to control weeds. Granular chloride was applied to the surface of all micro-plots on June 24 and 25, 1997. From June 24 to the fall sampling a total of 178 mm of rain was recorded.

Fall sampling was carried out from September 29 to October 1, 1997 with the intention of identifying variation in tracer redistribution that had occurred under fallow conditions during the summer growing season.

3.4.2. Chloride Background Levels

Samples for background chloride determination were collected from nine transects across the study site and included the area used in the moisture redistribution study as well as that used for the adjacent tillage experiments. The data were grouped to determine the mean background value over the 3-ha incorporating all the individual study/experimental locations. At each sampling position, composite samples were collected from two cores that were broken into increments from 0 to 0.10 m, 0.10 to 0.20 m, 0.20 to 0.35 m and 0.35 to 0.50 m. The background samples had a mean Cl^- concentration of 8.4 ug g^{-1} and a standard deviation of 6.2 ug g^{-1}; approximately 80% of the data fall within 2.5 standard deviations either side of the mean, i.e., they are less than 24 ug g^{-1}. In Figure 3.4 the combined data for all depths is shown in a histogram. Here we see that there is a break in the data continuity in the range 24 to 26 ug g^{-1}. The

background threshold value for chloride was thus estimated to be at 25 ug g^{-1}. This incorporates the range found in the data but excludes the relatively few samples with higher values. Any experimental values above 25 ug g^{-1} are unlikely to be due to background chloride.

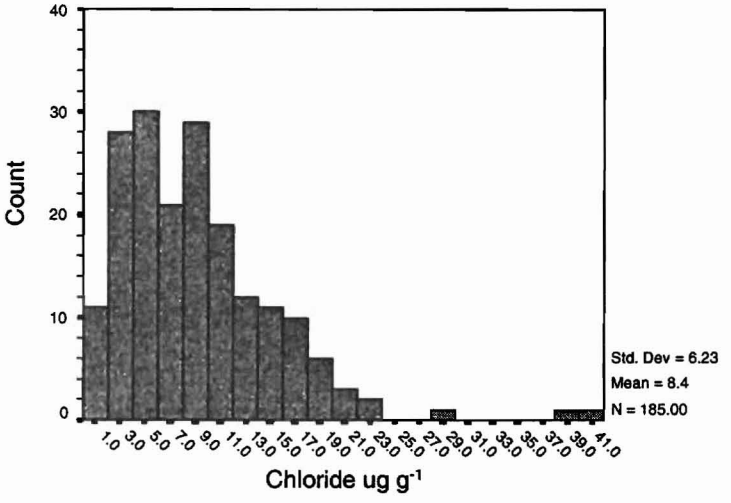

Figure 3.4 Histogram of chloride concentration values in background samples. Each bar has a range of 2.0 ug g^{-1}, the mid-point is shown for each bar.

3.4.3. Chloride Recovery

Mean total recovery (in the 0- to 0.50-m increment) across all locations was 103% with a standard deviation of 23%. The values for total recovery range from 57.5% to 155.2% (Table 3.1) and a similar range occurs in the recovery values by depth increment. The degree of variation in recovery within the third increment is much greater within the DSH and DBS landform elements than other landform elements.

There are fifteen locations with a total recovery > 100%, and of these seven are >120%. Three factors may have contributed to these high recovery values:

1. Preferential flow may have resulted in local high concentrations of chloride.

2. The interpolation of point values across the plot area may exaggerate the area truly affected by local high concentrations of chloride.

3. The use of the chloride selective electrode may have contributed to the overestimation of chloride concentration. Chloride selective electrodes have been shown to respond to humic substances in solution giving falsely high readings especially when the chloride concentration is low and the concentration of humic substances is high (Sikora and Stevenson, 1987). In the method employed for the Fall 1997 samples, gravity filtration did not remove all the suspended materials from the solution prior to the electrode being used.

There are eleven (out of twenty-nine) locations at which more chloride was recovered in the first increment than in the second increment (Table 3.1). These eleven locations include the six locations where gleyed profiles were observed (Gleysols or gleyed subgroups of Chernozemic order). These gleyed soils were found exclusively associated with DFS and CFS landscape elements. These landscape elements have their greatest mean recovered chloride in the surface increment. Note that non-gleyed soils occurring in DFS and CFS positions have either greater or equal amounts of chloride in the second increment than at the surface. In contrast, gleyed soils have at least 10% greater chloride in the surface increment than in the 0.10- to 0.20-m increment.

At the other five locations at which more chloride was recovered in the first rather than the second depth increment there is no clear pattern to their recovery. Two locations have CA.DBC profiles, one each at DBS and DSH positions. The remaining three locations, one Orthic Chernozem and two Calcareous Chernozems, all have less than 5% difference between the two increment depths.

Hence it would appear that chloride redistribution in gleyed soils is different to that for the non-gleyed soils. This in itself is not surprising, as we expect the different soil types to develop under different soil moisture regimes.

When plots are grouped by landform element, there is a large range in recovery values within sampling increments for the majority of the landform elements. Despite this variation, two patterns of chloride redistribution can be seen among the landform elements (Table 3.2, Figure 3.5):

Table 3.1 Fall 1997 chloride recovery (%) by sampling depth for each location.

Landform Element	Location*	Soil Subgroup	Chloride Recovery (%)				
			Sampling Increments (cm)				
			0-10	10-20	20-35	35-50	0-50
DSH	6	O.DBC	18.5	45.1	62.0	0.7	126.3
	26	O.R	37.1	53.1	13.7	0.0	103.8
	43	O.R	42.3	46.4	24.7	0.6	113.9
	52	CA.DBC	54.6	28.0	2.6	0.0	85.3
DBS	8	CA.DBC	32.9	20.2	4.3	0.2	57.5
	14	O.DBC	46.5	76.7	19.6	0.0	142.8
	15	O.DBC	32.7	45.3	38.0	6.5	122.5
	38	O.R	15.1	37.5	43.3	3.3	99.3
	40	CA.DBC	22.0	35.2	14.3	0.1	71.5
	50	CA.DBC	49.1	44.0	17.9	0.0	111.1
CBS	2	O.DBC	29.4	49.7	34.0	9.1	122.1
	12	O.DBC	29.3	36.4	15.8	0.3	81.9
	22	CA.DBC	45.1	53.1	15.3	0.0	113.5
	24	O.DBC	31.7	32.6	12.0	0.0	76.4
	28	O.DBC	29.2	49.4	15.9	11.9	106.5
	30	O.DBC	40.8	42.5	12.4	0.0	95.8
	32	O.DBC	30.3	41.1	14.9	5.3	91.6
DFS	19	R.DBC	36.8	38.8	8.2	0.0	83.8
	35	R.HG	39.3	27.2	7.8	0.1	74.3
	46	GLR.DBC	69.6	54.5	27.7	3.5	155.2
CFS	11	GL.DBC	79.1	28.2	5.9	1.1	114.2
	17	O.DBC	50.4	59.9	14.9	0.0	125.3
	20	HU.LG	87.4	19.3	5.1	1.1	111.7
	34	R.HG	49.3	29.7	20.6	21.3	120.9
	44	O.HG	38.1	21.2	7.4	1.3	68.0
	49	O.DBC	49.9	51.3	8.5	2.0	111.7
LEV	4	CA.DBC	12.2	31.6	36.4	26.3	106.5
	13	CA.DBC	37.8	34.6	11.4	0.0	83.9
	37	O.DBC	37.7	36.6	17.3	3.2	94.9

* See Figure 2.1

1. DFS and CFS landscape elements have their greatest mean recovery in the surface increment, and recovery then decreases with depth. These landform elements have more chloride in the 0 to 20 cm increment (>88%) than do the other landform elements (63 to 82%).

2. DSH, DBS, CBS and LEV landscape elements show the greatest mean chloride recovery in the second increment. Lesser amounts of chloride are found in the

first, third and fourth sampling increments, in that order. Within the different sampling increments there is little difference between these landform elements.

Table 3.2 Summary statistics for the Fall 1997 chloride recovery (%), data grouped by landform element.

		Chloride Recovery (%)				
		---------- Sampling Increments (cm) --------				
Landform Element		0-10	10-20	20-35	35-50	0-50
DSH	Mean	38.1	43.2	25.8	0.3	107.3
	Median	39.7	45.8	19.2	0.3	108.9
	Std. Deviation	15.0	10.7	25.8	0.4	17.3
	N	4	4	4	4	4
DBS	Mean	33.1	43.2	22.9	1.7	100.8
	Median	32.8	40.8	18.8	0.2	105.2
	Std. Deviation	13.3	18.7	14.8	2.7	31.9
	N	6	6	6	6	6
CBS	Mean	33.7	43.5	17.2	3.8	98.3
	Median	30.3	42.5	15.3	0.3	95.8
	Std. Deviation	6.5	7.5	7.6	5.0	16.7
	N	7.0	7.0	7.0	7.0	7.0
DFS	Mean	48.6	40.2	14.6	1.2	104.4
	Median	39.3	38.8	8.2	0.1	83.8
	Std. Deviation	18.3	13.7	11.4	2.0	44.2
	N	3	3	3	3	3
CFS	Mean	59.0	34.9	10.4	5.4	108.6
	Median	50.2	29.0	8.0	1.3	113.0
	Std. Deviation	19.5	16.7	6.1	8.9	20.6
	N	6	6	6	5	6
LEV	Mean	29.2	34.3	21.7	9.8	95.1
	Median	37.7	34.6	17.3	3.2	94.9
	Std. Deviation	14.8	2.5	13.1	14.4	11.3
	N	3	3	3	3	3
Total	Mean	40.5	40.3	18.3	3.5	102.5
	Median	37.8	38.8	14.9	0.7	106.5
	Std. Deviation	17.0	12.9	13.4	6.5	22.8
	N	29	29	29	28	29

As seen in Figure 3.6, it is apparent that the majority of the recovered chloride, to 0.50-m depth, is moving vertically downward below the 1.0-m^2 application area. Only minor amounts of chloride have moved laterally outside of area defined by the 1.0 m x 1.0 m plot perimeter.

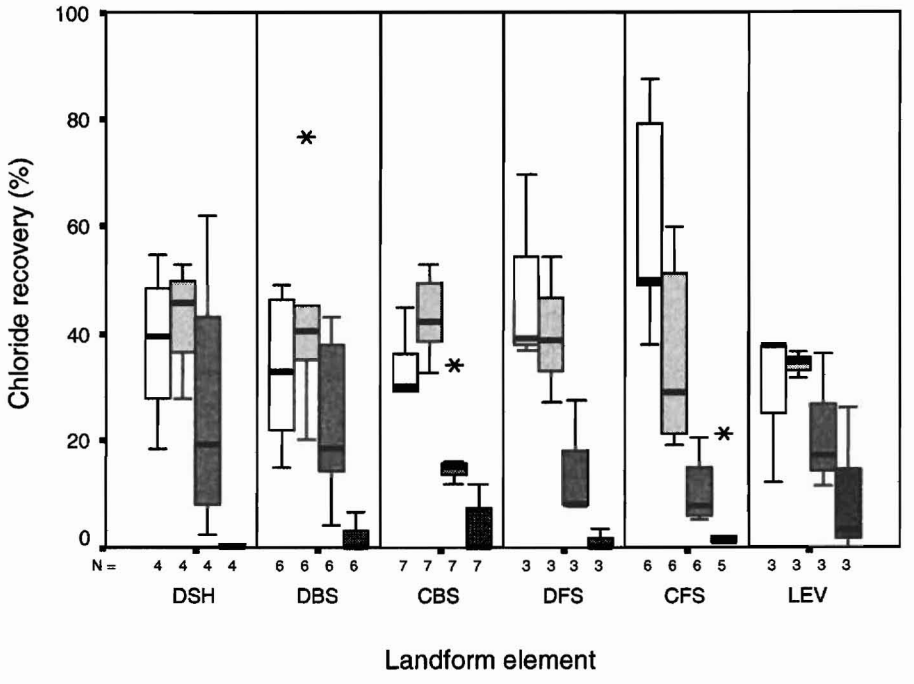

Figure 3.5 Fall 1997 chloride recovery (%) by depth increment and by landform element. Depth increments are read from the left to the right within each category: 0 to 0.10, 0.10 to 0.20, 0.20 to 0.35 and 0.35 to 0.50 m.

Locations were also grouped based on similarity in soil genesis into soil profile classes as discussed in Section 2.5 (Table 2.4). Orthic Regosols (O.R) and Rego Dark Brown Chernozems (R.DBC) were grouped together, Calcareous Dark Brown Chernozems (CA.DBC) and Orthic Dark Brown Chernozems (O.DBC) each form a group. Gleyed profiles are split into a calcareous group containing Gleyed Rego Dark Brown Chernozemic (GLR.DBC) and Rego Humic Gleysolic (R.HG) profiles, and non-calcareous group containing Gleyed Dark Brown Chernozemic (GL.DBC), Orthic Humic Gleysolic (O.HG) and Humic Luvic Gleysolic (HU.LG) profiles. The long term moisture status of these soils is presumed to increase in the sequence O.R/ R.DBC < CA.DBC< O.DBC <Gleyed.

The behaviour of the GLEYED and GLEYED-REGO soil profile classes is readily seen to be different from the other profile classes. The gleyed soils show a greater amount of chloride in the surface increment and less in the second increment than the other soil groups (Figure 3.7).

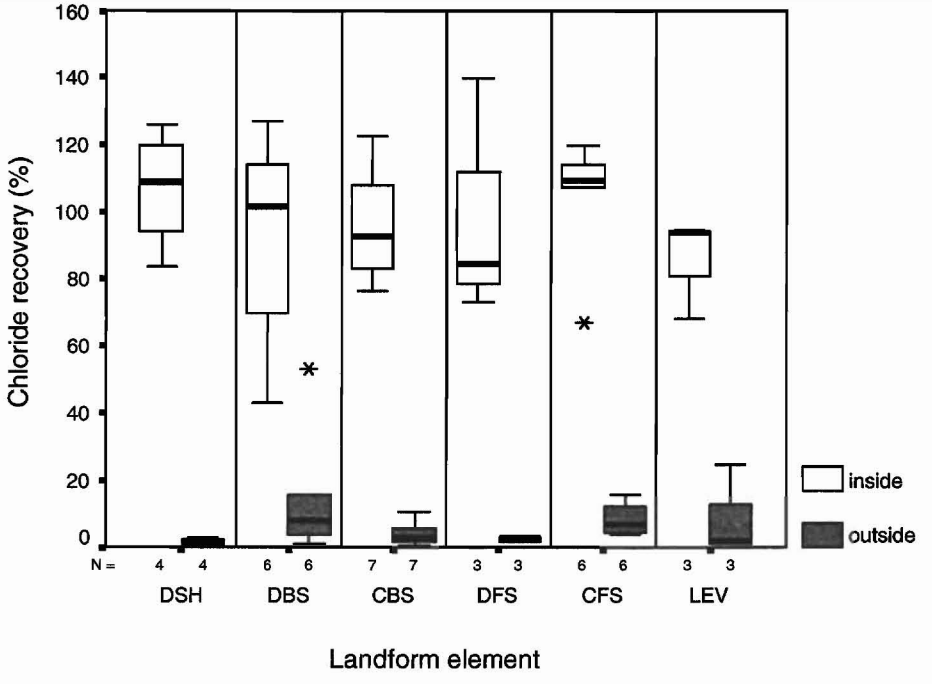

Figure 3.6 Fall 1997 chloride recovery (%) inside and outside the 1-m^2 plot area, 0- to 0.50-m depth

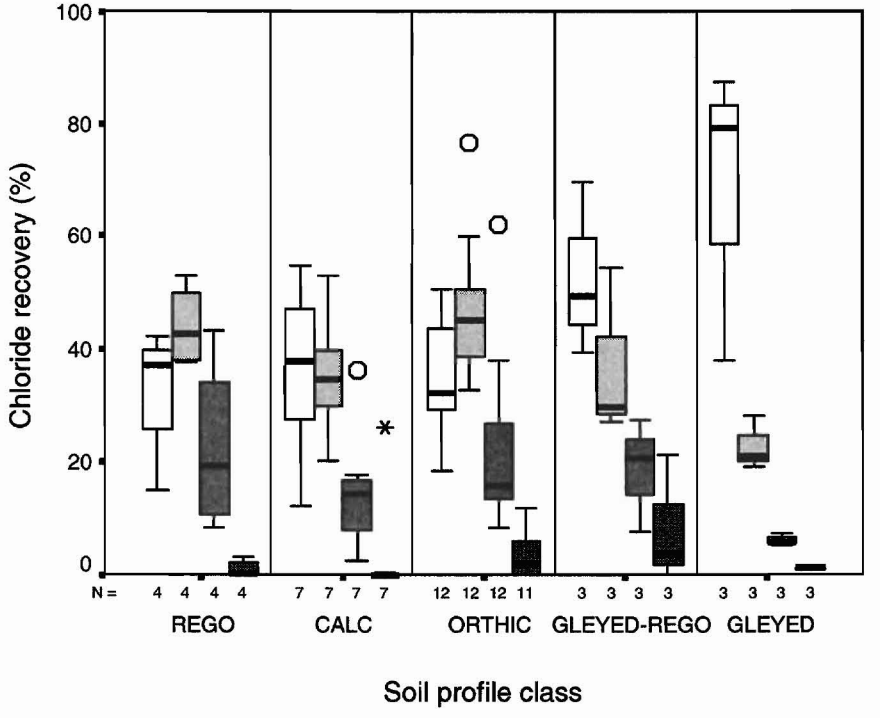

Figure 3.7 Fall 1997 chloride recovery (%) by depth increment and soil profile class. Within each soil profile class, depth increments from the left to the right are: 0 to 0.10, 0.10 to 0.20, 0.20 to 0.35 and 0.35 to 0.50 m.

3.4.3.1. Magnitude of Displacement

Chloride recovery can be used to scale the magnitude of the vector running from the initial centre of mass location through the new weighted centre of mass. However, because the percentage of total percent recovery exceeds 100% for many locations, it may not be appropriate to scale the vector magnitude using a percentage value. As an alternative, vector magnitude for each depth increment can be scaled using the sum of the chloride measured in each core, thus avoiding the problems associated with the interpolation process used to derive the percentage recovery. The observed patterns of redistribution are nearly identical to those suggested by the percentage recovery values in Figure 3.5. The sum of chloride recovered in each sampling increment (mg cm^{-2}) for each location is presented in Appendix A.

3.4.4. Chloride Centre of Mass

Movement of the chloride centre of mass was determined by calculating the coordinates for the weighted centre of mass following the Fall 1997 sampling. In Table 3.3 the coordinates to the weighted centre of mass are presented for the combined 0- to 0.50-m increment at each location. Also presented is the calculated displacement distance from the origin at the surface (i.e., the centre of the plot) to the new centre of mass at each depth, calculated using the x, y and z coordinates. The lateral displacement distance, calculated using only the x and y coordinate values, is also presented.

The data summarized in Figure 3.8 and Figure 3.9 show the shift in the centre of mass x, y, and z coordinates over the full 0.50-m sampling depth in the Fall of 1997, one growing season after the chloride was applied. Positive x values indicate a shift to the across slope to the right (assuming one is facing upslope), negative x values indicate a shift across slope to the left, positive y values indicate a shift upslope, negative y values indicate a shift downslope, and negative z values indicate movement into the profile.

Clearly, the displacement in the centre of mass has been dominated by vertical infiltration (Figure 3.8 and Figure 3.9). Displacement of the y coordinate is predominantly in the downslope direction although there is little distinction between

landform elements. The greatest individual downslope movement occurs at a single DBS location, followed by two of the Level locations (Table 3.3). In all but three cases vertical movement of the chloride exceeds that of lateral displacement (combined shift in the x and y coordinates) (Table 3.3).

Table 3.3 The Fall 1997 chloride centre of mass coordinates and displacement distance (cm) from the axes origin, 0- to 0.50-m combined increment.

			Centre of Mass Coordinates *			Displacement (cm)	
Landform Element	Location	Soil Subgroup	x	y	z	xy	xyz
DSH	6	O.DBC	-0.1	-1.1	-19.9	1.1	19.9
	26	O.R	-1.8	-5.3	-13.1	5.6	14.2
	43	O.R	-1.1	-4.7	-13.9	4.8	14.7
	52	CA.DBC	-0.3	1	-8.9	1	9
DBS	8	CA.DBC	-28.6	-23.5	-10.3	37	38.4
	14	O.DBC	0.1	-5.1	-12.9	5.1	13.9
	15	O.DBC	-0.7	-7.3	-17.6	7.3	19.1
	38	O.R	3.6	0.3	-19.6	3.6	19.9
	40	CA.DBC	0.6	-1.2	-14.7	1.3	14.8
	50	CA.DBC	1.1	1.5	-12.9	1.9	13
CBS	2	O.DBC	-3.5	-3.1	-17.6	4.7	18.2
	12	O.DBC	-2.5	-9.5	-14	9.8	17.1
	22	CA.DBC	-4.4	-4	-12.7	5.9	14
	24	O.DBC	5.8	-2.8	-13.2	6.4	14.6
	28	O.DBC	1.1	-5.1	-16.7	5.2	17.5
	30	O.DBC	1.8	-3.4	-12.3	3.8	12.9
	32	O.DBC	13.8	-7.2	-15	15.6	21.6
DFS	19	R.DBC	0.1	-7.2	-11.9	7.2	13.9
	35	R.HG	-2.1	-1.7	-11.2	2.7	11.5
	46	GLR.DBC	12.5	-9.7	-12.9	15.8	20.5
CFS	11	GL.DBC	-1.1	0	-9	1.1	9.1
	17	O.DBC	-1.6	-3	-12.6	3.4	13.1
	20	HU.LG	0.1	1.5	-8.4	1.5	8.5
	34	R.HG	4.5	-2.1	-17.9	5	18.6
	44	O.HG	-3.6	-5.8	-11.4	6.8	13.3
	49	O.DBC	3.9	5	-12.2	6.3	13.8
LEV	4	CA.DBC	-10.5	10.6	-24.4	14.9	28.6
	13	CA.DBC	-10.4	-16.3	-12.1	19.3	22.9
	37	O.DBC	0.8	-3.8	-14.1	3.9	14.6

*Negative x values indicate a shift across slope to the left (as one faces upslope), positive x values indicate movement to the right. Negative y values indicate movement downslope, positive y values indicate movement upslope. Negative z values indicate a movement into the soil.

Re-grouping the data by soil profile class, we see that the CALC class has a

greater range of displacement along the y-axis than do other soil profile classes (Figure 3.9). Generally the pattern of data for the coordinate values does not change between soil profile classes, however, the GLEYED-REGO class shows a trend towards greater movement in the x-dimension (across slope) than do the other soil profile classes.

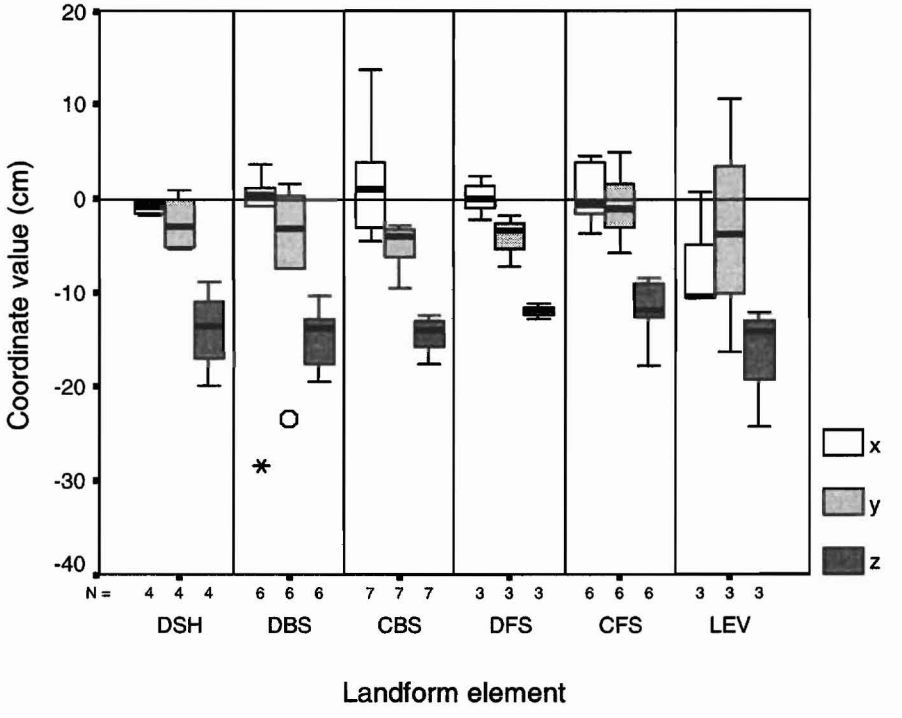

Figure 3.8 The Fall 1997 shift in the x, y and z coordinates for the chloride weighted centre of mass over the 0- to 0.50-m sampling increment, with data grouped by landform element. Negative x values indicate a shift across slope to the left (as one faces upslope), positive x values indicate movement to the right. Negative y values indicate movement downslope, positive y values indicate movement upslope. Negative z values indicate a movement into the soil.

The lateral displacement to the centre of mass in each depth can be explored by calculating the displacement distance using only the x and y coordinate values (Figure 3.10). There is little difference between sampling depths both within and between landform elements.

Large lateral displacement distances within the fourth sampling increment (Figure 3.10) are due to localized breakthrough of chloride in only a few of the sampling cores at any one location. For all locations, increments from 0 to 0.10 m, 0.10 to 0.20 m

and 0.20 to 0.35 m have increased chloride occurring in an average 66, 74 and 63% of their cores respectively. In the 0.35 to 0.50 m increment, only 20% of the cores contain chloride above the background level. The number of cores showing chloride above the background level at each location is summarized in Table 3.4

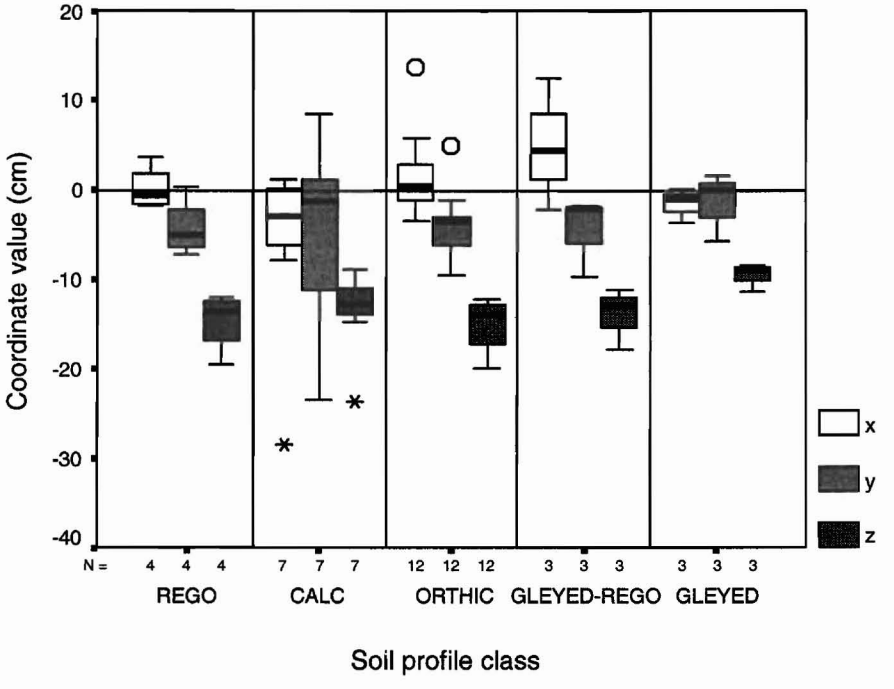

Figure 3.9 The Fall 1997 shift in the x, y and z coordinates for the chloride weighted centre of mass over the 0 to 50 cm sampling increment, with data grouped by soil profile class.

3.4.5. Summary

Calculated chloride recovery was very high, with only three locations having < 70% recovery. Recovery > 100% is believed to be largely due to the inability of the interpolation process to properly reflect the spatial influence of localized high chloride concentrations.

Displacement of the chloride centre of mass over the 0- to 0.50-m increment shows little difference between landforms or soil profiles. There is little difference between landforms or soil profiles when the data is split by individual depth increments. Within landforms or soil profile groups, displacement is dominated by movement into

the profile as opposed to lateral movement.

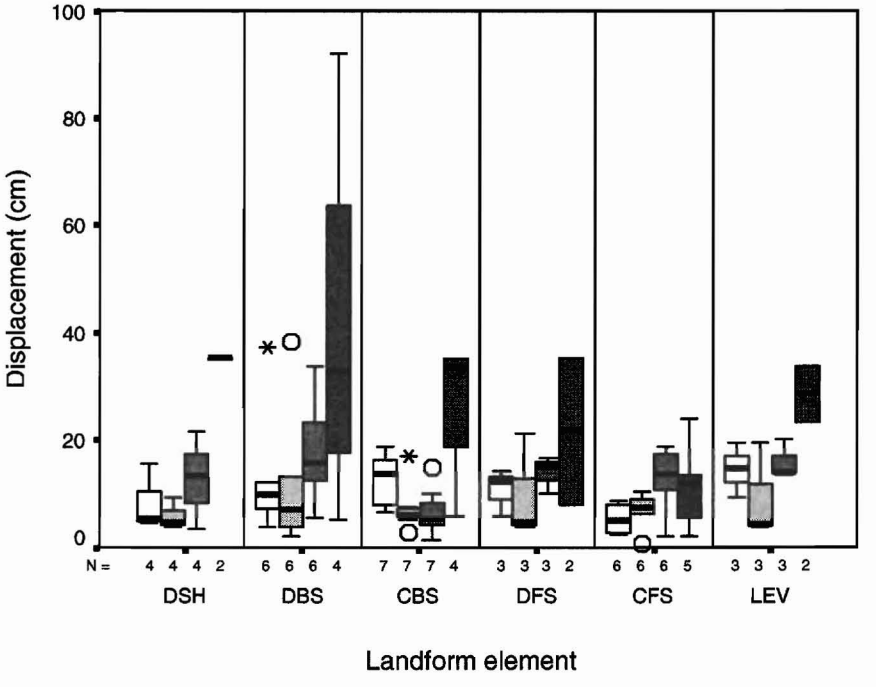

Figure 3.10 The Fall 1997 lateral displacement of the chloride centre of mass in each depth increment. Distance is calculated using the x and y coordinates only. Within each category, the increments from left to right are: 0 to 0.10, 0.10 to 0.20, 0.20 to 0.35 and 0.35 to 0.50 m.

Lateral displacement (displacement in the x and y axis) shows little difference between landform elements. There is a weak trend of increasing lateral displacement with depth. Large displacement distances in the fourth sampling depth are probably the result of isolated breakthrough of chloride heavily weighting the placement of the new centre of mass.

In summary, after one growing season, in which the field was fallow and precipitation was slightly above normal, there are few differences in the redistribution of chloride between landform elements. Only the gleyed soil profiles, which dominate divergent and convergent footslope positions, show a different pattern of chloride redistribution than is seen for other soil types.

Table 3.4 The number of cores at each depth with chloride above background levels, Fall 1997.

Landform Element	Location	Soil Subgroup	Number of Cores with Chloride				
			Total	0-10 cm	10-20 cm	20-35 cm	35-50 cm
DSH	6	O.DBC	9	4	5	4	1
	26	O.R	9	4	5	4	0
	43	O.R	9	6	6	4	1
	52	CA.DBC	9	6	6	3	0
DBS	8	CA.DBC	9	5	8	8	1
	14	O.DBC	9	4	6	4	0
	15	O.DBC	9	7	7	7	5
	38	O.R	9	5	7	7	2
	40	CA.DBC	9	6	5	6	1
	50	CA.DBC	9	7	6	5	1
CBS	2	O.DBC	9	4	5	6	2
	12	O.DBC	9	5	6	6	2
	22	CA.DBC	9	5	5	5	0
	24	O.DBC	9	6	6	6	0
	28	O.DBC	9	5	5	6	1
	30	O.DBC	9	8	8	5	0
	32	O.DBC	9	8	8	5	1
DFS	19	R.DBC	9	6	6	6	0
	35	R.HG	9	7	9	7	1
	46	GLR.DBC	12	6	8	6	3
CFS	11	GL.DBC	9	7	7	5	4
	17	O.DBC	9	7	8	7	1
	20	HU.LG	9	9	9	7	4
	34	R.HG	9	8	8	8	8
	44	O.HG	9	7	7	6	3
	49	O.DBC	9	6	9	9	6
LEV	4	CA.DBC	10	5	7	5	2
	13	CA.DBC	11	6	8	4	0
	37	O.DBC	9	6	6	6	3

3.5. Spring 1998 Results and Discussion

3.5.1. Introduction and Sampling Design

The Spring 1998 sampling was intended to identify spatial variations in moisture redistribution that were associated with the melting of the snow pack. The rapid release of the relatively large amount of moisture held in the snow (approximately 30% of the annual precipitation, de Jong and Kachanoski, 1987) provides an increased potential for

localized variation in moisture redistribution. Spatial variation in moisture redistribution associated with the spring melt is believed to be largely due to i) the enhanced redistribution of surface flows arising from the saturation of the soil surface and development of infiltration excess overland flow, ii) to the top-down thawing of the soil surface which, when accompanied by saturation, may enhance the potential for saturated lateral subsurface flow over top of the frozen soil (Miller, 1983), and iii) to the redistribution of the snow pack during the winter months. Landscape form will direct surface and near surface flows into convergent positions in the landscape. At these positions the accumulating water may temporarily saturate the profile, which can lead to further variations in subsurface flow patterns (Richardson et al., 1992; Reuter et al., 1998). Ultimately the greater flow volume collected in the convergent positions may infiltrate deeper into the profile as the soil continues to thaw.

A snow survey was conducted at the site on February 5, 1998. Snow depth and density were collected at all 52 of the original grid points; during the survey little to no snow was observed on exposed knolls. The calculated snow water equivalent (SWE) values (mm) are summarized by landform element in Figure 3.11. Mean SWE across all sampling positions was 24.4 mm, with average snow depth of 14.4 cm.

The data confirm that the least amount of snow was observed on the divergent shoulders. In general, divergent and level positions have a thinner snow pack than other landscape positions. The greatest amount of snow is found in the convergent footslope positions, with lesser amounts in other convergent positions. Note the large variability in the data associated with convergent footslopes and convergent backslopes (Figure 3.11).

An automated tipping bucket rain recorder was installed in the field April 8, 1998. Only 2 mm of rain was recorded from April 8 to April 21 and an additional 23 mm of rainfall was recorded between April 21 and June 24.

Spring sampling was conducted at fifteen micro-plot locations on April 21-24, 1998. The site had not been tilled since the previous June. Four other micro-plots located in a topographic low were under water or fully saturated through April and were

subsequently sampled June 24 and 25, 1998. These four locations were sampled after the cooperating farmer had seeded the field to canola using a 15.2-m wide air seeder equipped with 0.30-m sweeps on 0.22-m centres. Seeding depth was approximately 0.035 m and tractor speed was reported as 9.6 km h^{-1}. Seeding direction was from north to south.

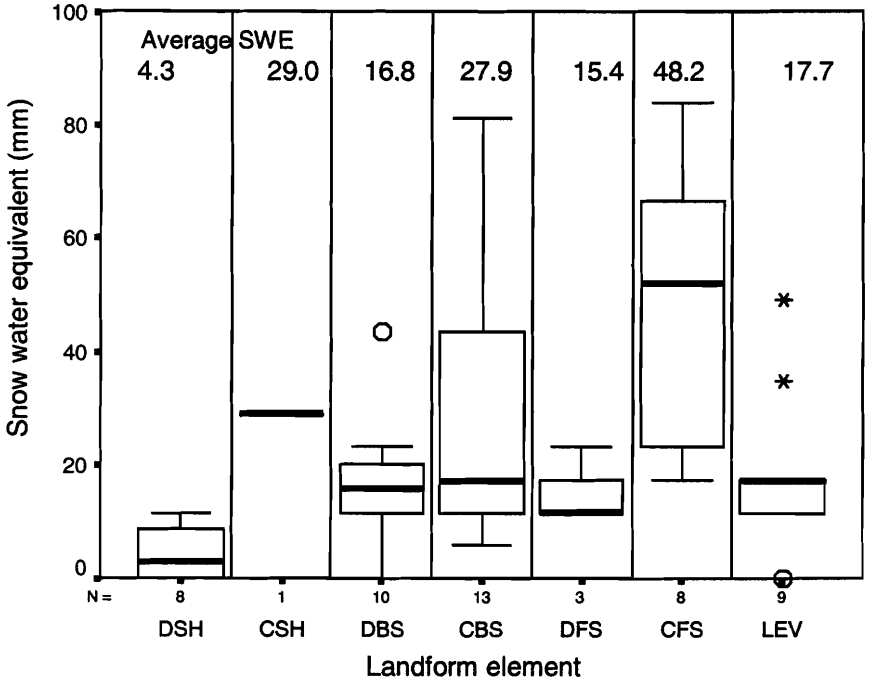

Figure 3.11 The snow water equivalents (mm) for February 5, 1998 organized by landform element. Average values for snow water equivalents (SWE) are listed above the boxplot in each category.

3.5.2. Chloride Recovery

Fifteen locations were sampled in Spring 1998, which gave only a few samples within each landform element or soil subgroup. However, the patterns observed suggested much greater differences among the landform elements than were observed in the Fall 1997 data set.

Mean chloride recovery to 0.50-m depth (Table 3.5) is still high (78%), and the majority of landform elements have lost approximately 10% of the chloride they held in

the previous fall. The greatest departure from the Fall 1997 results occurred in the divergent and convergent footslope elements which lost 60% or more of the chloride that they held in the fall of 1997.

Table 3.5 Summary statistics for the Spring 1998 chloride recovery (%), data grouped by landform element.

Landform Element		Chloride Recovery (%) Sampling Increments (cm)				
		0-10	10-20	20-35	35-50	0-50
DSH	Mean	68.5	30.9	17.5	1.6	118.5
	Median	68.5	30.9	17.5	1.6	118.5
	Std. Deviation	48.1	15.0	12.4	2.1	18.5
	N	2	2	2	2	2
DBS	Mean	72.9	24.6	8.1	0.4	106.0
	Median	72.9	24.6	8.1	0.4	106.0
	Std. Deviation	3.0	3.7	5.5	0.6	0.6
	N	2	2	2	2	2
CBS	Mean	29.0	24.4	24.7	3.9	82.1
	Median	31.8	27.2	26.1	2.6	86.3
	Std. Deviation	13.4	4.8	14.2	5.1	18.2
	N	5.0	5.0	5.0	5.0	5.0
DFS	Mean	3.7	4.4	4.4	1.3	13.8
	Median	3.7	4.4	4.4	1.3	13.8
	Std. Deviation	.	.	.	.	.
	N	1	1	1	1	1
CFS	Mean	24.1	13.5	5.2	0.4	43.2
	Median	7.1	8.3	4.6	0.2	15.9
	Std. Deviation	33.4	9.9	5.2	0.6	47.5
	N	3	3	3	3	3
LEV	Mean	37.1	33.9	17.9	0.9	89.8
	Median	37.1	33.9	17.9	0.9	89.8
	Std. Deviation	12.7	11.9	7.0	0.7	8.6
	N	2	2	2	2	2
Total	Mean	38.5	23.0	15.4	1.9	78.8
	Median	34.5	24.9	12.0	0.8	90.6
	Std. Deviation	29.1	10.9	12.2	3.2	37.0
	N	15	15	15	15	15

Figure 3.12 suggests that the landform elements have three different patterns of recovery with depth:

1. Divergent shoulder and DBS landform elements behave similarly, having a high recovery in the surface and decreasing with depth.

2. Convergent backslope and level landform elements behave alike. They lack the high recovery of the DSH and DBS locations. However

there is little difference between the DSH, DBS, CBS and LEV landform elements for recovery within the second increment or the third increments.

3. Divergent footslopes and convergent footslopes have much lower amounts of chloride in the upper three increments than all other landform elements. Convergent footslopes have a large variability within the surface increment.

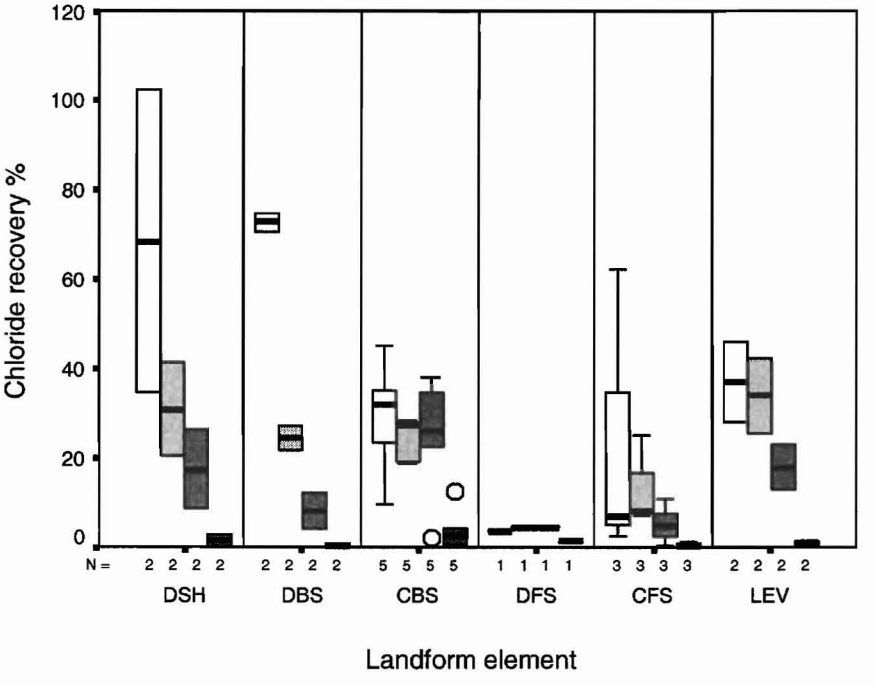

Figure 3.12 The Spring 1998 chloride recovery (%) by depth increment and landform element. From the left to the right within each landform element category, sampling depths are: 0 to 0.10, 0.10 to 0.20, 0.20 to 0.35 and 0.35 to 0.5 m.

The DFS and CFS landform elements are distinct from the others and show the lowest chloride recovery in all depths. In the Spring 1998 data set, recovery values in the surface increment of the DFS and CFS locations, with the exception of Location 49 (Figure 2.1), are an order of magnitude less than found at other landforms. Chloride recovery in the 0.10- to 0.20-m increments is also lower in DFS and CFS landform elements than among the other landform elements. Three of the DFS and CFS landform elements are at lower elevations near the tillage pond in the centre of the study area

(Locations 11, 17, and 46) in Figure 2.1. The fourth location (#49) is much further upslope. When locations are classified into the more general landform complex, all the DFS and CFS plots at the lower positions are footslope complexes whereas Location 49 is classified as a backslope complex. Attempts to distinguish Location 49 from the other footslope elements using several topography based indices - contributing area, dispersal area, contributing area/slope gradient (Burt and Butcher, 1985), contributing area x plan curvature ÷slope gradient (Burt and Butcher, 1985), and the log of (contributing area/tangent of the slope gradient)(Moore et al., 1993) - were unsuccessful.

As noted in Section 3.5.1, wet field conditions prevented CFS Locations 11 and 17, and DFS Location 46 from being sampled at the same date as the other locations, and these locations were tilled once before they could be sampled. The loss of chloride from the second and third increments as well as from the surface increment in these three locations (Table 3.6) shows that the chloride has been leached out of the 0.5 m sampling depth rather than removed from the surface by tillage.

Table 3.6 Spring 1998 chloride recovery (%) by sampling increment for each location.

			Chloride Recovery (%)				
			Sampling Increments (cm)				
Landform Element	Location	Soil Subgroup	0-10	10-20	20-35	35-50	0-50
DSH	26	O.R	34.5	41.5	26.2	3.1	105.4
	43	CA.DBC	102.5	20.3	8.7	0.1	131.6
DBS	14	O.R	70.8	21.9	12.0	0.8	105.5
	50	O.R	75.0	27.2	4.2	0.0	106.4
CBS	2	O.DBC	23.4	28.4	34.7	4.0	90.6
	12	O.DBC	31.8	19.0	1.9	0.0	52.7
	22	O.DBC	45.2	27.2	26.1	2.6	101.1
	24	O.DBC	35.1	28.2	22.6	0.4	86.3
	30	O.DBC	9.5	19.3	38.2	12.6	79.6
DFS	46	CA.DBC	3.7	4.4	4.4	1.3	13.8
CFS	11	HU.LG	2.6	8.3	4.6	0.2	15.7
	17	CA.DBC	7.1	7.3	0.3	1.1	15.9
	49	O.DBC	62.5	24.9	10.7	0.0	98.1
LEV	4	CA.DBC	46.1	25.5	22.8	1.4	95.9
	37	O.DBC	28.1	42.3	12.9	0.4	83.7

In the Spring 1998 sampling time chloride redistribution appears to be dominated by vertical displacement. The majority of the recovered chloride is found directly below the plots with comparatively little chloride being recovered outside the plot frame to suggest lateral flow (Figure 3.13). For those DFS and CFS locations that have lost >80% of their applied chloride, the chloride has moved either below 0.50 m or laterally beyond the outer ring of sampling cores. Among the LEV, CFS and DFS landform elements there has been some increase in chloride recovery outside the 1.0 m x 1.0 m plot frame since the Fall 1997 sampling, suggesting an increase in lateral flow at these positions.

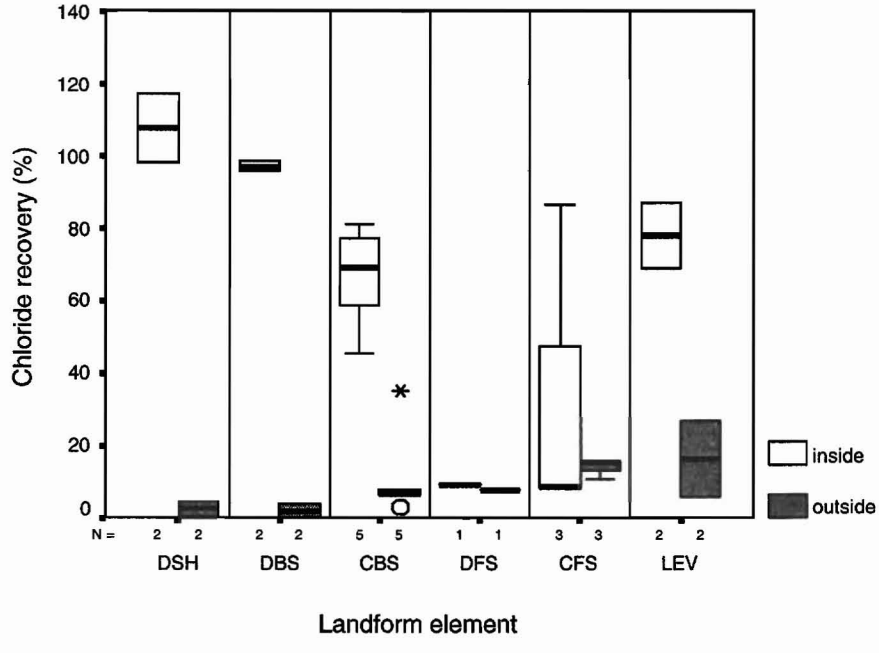

Figure 3.13 Spring 1998 chloride recovery (%) inside and outside the 1-m^2 plot area, 0- to 0.50-m depth.

3.5.2.1. Magnitude of Displacement

Again, the sum of the chloride (mg cm^{-2}) recovered from all cores at each depth was used to calculate an alternative measure of the magnitude of displacement to the percent recovery. As with the Fall 1997 results, the observed patterns of redistribution as determined by the sum of chloride values were nearly identical to those suggested by

the percentage recovery values. The sum of chloride values for the Spring 1998 data set are given in Appendix B.

3.5.3. Chloride Centre of Mass

Tables 3.7, 3.8, and 3.9 show the x, y and z coordinate values respectively for the weighted centre of mass. These values show the net movement away from the centre of the 1-m^2 plot at the soil surface. Data has been grouped by landform element and sampling depth. Note in Table 3.8, the y coordinate values for Locations 11, 17 and 46 show movement downslope (mean y coordinate value –37.3) that is an order of magnitude greater than that observed for the other locations (mean y coordinate value – 3.6).

The total displacement of the centre of mass for the combined 0- to 0.5-m increment is presented in Table 3.10; these data are summarized for each coordinate axis by landform element in Figure 3.14 and then by soil type in Figure 3.15. The total displacement distance for the footslope Locations 11, 17 and 46 is significantly greater

Table 3.7 The x coordinate value* to the weighted centre of mass, Spring 1998.

			X coordinate value (cm)			
			Sampling Increments (cm)			
Landform Element	Location	Soil Subgroup	0-10	10-20	20-35	35-50
DSH	26	O.R	0.3	-8.8	-5.3	-0.6
	43	CA.DBC	-7.3	0.7	-13.2	70.0
DBS	14	O.R	-7.1	5.6	10.1	18.8
	50	O.R	0.0	-6.3	4.2	.
CBS	2	O.DBC	-12.6	-7.6	0.1	3.3
	12	O.DBC	7.2	4.7	-5.5	.
	22	O.DBC	6.6	7.4	-4.3	-4.2
	24	O.DBC	15.6	0.9	-8.9	-25.0
	30	O.DBC	-3.1	-4.5	-0.5	-2.7
DFS	46	CA.DBC	26.2	44.7	36.7	54.4
CFS	11	HU.LG	-12.1	-18.1	-21.7	-34.0
	17	CA.DBC	-3.5	14.6	29.3	-25.0
	49	O.DBC	-6.0	-5.7	5.3	.
LEV	4	CA.DBC	0.8	9.6	9.5	25.0
	37	O.DBC	9.6	2.4	6.8	55.0

* Movement across the dominant slope. Positive values indicate movement to the right, negative values indicate movement to the left as you face upslope. Missing values indicate no chloride recovered.

Table 3.8 The y coordinate value* for the weighted centre of mass, Spring 1998.

Landform Element	Location	Soil Subgroup	Y coordinate value (cm) ---------- Sampling Increments (cm) ---------- 0-10	10-20	20-35	35-50
DSH	26	O.R	12.1	2.6	-5.1	-15.4
	43	CA.DBC	-7.2	4.7	6.8	-28.0
DBS	14	O.R	0.2	0.1	6.6	18.8
	50	O.R	2.0	7.7	5.2	.
CBS	2	O.DBC	0.0	-4.4	-4.4	-11.3
	12	O.DBC	-9.5	2.9	-24.1	.
	22	O.DBC	7.5	5.0	-11.5	-24.3
	24	O.DBC	-2.9	-3.2	-4.3	-9.2
	30	O.DBC	-9.2	2.7	-10.3	-11.8
DFS	46	CA.DBC	-23.4	-31.8	-39.0	-54.4
CFS	11	HU.LG	-32.5	-41.2	-52.6	-62.4
	17	CA.DBC	-29.4	-39.0	-10.7	-25.0
	49	O.DBC	-0.1	-3.9	5.0	.
LEV	4	CA.DBC	-12.1	-5.2	-3.0	-25.0
	37	O.DBC	-15.4	-10.3	-4.3	-55.0

*Movement along the dominant slope. Negative y values indicate movement downslope. Positive y values indicate movement upslope. Missing values indicate that no chloride was recovered at that increment depth.

Table 3.9 The z coordinate value* to the centre of mass for individual sampling depths, Spring 1998.

Landform Element	Location	Soil Subgroup	Z coordinate value (cm) ---------- Sampling Increments (cm) ---------- 0-10	10-20	20-35	35-50
DSH	26	O.R	-5.0	-15.0	-27.5	-42.5
	43	CA.DBC	-5.0	-15.0	-27.5	-42.5
DBS	14	O.R	-5.0	-15.0	-27.5	-42.5
	50	O.R	-5.0	-15.0	-27.5	.
CBS	2	O.DBC	-5.0	-15.0	-27.5	-42.5
	12	O.DBC	-5.0	-15.0	-27.5	.
	22	O.DBC	-5.0	-15.0	-27.5	-42.5
	24	O.DBC	-5.0	-15.0	-27.5	-42.5
	30	O.DBC	-5.0	-15.0	-27.5	-42.5
DFS	46	CA.DBC	-5.0	-15.0	-27.5	-42.5
CFS	11	HU.LG	-5.0	-15.0	-27.5	-42.5
	17	CA.DBC	-5.0	-15.0	-27.5	-42.5
	49	O.DBC	-5.0	-15.0	-27.5	.
LEV	4	CA.DBC	-5.0	-15.0	-27.5	-42.5
	37	O.DBC	-5.0	-15.0	-27.5	-42.5

* Negative values indicate vertical movement into the soil. Missing values indicate that no chloride was recovered.

than that for all other landform elements and locations (Table 3.10). Note the range of movement in the Calcareous Dark Brown Chernozemic (CA.DBC) soils (Figure 3.15). These soils occur across a range of landform elements and the data suggests that, for these soils at least, the chloride redistribution can be linked more to landscape position than to soil type.

Table 3.10 Spring 1998 displacement of the chloride centre of mass in the 0- to 0.50-m increment.

			center of mass coordinates			displacement distances (cm)	
landform element	location	soil subgroup	x	y	z	xy	xyz
DSH	26	O.R	-4.7	3.4	-15.5	5.8	16.6
	43	CA.DBC	-6.2	-4.4	-8.2	7.6	11.2
DBS	14	O.R	-2.4	1.0	-9.8	2.6	10.1
	50	O.R	2.6	-0.2	-8.5	2.6	8.9
CBS	2	O.DBC	-5.4	-3.5	-18.4	6.5	19.5
	12	O.DBC	5.9	-5.6	-9.3	8.1	12.3
	22	O.DBC	2.6	-0.8	-16.6	2.8	16.8
	24	O.DBC	4.3	-3.4	-14.2	5.5	15.3
	30	O.DBC	-2.1	-7.3	-24.2	7.6	25.4
DFS	46	CA.DBC	39.3	-34.8	-19.7	52.5	56.0
CFS	11	HU.LG	-18.4	-43.5	-17.4	47.2	50.3
	17	CA.DBC	5.2	-33.7	-11.8	34.1	36.1
	49	O.DBC	-4.7	-0.6	-10.1	4.8	11.2
LEV	4	CA.DBC	5.5	-8.3	-13.5	9.9	16.7
	37	O.DBC	5.9	-11.5	-13.5	12.9	18.7

3.5.4. Summary

The data suggest that during the spring melt period the divergent and convergent footslope landform elements undergo a different pattern of water flow than the other landform positions. Footslopes have lost more chloride, and have a greater displacement of the mean centre of mass than the other landform elements. Other landform elements show little change from the Fall 1997 sampling.

Within the footslope category three of the sampled locations occur within the large topographic low that is subject to periods of saturation (as observed in early April, 1998 and as evidenced by a dominance of gleyed and eluviated profiles). These locations show the chloride loss and displacement noted above. A fourth footslope

locations show the chloride loss and displacement noted above. A fourth footslope location (#49), is found considerably upslope from the topographic low, and does not exhibit the same pattern of chloride redistribution.

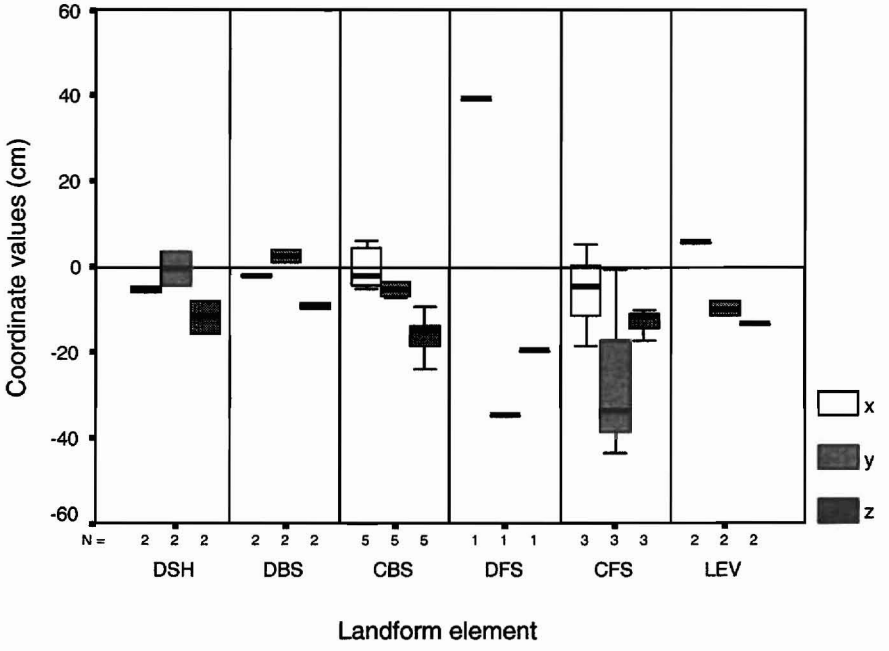

Figure 3.14 The Spring 1998 shift in the x, y, and z coordinates for the weighted centre of the chloride mass for the 0- to 0.50-m increment, with data organized by landform element. X values indicate movement across the slope, y values indicate movement either upslope (+) or downslope (-), z values indicate movement into the soil.

Greater amounts of water moving through the profile in the lower footslopes appears to have removed the majority of the chloride. While some of the water flow can be attributed to the direct influence of the snow pack, it is apparent that this is not the only contributing factor. Snow water equivalents were 43.4, 69.5, 23.2, and 17.4 mm for Locations 11, 17, 46, and 49 respectively. Clearly the local snow pack at Location 46 is not significantly different from most locations (Figure 3.11), thus additional moisture inputs to this location must have come as run-on and lateral flow. The mechanism by which moisture flow at these sites is increased appears to be largely related to their position in the landscape and their topographic form. Convergent sites (especially footslopes) capture more snow, and it is known that water flows will collect at convergent points in the landscape.

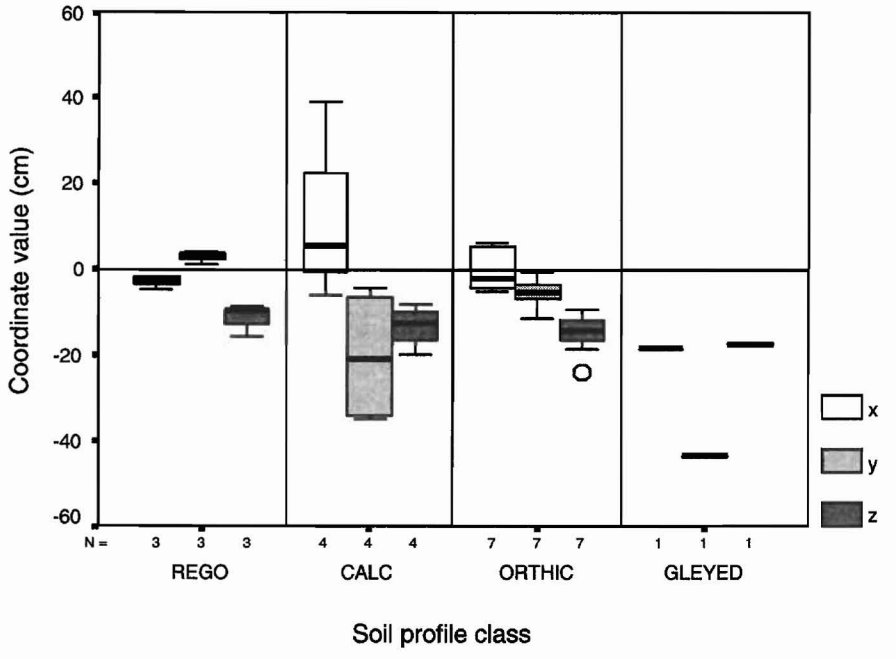

Figure 3.15 Spring 1998 shift in the x, y, and z coordinates for the weighted centre of the chloride mass for the 0- to 0.50-cm increment, with data organized by soil profile class. X values indicate movement across the slope, y values indicate movement either upslope (+) or downslope (-), z values indicate movement into the soil.

3.6. Fall 1998 Results and Discussion

3.6.1. Introduction

The intent of the Fall 1998 chloride sampling was to assess spatial variation in redistribution under cropping conditions common to the study area. Mechanisms of chloride redistribution would include both tillage and soil moisture flows. Since the last sampling (Spring 1998) the site had been tilled twice, once when seeded to canola, and again in September 1998 after the crop was harvested. Approximately 150 mm of rain was recorded from April 21 to Sept 29, 1998, with 23 mm from April 21 to June 24.

Seeding was conducted using a farm scale air-seeder equipped with 0.30-m wide sweeps. Tillage direction was from the north to the south. Seeding depth was approximately 0.035 m and tractor speed was reported as 9.6 km h^{-1}. In the fall of 1998, just prior to sampling, the site was again tilled with a cultivator having 0.40-m wide shovels. Tillage depth was approximately 0.10 m and tillage speed was estimated at

10.5 km h^{-1}. Tillage direction in this case was from south to north.

During the period September 29 to October 9, 1998 twenty-nine micro-plot locations were sampled to assess chloride redistribution during the past growing season. The sampling plan was the same as that used in the spring sampling period (Figure 3.3).

3.6.2. Chloride Recovery

The mean recovery in all landform elements is lower than the mean recovery from the earlier sampling periods. The overall mean recovery in the Fall 1998 samples is 45%, with a range from 7.5 to 93.9 % (Table 3.12). At four locations, sampling was conducted in the 0.50- to 0.65-m increment; chloride was recovered from this depth at only one of these locations. The results for the 0.50- to 0.65-m increment are presented in Table 3.11 and Table 3.12, but are not included in subsequent tables or images.

The percentage of recovered chloride (in the 0- to 0.50-m increment) is greatest in what is considered the driest portions of the landscape and decreases into the wetter parts of the landscape (Table 3.12, Figure 3.16). The greatest total recovery was in the DSH and DBS landform elements, which show sharply elevated chloride values in the 0.10- to 0.20-m and 0.20- to 0.35-m sampling increments.

It is apparent that the majority of the chloride has been removed from the surface increment in all cases (Table 3.11and Figure 3.17). In addition, little chloride was recovered from the 0.35- to 0.50-m sampling depth in all landform elements, with the exception of the CBS elements. The CBS elements had a median percentage recovery of approximately 20% in the 0.35- to 0.50-m sampling depth, more than double the recovery obtained at this depth for other landform elements. The DFS, CFS and LEV landform elements generally show low (<10%) recovery at all depths. However, the DFS elements show a trend towards greater chloride recovery in the 0.10- to 0.20-m increment and the LEV elements a trend towards greater recovery in the 0.20- to 0.35-m increment (Table 3.12 and Figure 3.17).

In this sampling time there is a notable increase in the amount of chloride recovered outside of the frame of the 1.0 x 1.0 m plot among all landform elements

(Figure 3.18) than at earlier times (Figures 3.6 and 3.13). This suggests that there has been an increase in displacement by lateral flows.

Table 3.11 Fall 1998 chloride recovery (%) by sampling increment for each location.

			chloride recovery %					
			sampling increments (cm)					
landform element	location	soil subgroup	0-10	10-20	20-35	35-50	50-65*	0-65
DSH	6	R.DBC	6.5	41.5	42.9	3.1	.	93.9
	26	O.R	1.6	24.3	26.9	1.8	.	54.6
	43	R.DBC	8.5	45.9	8.2	0.0	.	62.7
	52	O.R	9.2	34.8	28.3	14.7	.	87.0
DBS	8	CA.DBC	6.3	43.8	18.0	0.5	.	68.6
	14	O.R	2.1	30.0	22.9	0.0	.	55.0
	15	O.R	3.4	17.8	23.0	3.0	.	47.2
	38	O.DBC	2.1	12.8	30.4	19.9	.	65.2
	40	O.R	7.6	35.6	16.7	0.3	.	60.1
	50	O.R	1.5	23.4	28.3	1.8	.	55.1
CBS	2	O.DBC	1.3	10.9	23.0	25.5	.	60.7
	12	CA.DBC	0.7	13.4	5.9	0.0	.	20.0
	22	O.DBC	1.0	8.1	20.3	20.8	.	50.2
	24	O.DBC	2.4	16.1	28.0	23.0	.	69.5
	28	O.DBC	1.4	10.9	25.2	12.0	.	49.5
	30	O.DBC	7.0	16.7	21.4	22.1	11.7	78.9
	32	E.DBC	1.8	10.0	11.9	0.4	.	24.1
DFS	19	O.R	9.6	19.4	9.4	0.4	.	38.8
	35	O.HG	7.4	20.3	13.0	0.2	.	40.8
	46	CA.DBC	2.6	2.6	3.2	0.5	0.0	8.9
CFS	11	HU.LG	3.4	7.5	7.4	0.4	.	18.6
	17	O.DBC	6.3	3.8	0.8	0.0	.	10.9
	20	O.HG	6.0	8.4	4.9	2.2	.	21.5
	34	O.HG	9.9	10.5	1.5	0.3	0.0	22.2
	44	HU.LG	1.3	4.4	4.5	0.9	.	11.0
	49	CA.DBC	0.5	9.2	22.9	10.3	.	42.9
LEV	4	CA.DBC	0.1	8.5	29.5	5.4	.	43.5
	13	O.DBC	0.9	3.4	2.7	0.5	0.0	7.5
	37	E.DBC	3.7	13.9	18.6	7.8	.	44.0

*Only four micro-plots were sampled in the 0.50- to 0.65-m increment.

Table 3.12 Fall 1998 summary results, chloride recovery (%) by landform element.

landform element		chloride recovery % ----------sampling increment (cm) ----------					
		0-10	10-20	20-35	35-50	50-65	0-65
DSH	Mean	6.5	36.6	26.6	4.9	no sample	74.6
	Median	7.5	38.2	27.6	2.5		74.9
	Std. Deviation	3.4	9.4	14.2	6.7		18.9
	N	4	4	4	4		4
DBS	Mean	3.8	27.2	23.2	4.3	no sample	58.5
	Median	2.8	26.7	23.0	1.2		57.6
	Std. Deviation	2.5	11.5	5.4	7.7		7.8
	N	6	6	6	6		6
CBS	Mean	2.2	12.3	19.4	14.8	11.7	50.4
	Median	1.4	10.9	21.4	20.8	11.7	50.2
	Std. Deviation	2.2	3.2	7.8	10.8	.	22.0
	N	7	7	7	7	1	7
DFS	Mean	6.5	14.1	8.5	0.4	0.0	29.5
	Median	7.4	19.4	9.4	0.4	0.0	38.8
	Std. Deviation	3.6	10.0	5.0	0.2	.	17.9
	N	3	3	3	3	1	3
CFS	Mean	4.6	7.3	7.0	2.4	0.0	21.2
	Median	4.7	8.0	4.7	0.7	0.0	20.1
	Std. Deviation	3.5	2.7	8.2	4.0	.	11.7
	N	6	6	6	6	1	6
LEV	Mean	1.6	8.6	16.9	4.6	0.0	31.7
	Median	0.9	8.5	18.6	5.4	0.0	43.5
	Std. Deviation	1.9	5.3	13.5	3.7	.	20.9
	N	3	3	3	3	1	3
Total	Mean	4.0	17.5	17.2	6.1	2.9	45.3
	Median	2.6	13.4	18.6	1.8	0.0	47.2
	Std. Deviation	3.1	12.5	10.9	8.4	5.9	23.8
	N	29	29	29	29	4	29

When the chloride recovery data are organized by soil profile class (Figure 3.19), the major differences in redistribution reflect those seen with the data organized by landform element (Figure 3.17). Firstly, soils in the REGO soil profile class, dominated by O.R and R.DBC soil subgroups, tend to be found at divergent positions within the landscape. The elevated chloride recovery in the 0.10- to 0.20-m increment in the REGO class appears to correspond with the elevated levels of chloride found at DSH and DBS landform elements. Second, the CBS landform elements have elevated levels of chloride in the 0.35- to 0.50-m increment that correspond to those observed among soils in the ORTHIC profile class. Note that the CBS landform elements are dominated by the O.DBC subgroup, the sole soil subgroup within the ORTHIC soil profile class.

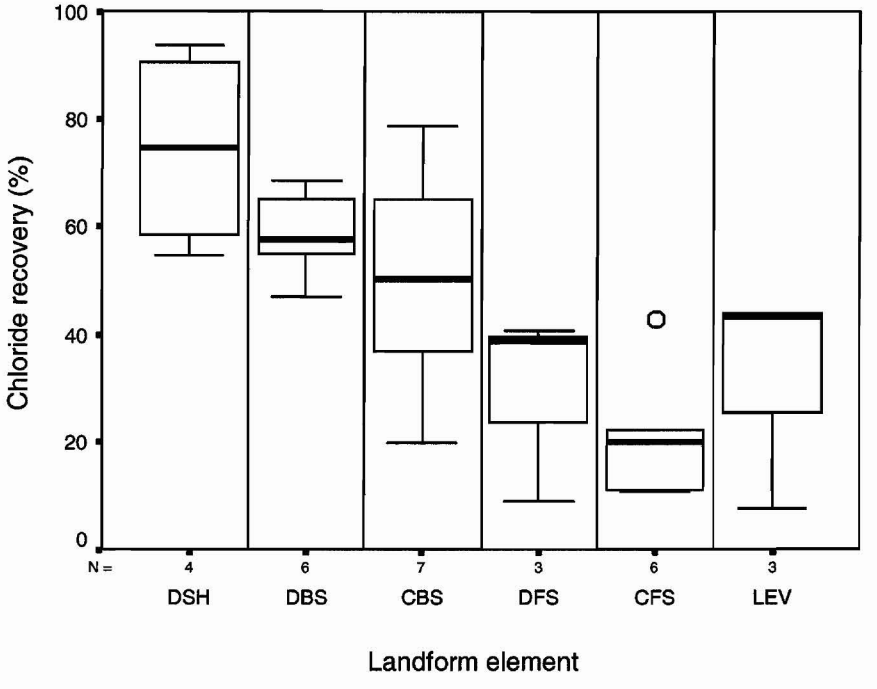

Figure 3.16 Fall 1998 total chloride recovered (%) in the 0- to 0.50-m sampling depth.

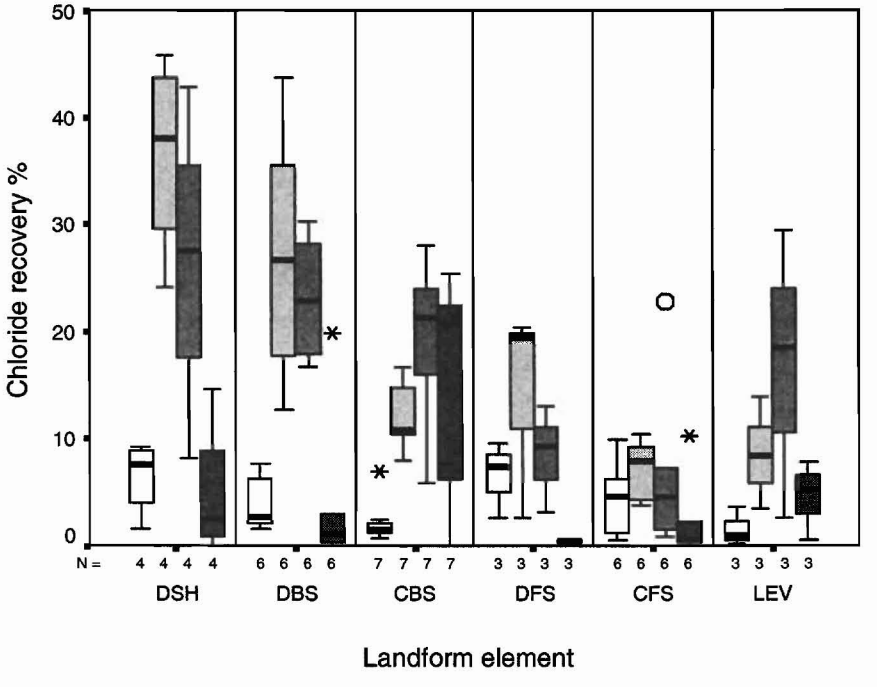

Figure 3.17 The Fall 1998 chloride recovery (%) by sampling increment and landform element. For each landform element category, the depth increments from left to right are: 0 to 0.10, 0.10 to 0.20, 0.20 to 0.35 and 0.35 to 0.50 m.

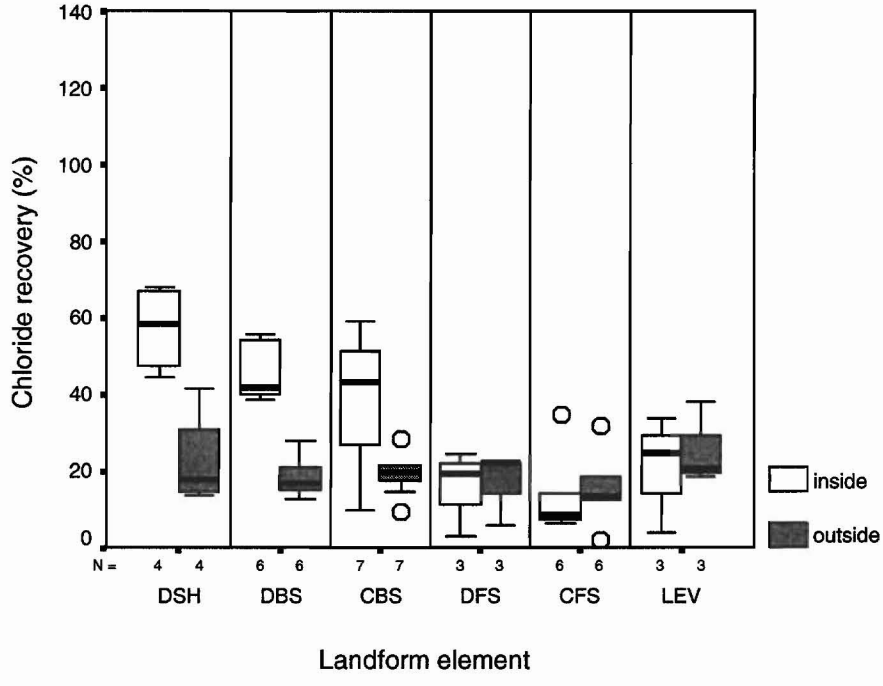

Figure 3.18 Fall 1998 chloride recovery (%) inside and outside the 1-m^2 plot area, 0- to 0.50-m depth.

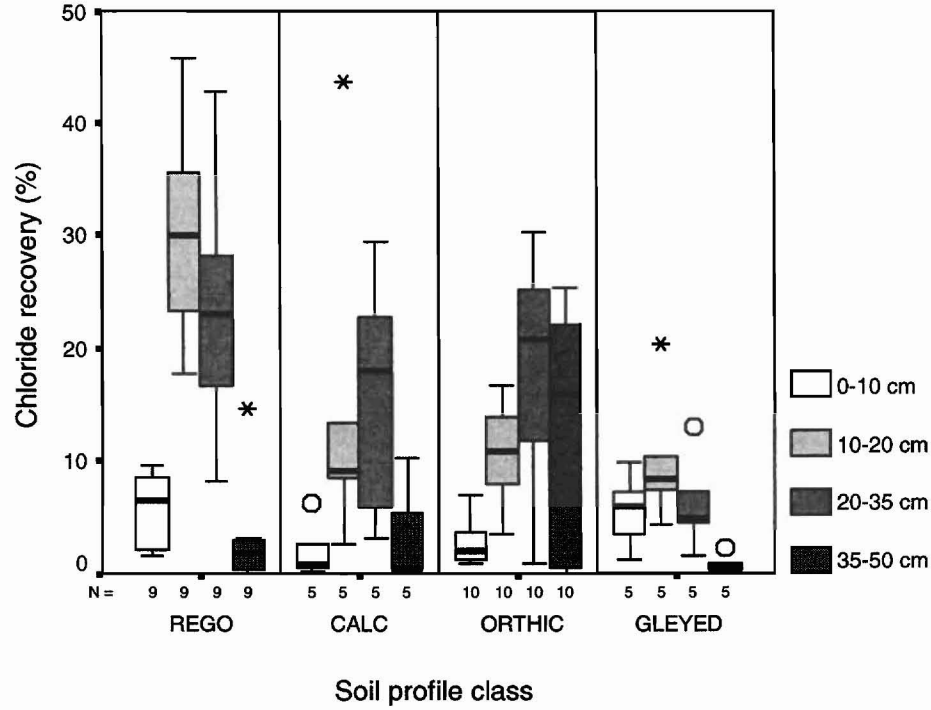

Figure 3.19 The Fall 1998 chloride recovery (%) by sampling depth and soil profile class.

Third, soils in the GLEYED profile category largely correspond to the CFS landform elements and have less than 10% recovery in any depth increment.

The pattern of chloride recovery with depth among soils within the CALC and ORTHIC profile classes is similar among the upper three sampling increments. The pattern differs in the 0.35- to 0.50-m increment. At this depth, the soils in the ORTHIC class show much greater median recovery than do the soils in the CALC class.

3.6.2.1. Magnitude of displacement

Again, the sum of the chloride recovered from all cores at each depth can be used as a measure of the magnitude of the chloride redistribution rather than the percent recovery. The sum of the chloride recovered from all the sampling cores at each micro-plot location provides the same pattern of recovery as seen for the percentage recovery data. The sums of chloride values for each location are supplied in Appendix C.

3.6.3. Chloride Centre of Mass

By the Fall of 1998 the net accumulated displacement of the chloride centre of mass over the 0- to 0.50-m sampling depth shows two major trends (Figure 3.20). (Displacement data for individual locations in the combined 0- to 0.50-m increment is listed in Appendix D). First, among DSH, DBS and CBS landform elements there is little variation in displacement within each landform element category. In contrast, displacement among DFS, CFS and LEV landform elements is highly variable. Among the DSH, DBS, and CBS landform elements the displacement appears to be dominated by vertical displacement along the z-axis (Figure 3.21). Among the DFS, CFS, and LEV landform elements there is an increase in the variability in lateral displacement along the y-axis and the x-axis that occasionally matches or exceeds the vertical movement. Second, it appears that landform elements can be grouped according to their median total displacement. Soils at DSH and DBS landform elements show similar behaviour and have the least net displacement of the chloride centre of mass. CBS, DFS and CFS landform elements show broadly similar behaviour and have a greater displacement. Level landform elements have the greatest displacement and they make up a third group.

The median value for vertical displacement was graphed against the calculated

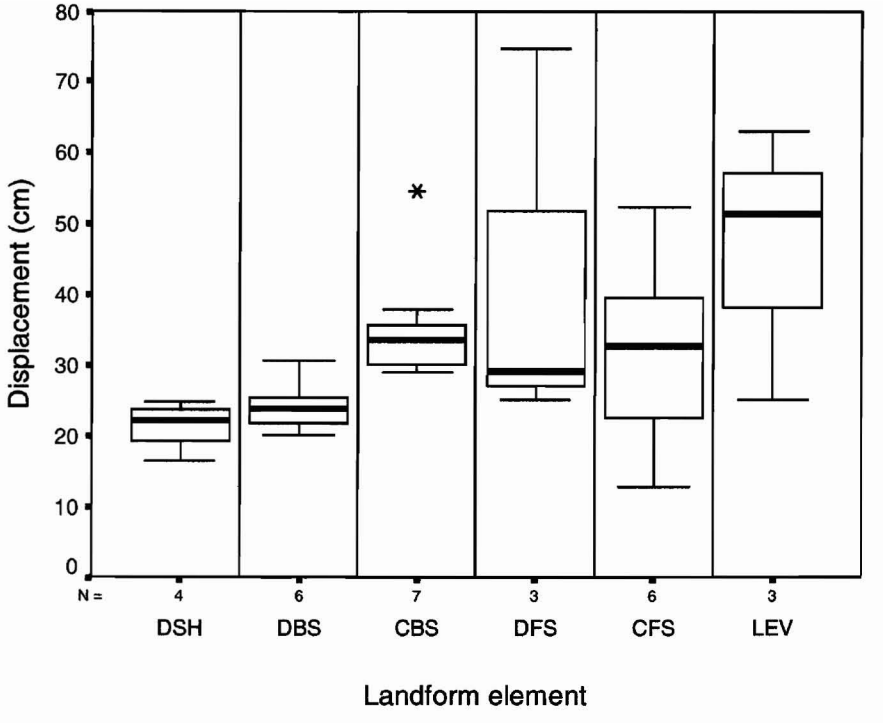

Figure 3.20 The Fall 1998 displacement distance (xyz) from the axes origin at the surface of the plot to the chloride centre of mass, 0- to 0.50-m sampling increment.

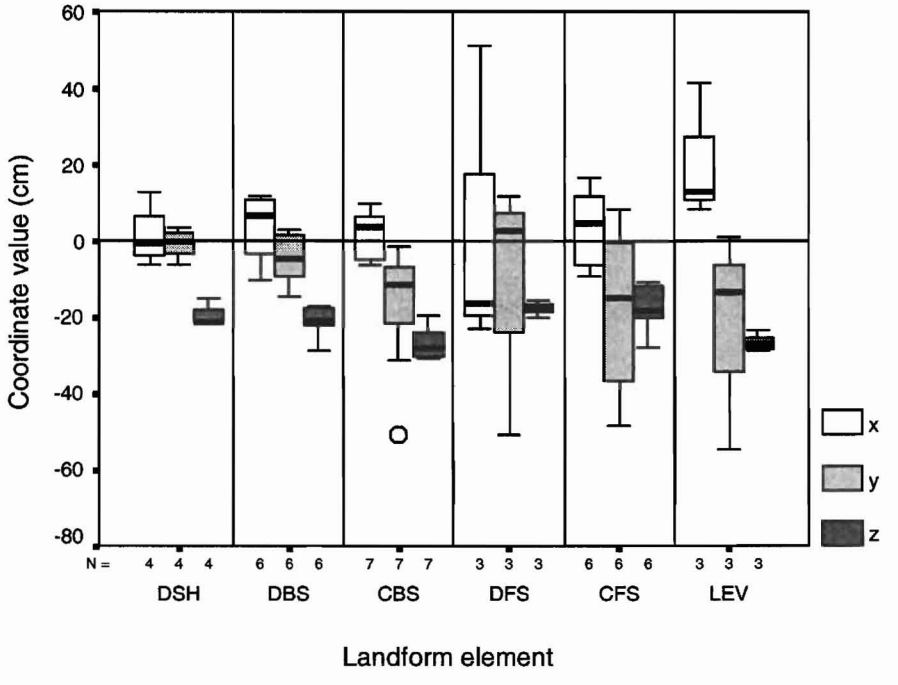

Figure 3.21 The Fall 1998 x, y, and z axis coordinates for the chloride weighted centre of mass in the 0-to 0.50-m sampling increment, with data grouped by landform element.

median lateral displacement for each landform element in Figure 3.22 to contrast the differences in direction and magnitude of displacement of the chloride centre of mass (0- to 0.50-m increment). The arrows in the image highlight the net direction of movement and the net distance of travel that the chloride centre of mass has moved from its origin at the centre of the plot at the soil surface to its new location. Negative lateral displacement values indicate net downslope movement; positive lateral displacement values indicate net upslope lateral movement. All landform elements with the exception of the divergent footslopes show a net downslope movement to the chloride tracer by the Fall of 1998. At this site divergent footslopes are dominantly found at the edge of the depression-centred tillage pond and they are dominantly associated with calcareous profiles, together these characteristics suggest that the DFS elements are sites of net

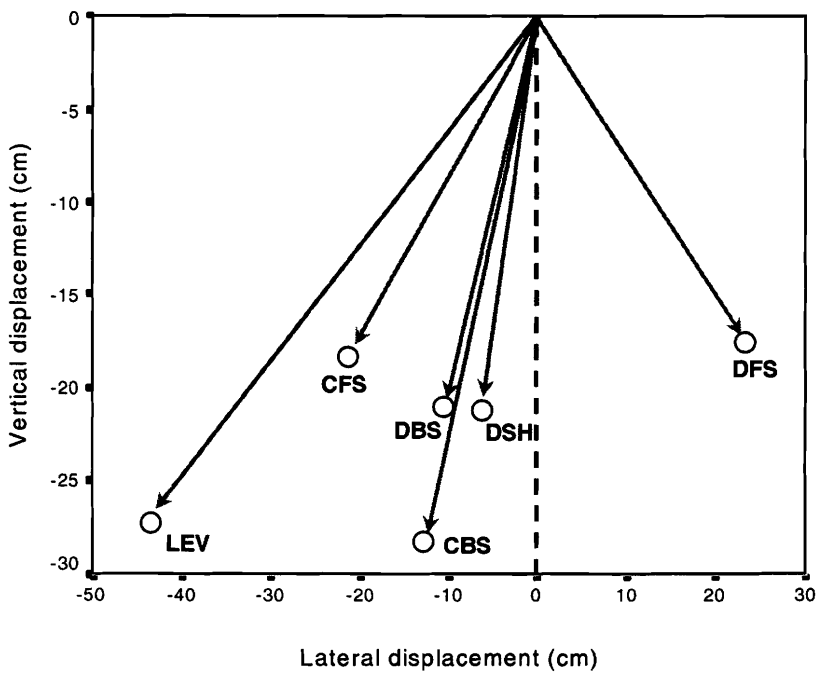

Figure 3.22 The Fall 1998 median lateral and vertical displacement of the chloride centre of mass for each landform element, 0- to 0.50-m sampling increment. The arrows highlight the net direction of movement of the chloride centre of mass from the centre of the 1-m^2 plot at the soil surface. Negative lateral displacement values indicate net downslope movement; positive values indicate net upslope movement.

groundwater discharge (as described by Miller, 1983; Mills and Zwarich, 1986; Richardson et al., 1992; Hayashi et al., 1998 and Richardson et al., 2001 among other

authors), resulting in upslope movement of the chloride tracer.

Surprisingly the chloride centre of mass was found at its deepest among level and convergent backslope landform elements, and not among footslope elements. This may be because within the footslopes the majority of the chloride had been leached from the profile during the spring melt period and the calculated centre of mass represents only that chloride remaining and not the total chloride mass. The low recovery among DFS and CFS elements limits the usefulness of the calculated displacement values, but the trends in the direction of movement should be representative. Level landform elements show the greatest lateral movement in this time period. Divergent backslope, divergent shoulder and convergent backslope landform elements show the least lateral displacement.

Differences in the pattern of lateral displacement with sampling depth are associated both with topographic form as defined by landform element and with soil profile development. In Figure 3.23 with the data grouped by landform element, three patterns of displacement are weakly apparent:

1. All divergent landform elements behave similarly, and DSH and DBS are especially alike. Similar in pattern to the DSH and DBS, but of greater magnitude, is displacement among DFS landform elements.

2. CBS and CFS make up a second group that has a large variability within the data set and as a result show little difference in displacement between sampling increments.

3. Level landform elements tend to show an increase in displacement with depth and they comprise the third group.

Re-grouping the data by soil profile class (Figure 3.24) removes some of the variability seen within the landform elements and helps to confirm the interpretation. It is apparent that the soils in the REGO profile class have a distinctive pattern of redistribution in which the displacement of the centre of mass decreases from the surface

to the third sampling increment and then shows a marked increase in the 0.35- to 0.50-m sampling increment. Soils in the REGO profile class dominate DSH and DBS landform elements. In contrast, the soils in the ORTHIC profile class, which dominate the CBS landform elements, do not show the increased displacement in the 0.35- to 0.50-m sampling increment.

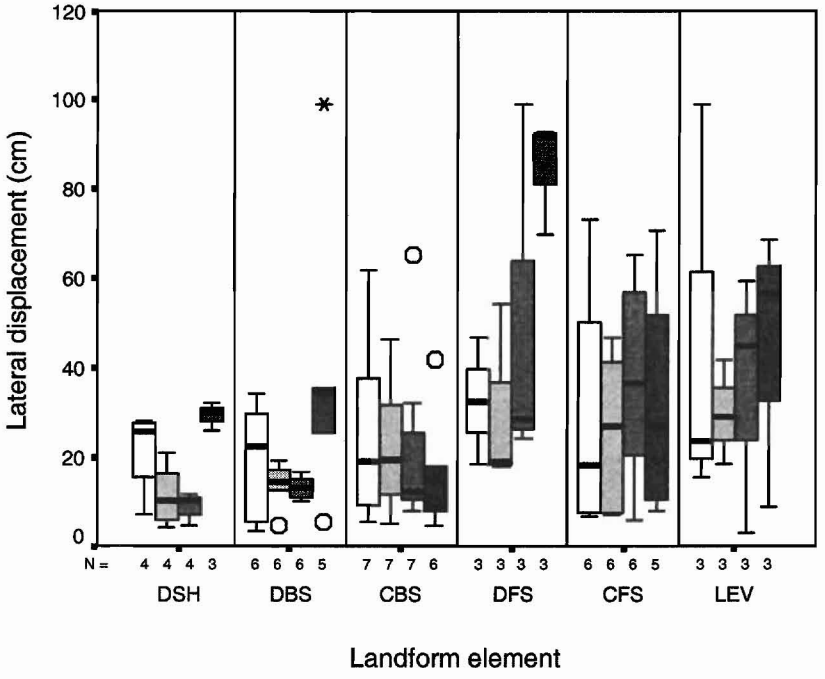

Figure 3.23 The Fall 1998 lateral displacement of the chloride centre of mass by depth and landform element. For each landform element category, the depth increments from left to right are: 0 to 0.10, 0.10 to 0.20, 0.20 to 0.35 and 0.35 to 0.50 m.

Soils subgroups included in the CALC profile class occur within most of the landform element categories, which may account for the large variation in the data apparent in Figure 3.24. The soils in the CALC class tend to have greater lateral displacement of the chloride mass in the surface increment than all other soil profile types.

Soils in the GLEYED profile category tend to occupy DFS and CFS landform elements; they show the least displacement in the surface increment, displacement increasing with depth.

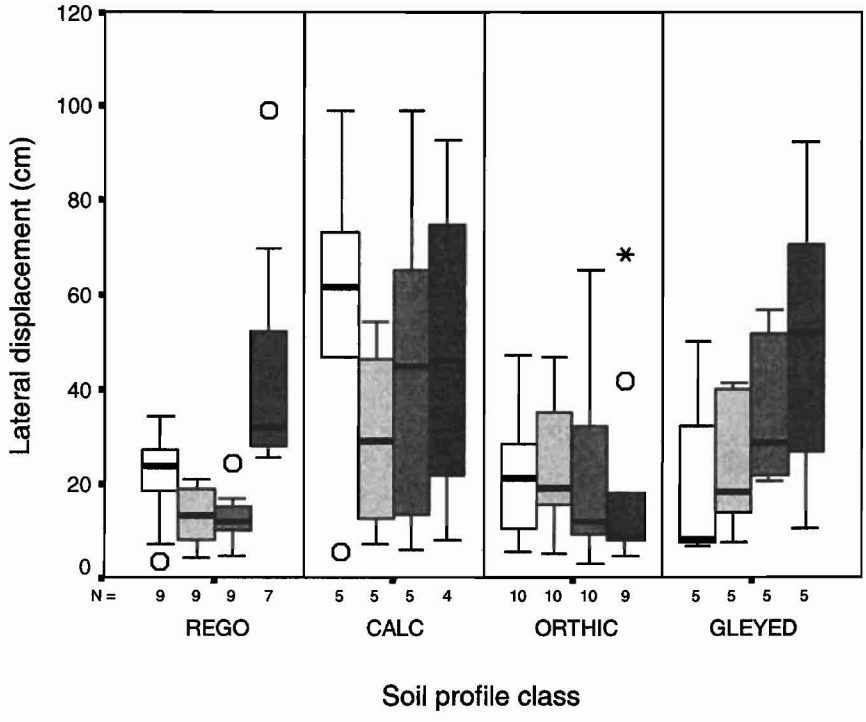

Figure 3.24 The Fall 1998 lateral displacement of the chloride centre of mass by depth and soil profile class. For each soil profile class, the depth increments from left to right are: 0 to 0.10, 0.10 to 0.20, 0.20 to 0.35 and 0.35 to 0.50 m.

Lateral displacement values for individual sampling depths and locations are attached in Appendix E

3.6.4. Summary

By the Fall of 1998 the pattern of chloride recovery (0- to 0.50-m) appears to correspond to the long term pattern of soil moisture that we expect in a hummocky landscape, with soil moisture increasing in the sequence shoulders < backslopes < footslopes (Zebarth and de Jong, 1989a). Chloride recovery is greatest in the divergent shoulder landform elements and then decreases in the sequence shoulders>backslopes>footslopes (Figure 3.18). Level elements have a median chloride recovery between that of CBS and DFS.

Chloride has been almost fully removed from the surface increment at all locations. The majority of the chloride is now contained within the 0.10- to 0.20-m and 0.20- to 0.35-m sampling increments. In the 0.35- to 0.50-m increment approximately

20% of the originally applied chloride mass was recovered from convergent backslope elements, which are dominated by soils of the ORTHIC profile class, while other locations have 5% or less in the same depth (Table 3.12 and Table 3.11).

Net total displacement of the chloride centre of mass (xyz) over the 0- to 0.50-m depth shows a weak trend of increasing displacement in the sequence DSH≈DBS<CBS≈DFS≈CFS<LEV landforms. Generally, displacement is greatest where chloride recovery is least. Variability within landform elements is very low among the DSH, DBS, and CBS elements, and is much greater among the DFS, CFS, and LEV landform elements where greater moisture accumulation would be expected. The chloride centre of mass has moved deeper into the soil profile among the convergent backslope and level landform elements than among other landform elements.

All landform elements show a greater recovery of chloride (0- to 0.50-m increment) outside of the 1-m^2 plot area than seen at previous sampling times, suggesting a greater amount of lateral movement. Overall there are four patterns of lateral displacement with depth. These appear to be associated with landform element and soil profile type. Soils and landforms can be grouped as follows:

1. Divergent positions which are dominated by soils with O.R and R.DBC profiles. Displacement decreases from the surface to the third sampling depth and then sharply increases in the 0.35- to 0.50-m depth.
2. Convergent backslope landform elements that correspond to soils with O.DBC profiles. Displacement is greatest at the surface and then decreases with depth.
3. Gleyed soil profiles which occur in DFS and CFS landform elements. Displacement is smallest at the surface and then increases with depth
4. CA.DBC profiles which occur in five landform element categories. Although data show a large variability within each sampling depth, they clearly tend towards greater movement in the surface increment than all other soil profile types.

3.7. Comparing chloride redistribution across time.

3.7.1. Recovery

Total recovery over the 0- to 0.50-m sampling depth is shown for all three sampling times with the data grouped by landform element in Figure 3.25. As seen in Figure 3.25, the majority of the chloride is recovered from all landform elements in the Fall 1997 sampling period. However, in the Spring of 1998 greater differences begin to emerge between landform elements and by the Fall of 1998 there appears to be a pattern of declining recovery that is associated with topographic form as defined by the landform elements.

In the Spring of 1998, the CFS and DFS positions show dramatic reductions in chloride, having lost approximately 80% of the chloride that was initially applied to the surface, while the remaining landform categories are essentially unchanged from the Fall 1997 sampling. The CFS and DFS positions that have lost the chloride are found in a topographic low that was covered by surface water for at least some portion of the spring. Chloride has been leached out of all sampling increments in these CFS and DFS positions.

A single CFS location (# 49) located at an upper slope position was not subject to spring flooding and had 98% chloride recovery in the Spring of 1998. Note that this location can be separated from the others in the CFS and DFS categories by the landform element complex (LFC) classification of Pennock et al. (1994b). Those footslope positions subject to spring flooding had a LFC classification of either footslope or level; whereas, Location 49, at an upslope position, had an LFC classification of backslope. As seen in Table 3.11 (Fall 1998 results) the pattern of recovery with depth for Location 49 more closely resembles those of the CBS landform elements than the other CFS elements.

The Fall 1998 results show an increased loss of chloride in all landform elements. The resulting pattern shows the greatest loss of chloride to be in the convergent footslopes (which appear to have been leached under saturated conditions in the spring), and the greatest recovery of chloride to be in the divergent shoulder

positions. Landforms have decreasing chloride recovery in order from DSH, DBS, CBS, LEV, DFS, and CFS (Table 3.12, Figure 3.25).

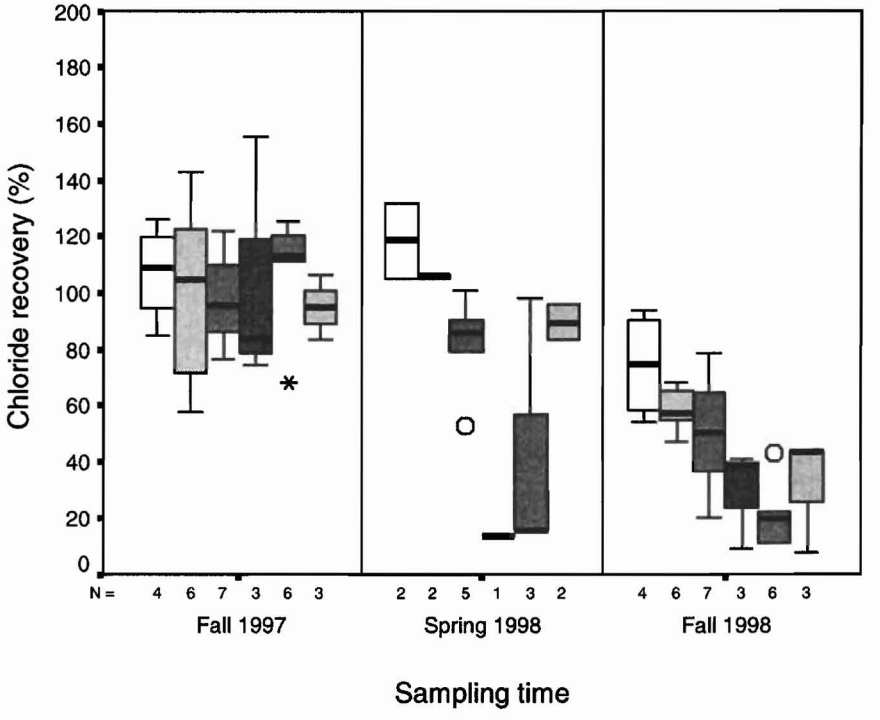

Figure 3.25 Chloride recovery (%) over time, with data grouped by landform element. Within each time period, landform elements from left to right are: DSH, DBS, CBS, DFS, CFS, LEV.

The variation in chloride distribution with depth is presented in Figure 3.26, with the data grouped by depth, sampling time and landform element. As discussed earlier, the data from the Fall of 1997 show few differences between landform elements irrespective of sampling depth. The notable exception to this pattern is the elevated chloride recovery in the surface of the CFS landform elements (10 to 20 % more chloride at the surface than other landform elements).

In the Spring of 1998 there is a greater variation between landform elements in the upper three sampling increments than was seen in the previous fall. The footslope elements show the greatest change from the Fall of 1997, and appear to have been largely leached of chloride at all sampling depths.

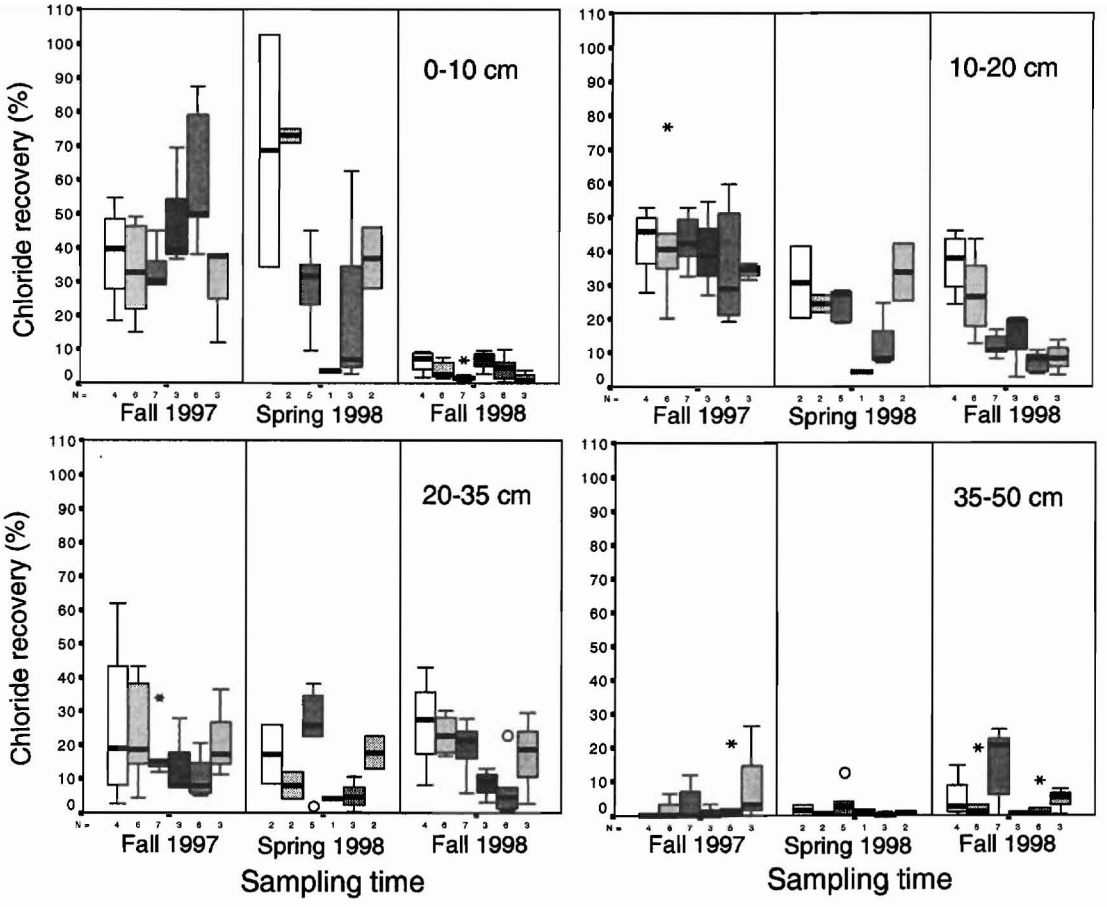

Figure 3.26 Chloride recovery (%) over time, with data grouped by sampling depth and landform element. Within each time period the landform elements from left to right are: DSH, DBS, CBS, DFS, CFS, LEV.

By the Fall of 1998 the variation between landform elements was largely limited to the 10-to 20 and 0.20- to 0.35-m sampling increments. Chloride appears to have been uniformly removed from the 0- to 0.10-m sampling increment where redistribution was affected both by moisture flows and by tillage.

Surprisingly, there is little accumulation of chloride in the 0.35- to 0.50-m increment in any sampling time. This suggests that any chloride moving below 0.35 m is probably moving rapidly and in localized channels, implying a dominance of preferential flow through this depth increment. The greatest recovery of chloride in this increment was in the CBS landform elements (Fall 1998) that are dominated by soils with Orthic Dark Brown Chernozemic profiles. Note that Location 49 is reported as an

outlier with elevated recovery among the CFS landform elements in both the 0.20- to 0.35-m, and 0.35- to 0.50-m increments for the Fall of 1998. A second outlier with elevated recovery in the 0.35- to 0.50-m increment is Location 38, the only Orthic Chernozemic profile among the DBS landform elements.

3.7.2. Chloride Centre of Mass

The displacement of the chloride centre of mass over the combined 0- to 0.50-m sampling depth is shown in Figure 3.27 for each sampling time. As with the changes in the percent of chloride recovered, major differences in displacement begin to emerge between landform elements in the Spring of 1998 with the probable leaching of the footslopes in the lower slope positions. Differences continue to develop between landform elements into the Fall of 1998 with CBS and LEV landform elements showing increasing displacement.

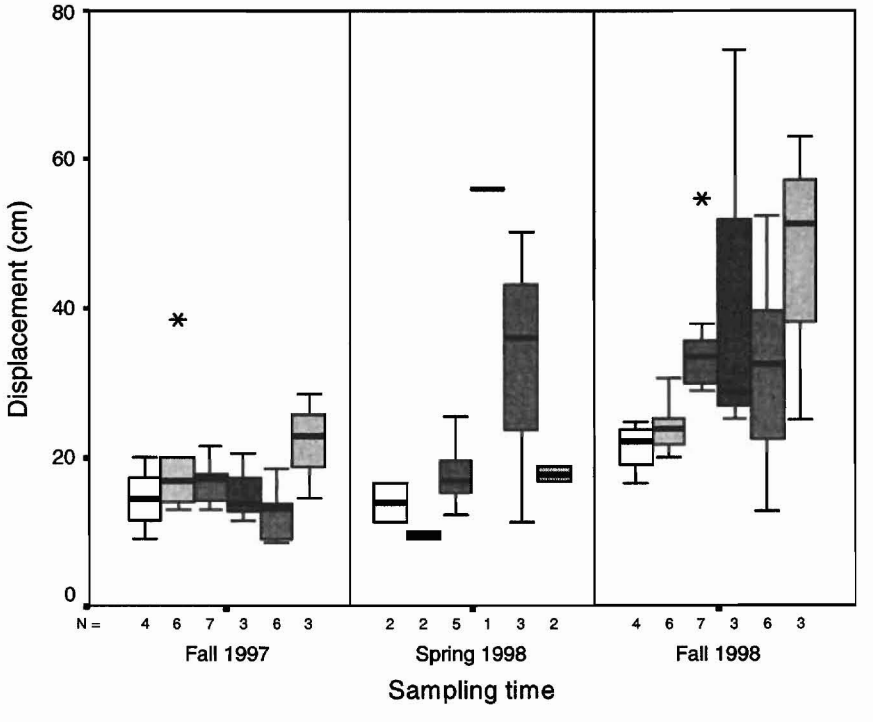

Figure 3.27 Total net displacement distance (cm) of the chloride centre of mass in the combined 0- to 0.50-m increment, with data grouped by time and landform element. Within each sampling time, landform elements from left to right are: DSH, DBS, CBS, DFS, CFS, and LEV.

All landform elements show an increase in the vertical displacement of the chloride centre of mass from the Fall 1997 results to the Fall 1998 (Table 3.13). By the Fall of 1998 the greatest vertical displacement has occurred in CBS and LEV landform elements.

Table 3.13 Median lateral and vertical displacement distance in the combined 0- to 0.50-m increment, with data grouped by landform element and sampling time.

Landform element	Lateral Displacement (cm)			Vertical Displacement (cm)		
	Fall 1997	Spring 1998	Fall 1998	Fall 1997	Spring 1998	Fall 1998
DSH	-3.0	-5.5	-0.9	-13.5	-11.9	-21.2
DBS	-3.2	0.4	-8.1	-13.8	-9.2	-21.0
CBS	-4.2	-4.4	-12.0	-14.0	-16.6	-28.2
DFS	-7.2	-52.5	16.6	-11.9	-19.7	-17.5
CFS	-1.2	-34.0	-15.6	-11.8	-11.8	-18.3
LEV	-11.1	-11.4	-18.7	-14.1	-13.5	-27.2

Displacement is measured from the axes origin in the centre of the plot at the soil surface. Negative lateral displacement values indicate a downslope orientation to the lateral movement (i.e., negative y-axis values). Positive lateral displacement indicates an upslope lateral movement. Negative vertical displacement indicates downward movement.

Between the Fall of 1997 and the Fall of 1998 median lateral displacement increases for all landform elements except for the DSH elements which show a small decrease (Table 3.13 and Figure 3.28). The CFS and DFS landform elements show anunexpected decrease in lateral displacement from the Spring of 1998 to the Fall of 1998 (Table 3.13). This may reflect the increase in sampling numbers during the fall sampling and the large variability within each landform element. Alternatively, it may be that the dispersed pulse present in the Spring of 1998 continues to undergo dilution during the intervening period.

With the exception of movement in the DFS and CFS landform elements during the Spring 1998 sampling, there is little accumulated lateral displacement among landforms within the upper three sampling increments June 1997 through May 1998. As suggested earlier, lateral movement in the fourth sampling increment in this time may be due to localized recovery in only a few of the sampling cores. During the period May 1998 to October 1998, there is much greater variability in total displacement within each landform element and sampling depth than observed earlier.

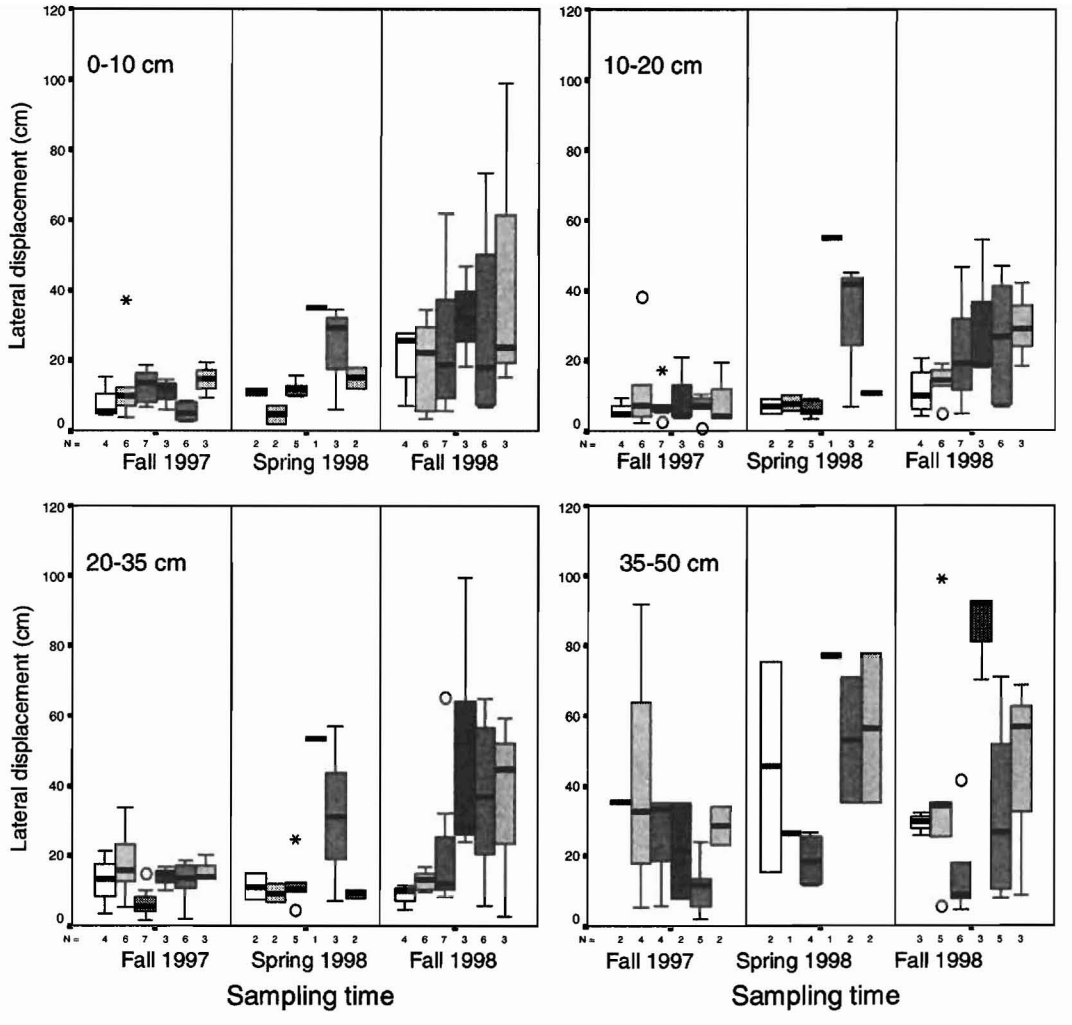

Figure 3.28 Net lateral displacement of the chloride centre of mass with data grouped by depth, time and landform element . Within each sampling time, landform elements from left to right are: DSH, DBS, CBS, DFS, CFS, and LEV.

The rate of displacement of the chloride centre of mass in the 0- to 0.50-m increment (Table 3.14) has a range from 0.4- to 2.7 x 10^{-8} m s^{-1}. Zebarth (1988) found that in a similar Saskatchewan landscape the unsaturated flux below 1.0-m depth was commonly 10^{-8} m s^{-1}at lower slope positions, 10^{-9} to 10^{-8} m s^{-1} in the saddle positions, and 10^{-9} to 10^{-10} m s^{-1} in the upper slope positions. The values in Table 3.14 represent the net movement of the centre of the chloride pulse over time. Values for DFS and CFS are underestimated after September 1997 as the majority of the chloride tracer has already been lost. The rate of displacement calculated for subsequent times is based on the remaining 20% of the chloride in the DFS and CFS positions.

Table 3.14 The median rate of displacement of the chloride centre of mass over time.

	median rate of displacement (10^{-8}m s^{-1})				
	June 1997 to September 1997	October 1997 to May 1998	May 1998 to October 1998	October 1997 to October 1998	June 1997 to October 1998
landform element	96 days	216 days	168 days	384 days	474 days
DSH	1.7	0.5	0.6	0.4	0.5
DBS	2.0	0.3	1.2	0.4	0.6
CBS	2.1	0.5	1.1	0.6	0.8
DFS	1.7	2.0	1.4	0.8	0.7
CFS	1.6	1.7	0.7	0.8	0.8
LEV	2.7	1.0	1.9	1.4	1.3

3.7.3. Summary

Data from the Fall 1997 sampling suggest that during the first summer the chloride pulse behaves largely the same at all landform positions. Infiltration is dominantly vertical with mean displacement of 16.6 cm (standard deviation 6.1 cm). The chloride pulse is largely contained within the upper three sampling increments with a mean recovery of 102.2 % (std. dev. 22.8%). There is little accumulation of chloride in the 0.35- to 0.50-m at any sampling time.

Data from the Spring 1998 sampling suggest that during the spring melt period there has been little net change to the chloride distribution among the upper slope positions, whereas positions occupying footslope landscape elements within an area subject to spring flooding have now lost approximately 85% of the original applied chloride. The chloride appears to have been leached equally from all depths within these footslope positions. The same positions that were subject to flooding also show the greatest displacement of the chloride centre of mass, with displacement an order of magnitude greater than at other positions. The rate of displacement in the upper slope positions (DSH, DBS, CBS, LEV) in the Spring of 1998 is less than half that observed the previous fall. For the lower slope positions that were flooded, the rate of displacement is equal to or greater than that seen in the Fall of 1997.

A footslope position that does not conform to this pattern of behaviour (Location 49) is located upslope from the area subject to flooding. It cannot be separated from the

other footslope positions based on individual topographic characteristics including specific catchment area (SCA), specific dispersal area (SDA), or the ratio SCA/SDA. However, it appears that it can be separated using the landform complex classification (LFC).

By the Fall of 1998 chloride recovery has declined further in all other landform elements. The resulting pattern of chloride loss (0- to 0.50-m) decreases in the sequence DSH<DBS<CBS<LEV≤DFS<CFS. This pattern of chloride loss matches the expected long-term pattern of moisture stability observed in similar landscapes, with greater chloride loss in positions that tend to have more water over the long term. Chloride has been almost fully removed from the surface increment at all positions; with the resulting recovery pattern largely determined by chloride distribution in the 0.10- to 0.20-m and 0.20- to 0.35-m increments.

4. TILLAGE REDISTRIBUTION

4.1. Introduction

Water redistribution is the major control on the formation of soil profiles in the period since deglaciation. The nature of the surficial horizons has, however, been altered from their native state by the combined effects of land clearing and decades of cultivation. The redistribution of soil by erosional processes in the landscape results in thinning of soils in erosional areas, and overthickening of A-horizons in depositional areas. The results of the combination of water action and soil material redistribution are illustrated by the present distribution of soils in these cultivated landscapes.

Recent studies in erosion processes suggest that erosion in cultivated fields in temperate and arid environments is dominated by tillage processes rather than water or wind driven processes (Lindstrom et al., 1990; Lindstrom et al., 1992; Govers et al., 1994; Govers et al., 1996). Prior to this, tillage was considered only a factor affecting the soil's sensitivity to erosion by water and wind rather than an erosion process per se. Research into the direct movement of soil by tillage operations had been largely neglected while researchers focused on water as the primary erosion mechanism in cultivated landscapes (Lindstrom et al., 1992; Govers et al., 1994; Govers et al., 1999). As a result, there is little historical literature on the subject other than the early work of Mech and Free (1942) (Lindstrom et al., 1992; Govers et al., 1993; Govers et al., 1994).

The movement of soil by tillage implements is variously referred to as tillage erosion, tillage translocation, and tillage redistribution. The terms *tillage redistribution* and *tillage translocation* are used interchangeably, referring to any displacement of soil due to tillage. Tillage redistribution and tillage translocation are commonly characterized as the average displacement distance of the tillage-layer following a tillage event (Lobb and Kachanoski, 1999). *Tillage erosion* has been more specifically defined

as the net loss of soil at a given location due to tillage translocation (Govers et al., 1999; Lobb et al., 1999).

Quine et al. (1999) introduce the term "soil flux due to tillage", which they define as the mass of soil displaced per meter of slope width per tillage event (kg m^{-1}). This is analogous to the term "unit soil transport rate" employed by Govers et al. (1999).

Research efforts through the early 1990's to confirm the importance of tillage as an erosive process were greatly aided by technical advances that improved the ability to collect and model spatially distributed data. Key among these technical advances was the development of the cesium-137 technique to assess soil redistribution. This method provides spatially distributed net soil redistribution data that is independent of the processes involved. This technique provided an observed baseline for total erosion against which the predictions of the erosion models could be compared (Govers et al., 1996, 1999).

4.2. Literature Review

4.2.1. The Redistribution Process

Quine et al. (1999) suggest that the process of tillage redistribution can be conceptualized as consisting of two parts: tillage detachment and tillage displacement. *Tillage detachment* refers to the mass of soil per square meter that can be moved during a tillage event. This is primarily dependent on the depth of tillage and the soil bulk density. *Tillage displacement* is defined as the distance soil is moved per tillage operation (translocation distance) and is dependent largely on slope gradient, implement type, implement speed, and soil cohesion.

Clearly, many factors influence tillage translocation. These include: slope gradient, slope curvature, soil bulk density, soil texture, tillage implement shape, tillage depth, tillage speed, the length of the tractor-tillage unit, slope length, and soil moisture at the time of tillage (Lobb et al. 1995, 1999).

Although many factors can influence the process of tillage redistribution,

research over the last decade has largely focused on soil and landscape factors, and of these, slope gradient and slope curvature have received the greatest attention. It has been demonstrated that soil *displacement* by tillage is primarily dependent on slope gradient (Mech and Free, 1942; Lindstrom et al., 1990; Lindstrom et al., 1992; Govers et al., 1994; Govers et al., 1996; Govers et al., 1999). Tillage can occur in either an upslope or a downslope direction, and it has been clearly demonstrated that there is a greater displacement when tillage is in the downslope direction (Mech and Free, 1942; Lindstrom et al., 1990; Lindstrom et al., 1992; Govers et al., 1993; Govers et al., 1994). Downslope tillage will result in greater displacement as the slope increases, whereas tillage upslope will show less displacement as the slope increases.

While slope gradient is the primary control on soil displacement at individual points within the landscape, the variation in soil loss and gain across the landscape (the field-scale pattern) is controlled by changes in slope gradient, i.e. slope curvature. Linear slopes show no net loss of soil, with the incoming soil equal to that which is removed. Convex positions show a net loss of soil, and concave positions show a net accumulation of soil. As noted above, this pattern of soil loss on convexities and consequent soil accumulation in concavities is typical for tillage-eroded landscapes (Govers et al., 1999; Lobb et al., 1999).

Govers et al. (1994) theoretically describe soil redistribution by tillage using the continuity equation for sediment movement on a hillslope section (equation 4.1). The equation shows that the change in soil mass over time (i.e. the rate of change), on the left hand side of the equation, equals the flux of soil in the x direction per unit width of the slope.

$$\rho_b \frac{\partial h}{\partial t} = -\frac{\partial Q_s}{\partial x} \tag{4.1}$$

where,

ρ_b = the bulk density of the soil
h = height at a given point on the hillslope,
t = time,
x = distance in the horizontal direction.
Qs = flux of soil in the x direction

Govers et al. (1994) show that this equation can be transformed into equation 4.2, where the change in soil mass at any point on the hillslope is equal to the proportionality constant, k, multiplied by the second derivative of the slope. The second derivative of elevation is curvature; thus, these authors show in mathematical form that the pattern of soil loss and soil gain is governed by the slope curvature, rather than slope gradient. The rate of erosion or deposition will depend on both the value of k and the curvature of the slope. If we assume that the components of k - bulk density, depth of tillage, and the slope of the linear regression between soil displacement and slope tangent – are constant over some study area, then we can say that erosion and deposition will be controlled by slope curvature.

$$\rho_b \frac{\partial h}{\partial t} = k \frac{\partial^2 h}{\partial x^2} \tag{4.2}$$

where,

ρ_b = the bulk density of the soil,
h = height at a given point on the hillslope,
t = time,
x = distance in the horizontal direction.
k = tillage transport coefficient

Govers et al. (1994, 1996) refer to the k value as a 'diffusion coefficient', but in a brief and informative overview of tillage erosion and translocation Govers et al. (1999) suggest the term 'tillage transport coefficient' to avoid any confusion with other classical diffusion-type processes. The use of the tillage transport coefficient and its experimental derivation are more fully discussed in Section 4.2.3.

Erosion processes in which the soil displacement is primarily determined by the slope gradient are called diffusive processes by geomorphologists (Govers et al., 1999). Such processes tend towards infilling of the landscape and a decrease in relief, in contrast to fluvial processes which tend towards incision and an increase in relief. Govers et al. (1994, 1996) point out that the magnitude of similar diffusive-type processes (such as soil creep and soil movement by splash) can be compared using the coefficient, k. The values calculated for tillage redistribution are more than an order of magnitude greater than those for soil creep or splash.

As noted above there are many sources of variability other than slope gradient and curvature that impact soil redistribution by tillage. Lobb et al. (1999) point out that the complex relationship between tillage depth, tillage speed, slope gradient, slope curvature and implement shape can not readily be extrapolated from small plot trials to topographically complex landscapes. For example, Govers et al. (1994), Lobb et al. (1999) and Quine et al. (1999) have all noted that actual tillage depth varied over their study landscapes, most likely in response to the interaction between micro-topography and the fixed frame of the tillage implement. This will have a direct impact on the mean translocation distance and the tillage flux. Gerontidis et al. (2001) compare the impact of three different tillage depths using a moldboard plough. They found that mean soil displacement (i.e., mean translocation distance) was decreased as plough depth increased when ploughing perpendicular to the contours.

4.2.2. Magnitude and Spatial Pattern

To establish the magnitude of tillage erosion Lindstrom et al. (1990, 1992) and Govers et al. (1994, 1996) used the results of small plot tillage trials as the basis of predictive models. Their model predictions suggested that erosion due to tillage would be of a magnitude equal to or greater than that of water erosion. Lindstrom et al. (1992) showed that the predicted magnitude of erosion by tillage (30 Mg ha^{-1} yr^{-1} over a 90 year simulation) is sufficient to account for the observed loss of organic rich topsoil along ridges and adjacent upper slopes in Minnesota and South Dakota. Govers et al. (1996) determined that the magnitude of tillage translocation may often exceed 10 Mg ha^{-1} yr^{-1} on irregular topography. This rate of tillage translocation is of the same magnitude as total erosion (established using the cesium-137 method), whereas the redistribution by soil creep and splash have a magnitude in the tens of kilograms ha^{-1} yr^{-1} (Govers et al., 1994).

The model results of Lindstrom et al. (1990, 1992) and Govers et al. (1993, 1994, 1996) predicted the long-term impact of tillage to result in soil loss on convex landforms and soil gain in concavities. This was noted to be different from the predicted pattern in response to water erosion, in which erosion from overland flow would be maximized where contributing area and slope where greatest, i.e. the concavities. Their model

results were supported by the field data from the cesium-137 investigations. This prompted Govers et al. (1996) to conclude that "landscapes dominated by overland flow erosion will tend towards incision and increase in relief, those dominated by tillage will tend towards infilling and relief reduction."

Lobb et al. (1995) using labelled soil on small plots in Ontario reported an average soil loss of 54 Mg ha^{-1} yr^{-1} due to tillage. They found that 70% of the total soil erosion at shoulder positions could be accounted for by tillage.

In a series of ^{137}Cs investigations in Saskatchewan, de Jong et al. (1983), de Jong and Kachanoski (1988), and Pennock et al. (1994b) observed that the erosion rates on cultivated landscapes varied from approximately 8 to 26 Mg $ha^{-1}yr^{-1}$ in the Brown, Dark Brown and Black soil zones depending on landscape position and soil texture. Losses up to 60 Mg $ha^{-1}yr^{-1}$ were reported for sandy soils and for Dark Gray Luvisols (de Jong et al., 1983). The greatest losses where from the convex upper slope positions, with relatively minor losses or even net gains occurring in the concave lower slopes.

4.2.3. Measuring Tillage Displacement on Small Plots

Historically, relatively few plot studies have been undertaken to assess soil translocation due to tillage. Mech and Free (1942) used small boxed plots over which they drew tillage implements. Following tillage, the boxes were re-weighed to determine the mass of soil moved from one end of the box to the other. More recently, field experiments by several authors have employed a variety of tracers to monitor soil displacement following tillage. Tracers can be point-tracers such as small metal nuts or plastic spheres (Lindstrom et al., 1990; Lindstrom et al., 1992; Govers et al., 1993; Govers et al., 1994). Tracers can also be plot-tracers, in which the soil within the plot is labelled, either with a physical tracer such as gravel (Guiresse and Revel, 1995), or the soil can be labelled with chemical tracer such as potassium chloride or cesium-137 (Lobb et al., 1995; Lobb et al., 1999). Following tillage, the tracer distribution is determined, which involves either some excavation of the plot area if using point–tracers, or a systematic soil sampling if using plot-tracers.

As noted earlier, tillage translocation is commonly characterized as the average

displaced distance of the tillage-layer. The mean displacement of the tillage layer is considered an adequate measure to characterize relative soil redistribution in landscapes (Lobb and Kachanoski, 1999). Two primary methods have been identified by Lobb et al. (2001) for calculating the mean displacement distance. These are known as 1) the distribution-curve method and 2) the summation-curve method.

When using the distribution-curve method, translocation is calculated directly from the difference in the distribution of tracer before and after tillage. Following tillage, the distribution of the tracer is determined and mean displacement distance can be calculated. Examples of this methodology are presented by Lindstrom et al. (1990, 1992) and Govers et al. (1993, 1994) who used metal nuts and plastic spheres as point tracers on small plots.

An alternative method to evaluate tillage translocation is the use of a summation curve or convolution method as reported by Lobb et al. (1995, 1999). Following tillage, the tracer concentration is determined at points along the tillage path. The concentration of tracer is then integrated over the sampling distance and the form of the integrated curve is then shifted forward (in the direction of tillage) by the width of the plot.

The use of paired plots, where one is tilled in the upslope direction and the other in the downslope direction, allows for the estimation of net (downslope) soil translocation (Lobb et al., 1995; Lobb et al., 1999; Quine, 1999; Gerontidis et al., 2001).

Once mean displacement distance is determined, the results from several plots can be graphed against the tangent of the slope gradient (i.e., the gradient at a point on the hillslope). Several authors have shown that a linear model approximates the relationship between the tangent of the slope gradient and mean displacement distance (Govers et al., 1996; Govers et al., 1994; Lindstrom et al., 1992; Lindstrom et al., 1990). This can be expressed as equation 4.3.

$$\bar{d} = A + BG \qquad (4.3)$$

where,

$\bar{d}$ = the mean displacement distance of the plough layer in the direction of tillage, at a

point on the hillslope

G = the tangent of the slope gradient at a point on the hillslope

B = the slope of the linear regression function between the experimentally determined displacement distance ($\vec{d}$) and tangent of the slope gradient, determined using a range of slope gradients in the study landscape.

A = the y intercept of the linear regression function

The unit soil transport rate, T_M, for a single pass of the tillage implement, at a specific point on the hillslope can be calculated using the experimentally determined mean displacement distance with equation 4.4:

$$T_M = D.\rho_b \bar{d} \tag{4.4}$$

where,

T_M = the unit soil transport rate (kg m^{-1}), the flux of soil in the tillage direction

$\bar{d}$ = the experimentally determined mean displacement distance of the plough layer (m)

D = the depth of tillage (m)

ρ_b = the bulk density of the soil (kg m^{-3})

The proportionality coefficient k (kg m^{-1}) (equation 4.5), also known as the tillage transport coefficient, has been shown by Govers et al. (1994) to define the average relationship between slope gradient and net tillage displacement (T_{MNET}) in a landscape where tillage is equally in the upslope and downslope directions (Govers et al., 1994; Gerontidis et al., 2001). The value for k (equation 4.6) provides a landscape averaged measure of the relationship between tillage flux and slope tangent; it is one value that can be used to compare the intensity of different tillage operations. The value for k is only valid within the range of slope gradients used to determine B.

$$T_{MNET} = -k\frac{\partial h}{\partial x} \tag{4.5}$$

$$k = D.\rho_b B \tag{4.6}$$

where,

T_{MNET} = the net unit soil transport flux for a landscape, established using a range of slope gradients and assuming tillage in both the upslope and downslope directions, (kg m^{-1})

$\frac{\partial h}{\partial x}$ = the slope gradient (4.7)

It should be noted that in all the small plot trials referred to above, the tillage pathway has been oriented so that it is aligned with the dominant gradient at each plot location, i.e. cross slope influence has been minimized. Virtually all of the studies select plot locations to minimize across slope curvature (i.e., plan curvature). Most researchers with the exception of Lobb et al. (1995, 1999) have attempted to minimize the influence of profile curvature (changes in slope gradient) by selecting plot locations with near linear slope.

4.3. Tillage Experiment No. 1

4.3.1. Introduction

Surface application of granular fertilizers and other materials is a common practice in agricultural fields. These materials are often incorporated into the soil shortly after their application and subsequently redistributed by the tillage implements. The primary purpose of this experiment was to identify differences in the redistribution of surface applied granular materials with respect to landscape position. These results may prove useful as an indicator of bulk soil redistribution in the tillage layer.

4.3.2. Experimental Design

A 150-m transect running from the north to south was established in the study field (SE 24-37-2-W3). The transect descended from a height of land in the north to a low point at approximately 125 m and then climbed the remaining 25 m (Figure 4.1). Slope gradient, curvature and aspect change along the transect. At seven locations along this transect (25-m intervals) coarse granular potassium chloride (with 60% equivalent K_2O) was mechanically broadcast at the rate of 672 g m^{-2} over a 1.8 x 9.1 m strip perpendicular to the initial transect.

Immediately following KCl application the strips were tilled using a 3.0-m wide cultivator with 0.35-m wide shovels on 0.30-m spacing and a tine harrow with tines on 0.15-m spacing. At each KCl strip, tillage was conducted once from the north to the south, and then adjacent to the initial tillage, once from the south to the north (see schematic diagram in Figure 4.2. Thus for each of the seven locations there is one tillage pass in either direction, creating fourteen individual plots. Tillage speed was estimated at

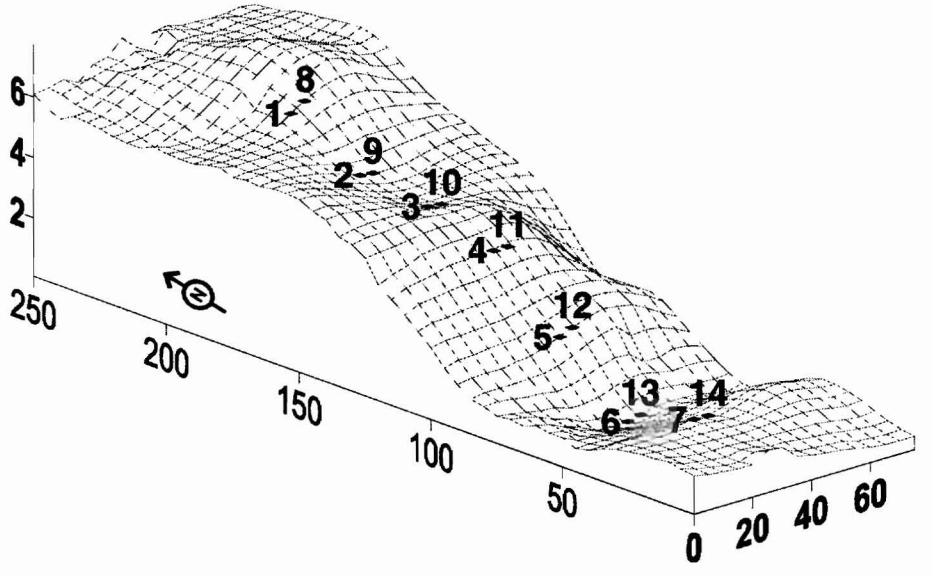

Figure 4.1 Wireframe image of the study area for Tillage Experiment No.1 showing the location of individual plots. Axes units are in meters.

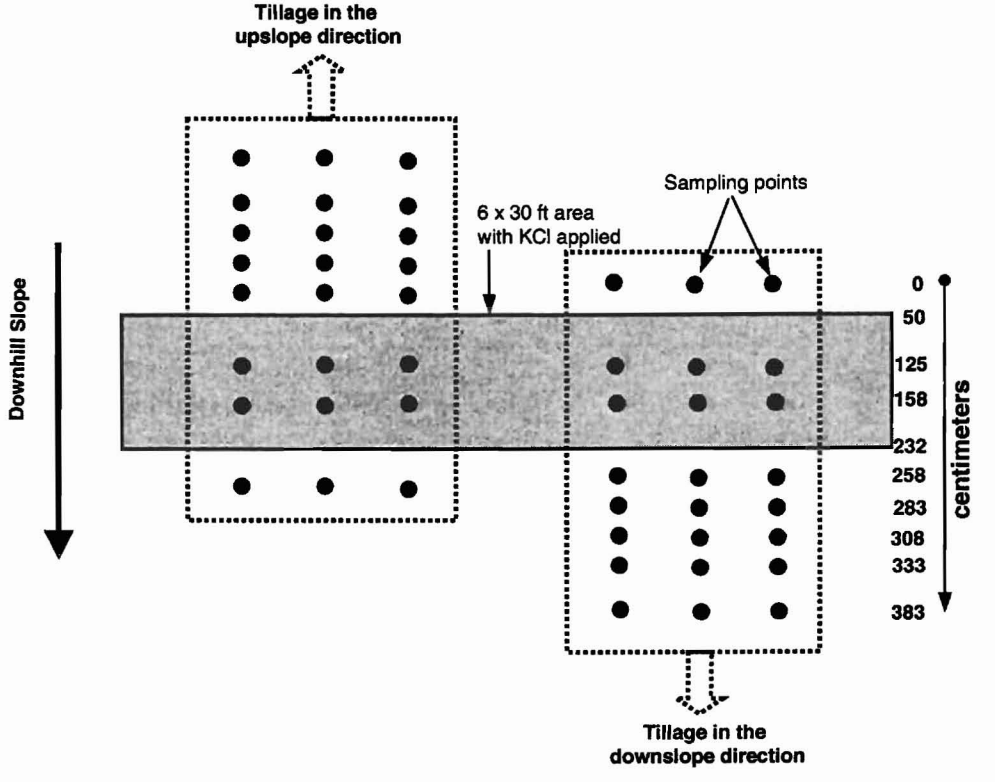

Figure 4.2 Schematic diagram of the sampling pattern at each plot, Tillage Experiment No.1.

8 km h^{-1} for both tillage passes.

It is important to note that plot alignment and thus tillage direction at each location were not specifically arranged so that tillage would be conducted up or down the maximum slope. Instead tillage was initiated at one end of the transect and moving in a continuous line was terminated at the other end having crossed all the KCl strips. The intention was to replicate the impact of normal farm tillage practice, in which the pattern of mechanical tillage is such that the tillage equipment is not always aligned with the direction of maximum slope, but may be running across the slope at any given point. The range of slope-tillage unit interactions would be the same as that encountered by the farm operator during a tillage operation in a single pass across the field. Thus, tillage direction is nominally up or down the slope at any plot location. This plot arrangement is different from the majority of those in the literature where plot alignment is determined so that tillage direction is directly up or down the maximum slope, and plot locations are generally chosen to minimize slope curvature.

4.3.3. Sampling Procedure

Post-tillage sampling was conducted using a truck-mounted hydraulic punch with a 0.065-m diameter corer. The sampling pattern followed that shown in Figure 4.2. Individual cores were taken at eight positions from 0.50 m back of the KCl strip to 1.50 m beyond the KCl plot in the direction of tillage. Samples were collected for the 0 to 0.10 m depth. Cores were taken in the centre of the 3.0 m wide tillage strip and 0.90 m to either side. This gave a total of 24 cores for each slope position and each tillage direction.

In addition, a single core was taken from the untilled area between the paired plots at four locations to evaluate the initial broadcast distribution of the KCl. Two further cores were taken at each slope location to a depth of approximately 1.0 m in order to record the profile description.

As discussed more fully in Section 2.4, topographic data were collected in the field using a total station and single prism. The distance between measurement points was adjusted in order to capture as much topographic variation as possible.

Approximately 600 data points were used within the 3.0-ha area where the experiments were performed. The field data was converted into an x, y, z format, and then a digital elevation model (DEM) was constructed using the Surfer 7.0 suite of programs (Golden Data Software, Inc.). The DEM was constructed with a 5 x 5 m grid size. Interpolation between known data points was done by kriging.

For each grid cell of the DEM, landform was characterized into landscape elements defined by a combination of slope gradient, plan curvature and profile curvature following the method of Pennock et al. (1987, 1994b).

4.3.4. Laboratory Procedures

Soil samples were air dried, weighed and ground to pass through a 2-mm sieve. Chloride content was determined colormetrically using a Technicon® AutoAnalyzer®. Following the method of Janzen (1993) a 2:1 solution of de-ionized water:soil was mixed and shaken for 1 h. The mixture was filtered to remove solids and the extract compared against known standards for chloride content using the colorimeter.

4.3.5. Data Analysis

The measured chloride concentration (ug g^{-1}) for each sample was reduced by the background threshold value of 25 ug g^{-1} (Section 3.4.2). The results were then converted to a mass per area basis using the soil bulk density and sampling depth (0.10 m). The corrected values for each sample are presented in Table 4.1.

Mean tracer displacement distance of the tracer was determined as the difference between the centre of the chloride mass before tillage and after tillage. To establish the chloride centre of mass following tillage, the mean chloride concentration from the combined samples (Table 4.1) was graphed against distance along the tillage path and a function fit to these points using the computer program Mathcad® 8 Professional. A spline function was used to predict the continuous chloride concentration between the sampling points. The area under the spline function was integrated, allowing the chloride recovery and centre of mass to be determined. Figure 4.3 shows an example of the Mathcad® worksheet.

Table 4.1 Post-tillage chloride concentration data for individual sampling points, Tillage Experiment No.1.

Plot	Distance Along Sampling Transect (cm)	Chloride ($g\ m^{-2}$)				Standard Deviation	CV %
		Left	Centre	Right	Combined Mean		
1 u*	0	0.0	0.0	0.0	0.0	0.0	0.0
	125	473.9	154.6	240.5	289.7	134.9	46.6
	158	8.7	230.0	300.0	179.6	124.2	69.2
	258	61.8	46.9	218.0	108.9	77.4	71.1
	283	21.2	64.9	24.5	36.8	19.9	53.9
	308	13.5	13.6	0.0	9.0	6.4	70.7
	333	4.2	0.1	7.7	4.0	3.1	77.6
	383	0.9	2.4	0.5	1.3	0.8	63.3
2 u	0	0.0	0.0	0.0	0.0	0.0	0.0
	125	24.4	136.5	34.9	65.3	50.5	77.5
	158	191.1	350.6	145.4	229.0	88.0	38.4
	258	21.2	83.9	85.0	63.4	29.8	47.0
	283	37.6	53.9	123.6	71.7	37.3	52.0
	308	3.1	0.0	9.2	4.1	3.8	92.8
	333	19.8	0.0	6.8	8.9	8.2	92.6
	383	0.0	0.0	0.0	0.0	0.0	0.0
3 d*	0	2.6	2.9	0.0	1.8	1.3	71.0
	125	109.0	498.4	393.0	333.4	164.5	49.3
	158	306.4	419.9	340.7	355.7	47.5	13.4
	258	136.4	30.0	21.3	62.6	52.3	83.6
	283	66.5	7.8	19.5	31.3	25.3	81.0
	308	15.3	8.4	1.0	8.3	5.8	70.7
	333	2.9	19.5	201.2	74.5	89.8	120.5
	383	0.0	0.0	0.0	0.0	0.0	0.0
4 u	0	0.0	0.0	0.0	0.0	0.0	0.0
	125	532.1	827.4	417.9	592.5	172.5	29.1
	158	282.9	305.9	728.4	439.0	204.8	46.6
	258	14.7	0.0	185.3	66.7	84.1	126.2
	283	1.2	9.5	47.2	19.3	20.0	103.8
	308	0.0	42.4	41.9	28.1	19.9	70.7
	333	3.5	6.5	24.4	11.5	9.2	80.6
	383	0.7	0.0	0.0	0.2	0.3	141.4
5 u	0	0.0	0.0	0.0	0.0	0.0	0.0
	125	10.9	246.1	504.4	253.8	201.5	79.4
	158	293.1	98.2	89.4	160.2	94.0	58.7
	258	17.0	70.5	12.2	33.2	26.4	79.5
	283	60.9	28.5	67.2	52.2	16.9	32.4
	308	32.1	20.0	0.0	17.4	13.2	76.3
	333	4.6	0.0	0.0	1.5	2.2	141.4
	383	21.3	0.0	0.0	7.1	10.1	141.4

* u indicates tillage direction is upslope, d indicates tillage direction is downslope.

Table 4.1 continued...

Plot	Distance Along Sampling Transect (cm)	Chloride ($g\ m^{-2}$)				Standard Deviation	CV %
		Left	Centre	Right	Combined Mean		
6 u	0	0.0	0.0	0.0	0.0	0.0	0.0
	125	3.3	650.6	301.2	318.4	264.5	83.1
	158	191.5	25.3	240.1	152.3	92.0	60.4
	258	281.9	113.8	231.9	209.2	70.5	33.7
	283	24.1	35.7	99.4	53.1	33.1	62.4
	308	20.2	0.0	52.2	24.2	21.5	89.0
	333	21.2	0.6	40.8	20.8	16.4	78.8
	383	0.0	0.0	0.0	0.0	0.0	0.0
7 d	0	0.0	0.0	0.0	0.0	0.0	0.0
	125	179.6	171.8	15.6	122.3	75.5	61.7
	158	262.1	313.3	82.9	219.4	98.8	45.0
	258	64.4	93.5	59.4	72.4	15.0	20.8
	283	69.7	22.9	200.2	97.6	75.0	76.8
	308	65.9	13.3	224.5	101.3	89.8	88.7
	333	48.2	28.5	20.3	32.3	11.7	36.3
	383	5.5	0.0	0.0	1.8	2.6	141.4
8 d	0	0.0	0.0	0.0	0.0	0.0	0.0
	125	80.8	58.2	34.2	57.7	19.0	32.9
	158	249.4	159.1	82.0	163.5	68.4	41.8
	258	14.4	70.9	131.4	72.2	47.8	66.2
	283	197.5	115.2	34.3	115.6	66.6	57.6
	308	165.4	44.9	13.0	74.4	65.6	88.2
	333	11.9	17.2	6.8	11.9	4.2	35.5
	383	0.0	0.0	16.6	5.5	7.8	141.4
9 d	0	0.0	2.4	0.0	0.8	1.1	141.4
	125	282.1	16.0	91.8	130.0	111.9	86.1
	158	479.9	33.4	150.7	221.3	189.0	85.4
	258	46.9	177.5	300.4	174.9	103.5	59.2
	283	113.6	51.3	63.4	76.1	27.0	35.4
	308	65.7	22.6	53.3	47.2	18.1	38.4
	333	54.2	26.4	0.9	27.1	21.8	80.3
	383	13.0	7.7	16.2	12.3	3.5	28.3
10 u	0	0.0	0.2	0.0	0.1	0.1	141.4
	125	67.3	57.9	223.5	116.2	75.9	65.3
	158	141.2	98.3	604.2	281.2	229.1	81.4
	258	97.4	63.2	43.7	68.1	22.2	32.6
	283	13.9	190.6	35.2	79.9	78.8	98.6
	308	14.2	0.0	11.1	8.4	6.1	72.3
	333	15.3	2.7	55.0	24.3	22.3	91.7
	383	0.0	4.3	7.5	3.9	3.1	77.9

Table 4.1 continued...

Plot	Distance Along Sampling Transect (cm)	Chloride (g m^{-2})				Standard Deviation	CV %
		Left	Centre	Right	Combined Mean		
11 d	0	0.0	0.0	0.0	0.0	0.0	0.0
	125	713.8	752.9	91.9	519.5	302.8	58.3
	158	172.9	184.2	284.8	213.9	50.3	23.5
	258	176.2	134.6	5.2	105.3	72.8	69.1
	283	111.2	47.0	30.1	62.8	34.9	55.7
	308	48.8	50.7	29.7	43.1	9.5	22.0
	333	66.5	42.6	7.1	38.7	24.4	63.1
	383	19.9	10.2	4.2	11.4	6.5	56.9
12 d	0	0.0	0.0	0.0	0.0	0.0	0.0
	125	135.2	22.8	174.3	110.8	64.2	58.0
	158	528.7	61.9	123.5	238.0	207.0	87.0
	258	24.2	376.5	43.1	147.9	161.8	109.4
	283	31.4	91.8	167.3	96.8	55.6	57.4
	308	64.7	102.5	106.4	91.2	18.8	20.6
	333	2.5	80.5	23.3	35.4	33.0	93.2
	383	14.5	6.4	0.0	7.0	5.9	85.4
13 u	0	0.0	0.0	0.0	0.0	0.0	0.0
	125	299.8	0.0	889.3	396.4	369.4	93.2
	158	716.7	11.8	628.0	452.1	313.5	69.3
	258	119.1	296.4	80.1	165.2	94.1	57.0
	283	43.1	185.5	324.7	184.5	115.0	62.3
	308	19.7	36.8	7.3	21.2	12.1	56.8
	333	9.1	18.7	3.6	10.4	6.2	59.7
	383	0.0	0.0	0.0	0.0	0.0	0.0
14 u	0	0.0	0.0	0.0	0.0	0.0	0.0
	125	263.5	298.3	458.2	340.0	84.8	24.9
	158	439.3	184.2	328.6	317.4	104.5	32.9
	258	145.8	100.8	92.8	113.1	23.3	20.6
	283	175.3	66.4	63.9	101.9	52.0	51.0
	308	4.2	22.4	55.7	27.4	21.3	77.6
	333	25.2	0.0	9.9	11.7	10.4	88.5
	383	0.0	0.0	0.0	0.0	0.0	0.0

$$y := \begin{bmatrix} 49 \\ 125 \\ 157.8 \\ 257.8 \\ 282.8 \\ 307.8 \\ 332.8 \\ 382.8 \end{bmatrix} \quad c := \begin{bmatrix} 0.000 \\ 289.657 \\ 179.574 \\ 108.895 \\ 36.849 \\ 9.015 \\ 3.994 \\ 1.261 \end{bmatrix}$$

location: plot 1 tillage1
chloride (grams meter $^{-2}$)
averaged for each y value

y = distance along sampling transect (cm)
c = chloride concentration (g m $^{-2}$)

pre-tillage boxcar distribution

the initial concentration of chloride was 305 grams meter $^{-2}$

$pt := 305$

$rp := 0..305 \qquad p := \begin{bmatrix} 50 \\ 232.8 \end{bmatrix}$

$xx := 50..232.8$

$boxcararea := 55754$

$i := 0..12 \qquad x := y^{<0>}$

$root1 := 49$ first sampling point

$ci := lspline(x, c) \qquad rx := -250..500$

$cl(rx) := interp(ci, x, c, rx)$

$root2 := 382.3$ last sampling point

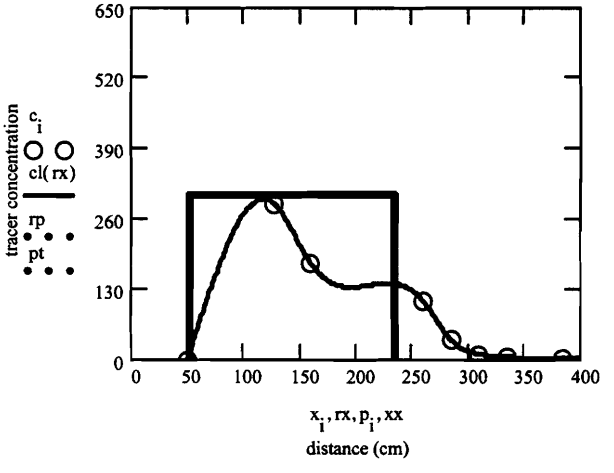

$$area := \int_{root1}^{root2} cl(x)\,dx \qquad area = 3.923 \cdot 10^4$$

area under curve post-tillage

$$mean := \left(\frac{1}{area}\right) \cdot \int_{root1}^{root2} cl(x) \cdot x\,dx \qquad mean = 156.011$$

chloride centre of mass along sampling transect

$$var := \left[\int_{root1}^{root2} cl(x)\,(x - mean)^2\,dx\right] \cdot \left(\frac{1}{area}\right) \qquad var = 3.736 \cdot 10^3$$

calculated variance

$$totalrecov := \frac{area}{boxcararea} \qquad totalrecov = 0.704$$

chloride recovery

Figure 4.3 Example of a Mathcad® worksheet.

During the spline fitting and graphing operation it became obvious that the first sampling point at the zero position along the sampling path (Figure 4.2) was heavily weighting the graphic outcome. The spline function regularly appeared to over-estimate both the chloride in front of the plot (i.e., from 0- to 0.50-m along our sampling path) and the chloride remaining in that portion of the plot first struck by the tillage implements. This in turn caused the post-tillage centre of mass to be shifted towards the left of the graph. This over-estimation is believed to be due to the great difference between the very low chloride values at the zero position and the very high values at the next sampling position (1.25 m), coupled with the lack of sampling points across this span of 1.25 m. Had there been more sampling points within this span, the problem would not have arisen.

In order to counter this over-estimation by the spline function, a decision was taken to begin graphing just outside the plot boundary at 0.49 m, rather than at 0 m. Essentially this meant accepting the assumption that redistribution of chloride occurred only in the direction of tillage. This seemed a valid decision for the following reasons:

1. Only two of the fourteen plots show any chloride at the first sampling position (plots 3 and 9) (Table 4.1). The chloride identified at these points is a minor amount of the total applied to the plot, less than 0.6 % of the applied 305.0 g m^{-2}.

2. The chloride at these points may be the result of back translocation or it may be due to irregular broadcast of the granular KCl, or improperly re-locating the plot boundaries following tillage.

Back translocation would be expected to play a minor role in the tillage redistribution process and ignoring this would introduce negligible error into the calculations. Lobb et al. (1999), in a similar tillage experiment, assumed that back translocation would be insignificant. The results from their investigations suggested that back translocation from cultivation with a field cultivator using a C-tine shank would only occur at slopes with a slope tangent of 1.0 or greater.

Figure 4.4A shows an example of the spline fit where the graph is initiated at the zero position along the sampling path (0.50 m before the plot). Clearly seen is the chloride mass that is represented to the left of the plot area (the initial application pulse).

Figure 4.4B shows the same data where the graph is initiated at 0.49 m along the sampling transect at each plot; the over-estimation of the chloride to the left of the plot has been removed.

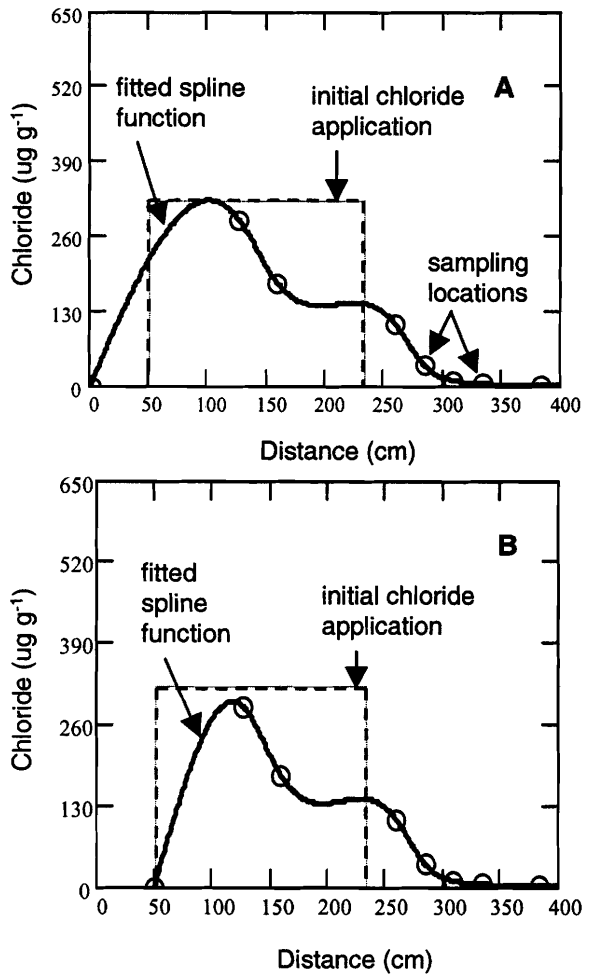

Figure 4.4 Fitting a spline function to the data from Tillage Experiment No.1. In Figure 4.4A the data is graphed from 0, the actual sampling position; and in Figure 4.4B the graph is initiated at 49 cm, just outside the plot.

In this chapter the impact of different tillage operations are reported using three different measures of soil translocation:

1. The experimentally determined mean displacement value ($\overline{d}$) of the tracer, which varies with slope, soil and implement properties, as well as slope-implement interaction. This is calculated using the spline function as noted above.

2. The unit soil transport flux (T_M) for a single tillage pass at a single location (equation 4.4). This measure converts the mean displacement value into a mass of soil transported per meter of tillage width (kg m^{-1}) using the depth of tillage and soil bulk density (Lobb et al., 1999).

3. The proportionality coefficient, k (kg m^{-1}) (equation 4.6) provides a landscape averaged measure of the net relationship between tillage flux and slope gradient, assuming tillage in both the upslope and downslope directions.

4.3.6. Results and Discussion

At any position along the tillage path, the chloride concentrations at individual sampling points at the left, centre, and right side of the plot can be highly variable (Table 4.1). The pattern of variability along the tillage path, as expressed by the coefficients of variation, differs between plots.

The variability may be due to inconsistent tracer application but visual field observations at the time did not detect this. In an effort to confirm the actual application rate of the tracer, single cores were collected in the centre of the non-tilled area between the paired plots at four locations along the study transect. These samples were collected after all other samplings had been completed. At two of these locations the chloride concentration in the sample was approximately 80% of that applied, while at the other two locations the results showed approximately 40% of the application concentration. The difference between these values should be viewed with caution as the sites had been disturbed by foot and vehicle traffic during the plot sampling and it is not certain that the samples are representative.

A second and more likely cause of this variability, assuming a consistent tracer application, is that the post-tillage pattern of the surface applied tracer has an underlying pattern linked to the design of the tillage unit, i.e., point sampling may reflect the variability introduced at the micro-topographic level by the tillage implement. Soil displacement has been shown to be greatest at the centre of the cultivator shovel and rapidly decreases towards the wing tips (Sharifat and Kushwaha, 1997). Thus redistribution of the surface tracer will depend on its in initial placement relative to the tillage implement. In addition, tillage with a cultivator produces a micro-topography of furrows and mounds. Sharifat (1999) has shown that as tillage speed is increased the

distance material is thrown laterally from the furrow is also increased. At tillage speeds in excess of 3.6 km h^{-1} most of the particles that are thrown sideways will remain in the mound and will not fall back into the furrow (McKyes, 1985). The tillage speed in this experiment was approximately 8 km h^{-1}. Thus point sampling may give very different results depending on whether the sample is collected from the furrow or the mound. The inability to detect a consistent pattern in the variability along the tillage pathway may be due to the scale at which samples were collected.

Chloride recovery, mean tracer displacement distance, and topographic properties for each of the fourteen plots are presented in Table 4.2. Following the methodology employed by Gerontidis et al. (2001), Govers et al. (1994), Lindstrom et al. (1992), Lindstrom et al. (1990), Quine et al. (1999) and van Oost et al. (2000) the displacement distance is graphed against the tangent of the slope gradient in Figure 4.5 to Figure 4.7. Tillage upslope is indicated by a positive tangent, whereas a negative tangent indicates tillage in the downslope direction. In these figures the data show a clear trend of greater displacement when tillage is downslope on steeper gradients. The least displacement occurs when tillage is in the upslope direction on a steep gradient. This pattern is similar to that observed by the researchers cited above.

The mean displacement value ranges from 0.02 to 0.69 m at individual plots (Table 4.2). Clearly, shoulder and backslope elements occupy the extremes of the data set with level elements occupying the mid-range (Figure 4.5, Figure 4.6). The values for mean displacement distance found in the literature rarely exceed 0.80 meters (Table 4.3).

The slope of the linear regression function between the mean tracer displacement distance and the tangent of the slope gradient provides the value *B* used in equation 4.6. This value is the basis of the tillage translocation coefficient (*k*). Assuming that depth of tillage and bulk density are constant through a given field then the *B* value alone can be used to compare the general relationship between slope gradient and translocation across different fields and different tillage implements.

Table 4.2 Summary results and topographic properties for each plot in Tillage Experiment No.1.

Location	Nominal Tillage Direction	Tangent of the Slope Gradient	Profile Curvature ($^{O}m^{-1}$)	Plan Curvature ($^{O}m^{-1}$)	Aspect (^{O})	Landform Element	Chloride Recovery Total (%)	Chloride On Plot (%)	Chloride Off Plot (%)	Mean Displacement (m)	Bulk Density (g cm^{-3})	T_M* (kg m^{-1})
1	upslope	0.079	-0.01	4.61	235.5	DBS	71.5	61.0	10.6	0.15	1.54	18.0
2	upslope	0.043	-0.04	-4.79	152.6	LEV	47.6	37.1	10.5	0.55	1.49	65.8
4	upslope	0.085	0.08	-0.39	190.4	CBS	129.5	121.0	8.5	0.03	1.58	4.1
5	upslope	0.091	0.11	-0.50	203.7	CSH	51.5	45.9	5.5	0.02	1.59	2.7
6	upslope	0.014	-0.09	-47.35	264.4	LEV	90.9	70.4	20.5	0.27	1.44	31.4
10	upslope	0.019	-0.02	-4.71	287.2	LEV	60.1	48.1	12.0	0.53	1.34	56.9
13	upslope	0.024	-0.05	-27.18	259.6	LEV	123.5	101.2	22.3	0.31	1.49	36.9
14	upslope	0.033	-0.04	-9.45	345.6	LEV	94.3	79.2	15.1	0.24	1.44	27.4
3	downslope	-0.024	0.00	-5.59	313.9	LEV	96.5	82.3	14.2	0.29	1.34	31.5
7	downslope	-0.036	-0.06	0.32	279.0	LEV	58.0	42.0	16.0	0.56	1.49	66.8
8	downslope	-0.078	0.01	3.76	220.3	DBS	41.4	27.1	14.4	0.69	1.53	84.4
9	downslope	-0.046	-0.10	-4.97	173.7	CFS	75.2	53.8	21.3	0.60	1.58	75.2
11	downslope	-0.081	0.08	3.07	184.0	DBS	102.5	87.2	15.3	0.04	1.54	4.6
12	downslope	-0.085	0.14	0.11	204.8	DSH	73.0	51.0	22.1	0.64	1.43	73.7
mean							79.7	64.8	14.9	0.35	1.49	41.4
std dev							27.5	26.6	5.2	0.24	0.08	28.7

* T_M = the unit soil transport flux

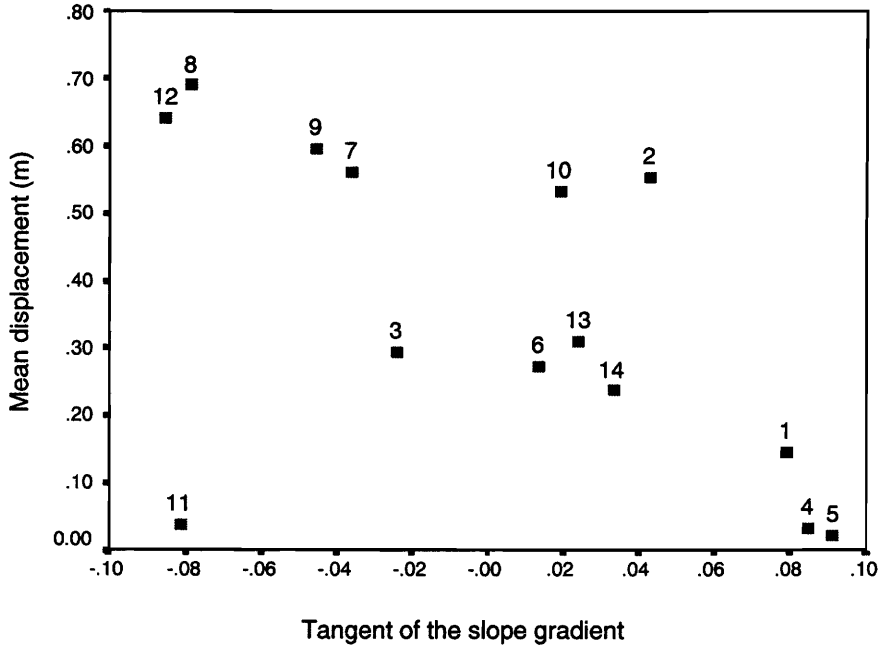

Figure 4.5 Mean tracer displacement versus the tangent of the slope gradient for Tillage Experiment No 1., with data points identified by plot number. Tillage downslope is indicated by a negative tangent.

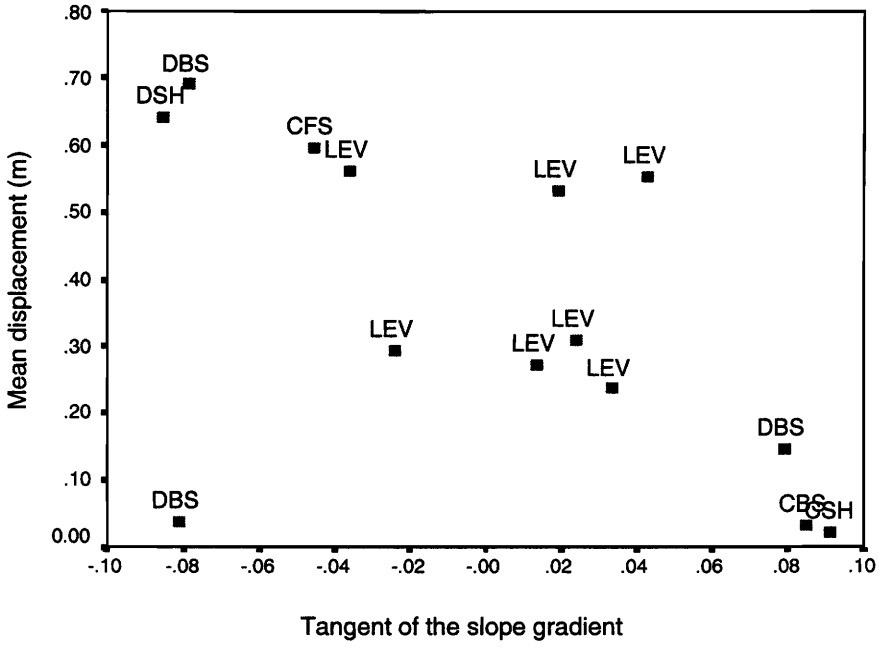

Figure 4.6 Mean tracer displacement versus the tangent of the slope gradient for Tillage Experiment No. 1, with data points identified by landform element. Tillage downslope is indicated by a negative tangent.

Table 4.3 Tillage translocation values from the literature.

Tillage Experiment	Maximum Slope Tangent		Bulk Density	Tillage Speed	Tillage Depth	$\bar{d}$ (m)		B	T_M (kg m^{-1})		k (kg m^{-1})
	Downslope	Upslope	(kg m^{-3})	(km h^{-1})	(m)	min	max		min	max	
Duckfoot Cultivator. Quine et al. ,1999	-0.16	0.16	1382	2.5	0.19	0.15	1.13	-2.30	39.4	296.7	604
Tillage Experiment No.1. This project.	-0.08	0.08	1482	8.0	0.08	0.03	0.69	-2.22	3.6	81.8	263
Chisel Plough. Govers et al., 1994	-0.22	0.22	1350	4.5	0.15	0.20	0.63	-0.55	40.5	127.6	111
C-tine Field Cultivator and Harrows. Lobb et al., 1999	-0.12	0.12	1211	6.5	0.15	0.21	0.47	-0.09	38.1	85.4	16
* Moldboard Plough. Lindstrom et al., 1994	-0.10	0.10	1350	7.5	0.24	0.26	0.52	-1.12	84.2	168.5	363
** Moldboard Plough with Tandem Disc. Lindstrom et al., 1994	-0.08	0.08	1450	7.5	0.24	0.40	0.82	-2.40	139.2	285.4	835
Moldboard Plough. Van Oost et al., 2000	-0.22	0.22	1570	5.4	0.20	0.24	0.72	-0.93	75.4	226.1	292
Moldboard Plough. Govers et al., 1994	-0.22	0.22	1350	4.5	0.28	0.11	0.49	-0.62	41.6	185.2	234
Moldboard Plough. Gerontidis et al., 2001	-0.22	0.22	1420	4.5	0.20	0.02	0.35	-0.54	5.7	99.4	153

* Two tillage operations traveling in the same direction.
** Tillage upslope and then downslope over the same plots.

In Figure 4.7 a linear regression function is fitted to the complete data set giving a *B* value of -2.22. Location 11, however, clearly does not fit the general trend; the difference between this value and its predicted value (using the regression equation) is more than 2.0 standard deviates from the mean predicted difference for all locations and hence it is an outlier in the data set. If Location 11 is removed from consideration then the regression slope (*B*) changes to –3.30, and the R^2 value becomes 0.70.

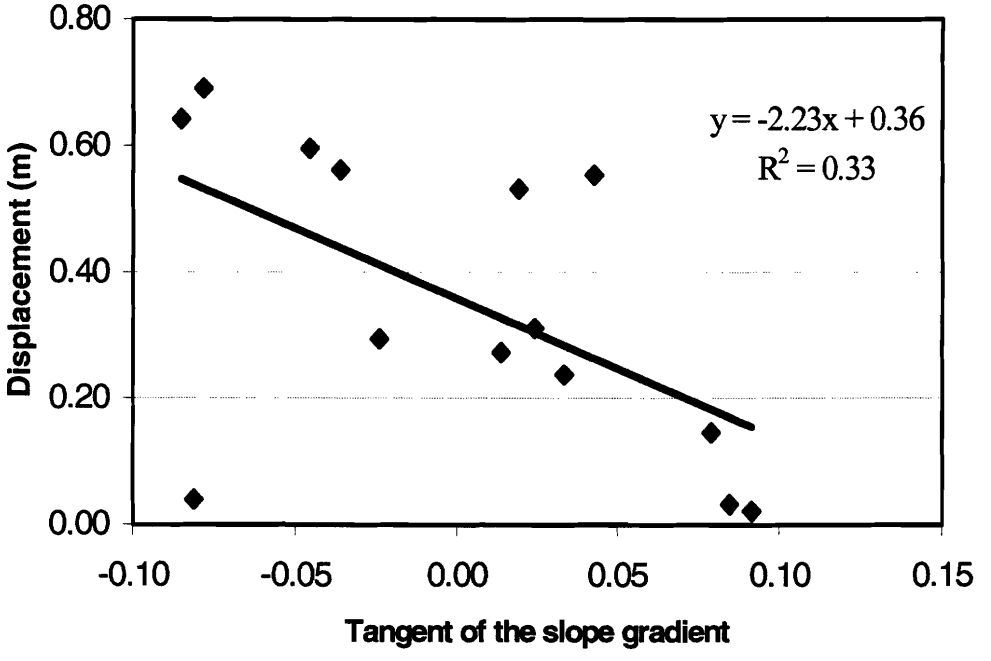

Figure 4.7 Mean displacement distance versus the tangent of the slope gradient with the plotted regression line, Tillage Experiment No.1.

Quine et al. (1999) found a comparable value of -2.30 for *B* when using a similar tillage implement (a 0.26-m wide 'duckfoot cultivator' shovel) on a similar range of slopes. Individual mean displacement values from Quine et al. (1999) range from 0.21 to 1.13 m. In this experiment the measured displacement values ranged from 0.03 to 0.69 m.

Lobb et al. (1999) reported their results from a series of tillage implements that included a field cultivator with a C-tine cultivator shovel of 0.10 m width. For this implement they report tillage displacement distances ranging from 0.21 to 0.47 m over a range of slope tangents from -0.127 to 0.127. Their results show relatively uniform

displacement regardless of slope tangent; a *B* value of -0.09 is obtained from plotting their data. This difference in results may be largely explained by the width of the cultivator shovels used. The very narrow shovel used by Lobb et al. (1999) will tend to slice through the soil with much less disturbance than the wider shovels employed in this experiment and by Quine et al. (1999) (Sharifat and Kushwaha, 1997; Sharifat, 1999).

An additional source of difference between the *B* values determined by Lobb et al. (1999) and Quine at al. (1999) may be the method by which displacement distance is determined. In this experiment and that of Quine at al. (1999), the displacement distance is the calculated as the difference in the centre of the tracer mass before and after tillage. Lobb et al. (1999) calculated the displacement distance from the total volume of tracer recovered (using the convolution method) multiplied by the soil bulk density and then divided by the depth of tillage.

Much of the variability in displacement distance surrounding the trend line in Figure 4.7 may be due to the influence of the complex topography on the behaviour of the tractor-tillage unit (Lobb et al., 1995; Lobb et al., 1999). Topography before or behind the plot may influence the alignment of the tillage unit thus changing the depth of tillage and the potential for redistribution. Quine et al. (1999) discuss their own experience in which topography-tillage unit interaction influenced the depth of the tillage operation and thus the degree of mixing and drag experienced on the plot. Another source of variability may be that reported slope gradients do not represent the true tillage gradient (as discussed above in section 4.3.2 on experimental design).

The *B* values presented in Table 4.3 show that the displacement distances attained by the field cultivator used in this experiment and that used by Quine at al. (1999) are more highly responsive to slope gradient than all other experiments employing a single tillage pass. These higher values for *B* suggest considerable differences in local displacement distance in response to changing slope gradient. If Location 11 is excluded from the results of this experiment, the resulting *B* value of -3.30 exceeds all others encountered in the literature. Given the speed of tillage in this experiment, and the relatively shallow depth of tillage (0.08 m), it is not altogether surprising that a change in slope gradient would show a strong influence on

displacement distance.

As noted above, measures of soil translocation ($\bar{d}$, T_M, k) are subject to a variety of influences including the soil bulk density, depth of tillage, implement type, tillage speed and the range of slopes encountered. The experimental results presented in the literature are difficult to compare directly because of these differences. However, it is apparent from Table 4.3 that the translocation encountered in this experiment is well within the range of that observed in the literature.

The value for T_M (the mass of soil moved per meter width of tillage, equation 4.4) is reliant on the soil bulk density and depth of tillage for its calculation and is best used to compare translocation at individual locations within fields. In the calculation of T_M, the value for $\bar{d}$ is believed to reflect the mean displacement distance of the entire plough layer (Poesen et al., 1997). However, in this experiment the tracer is applied only at the surface, and was not subsequently mixed through the plough layer prior to tillage. This is different to the methodology employed by other authors who placed the tracer uniformly through the depth of the plough layer. Thus the values presented for T_M from this experiment (Table 4.2) using a plough depth of 0.08 m, must be viewed with care when compared to those in the literature (Table 4.3).

The proportionality constant, k, can be used as a single value by which to compare the impact of different cultivation systems across a landscape (van Muysen et al., 2000). However, as with T_M, the k value relies in part on tillage depth in its calculation and assumes that any tracer has been applied equally through the full plough depth. Thus, these values too must be viewed with care as noted above. In this experiment, k was determined to be 263 kg m^{-1}, which is very close to the values of 282 and 275 kg m^{-1} reported by van Muysen et al. (2000) for a duckfoot chisel plough employed by Poesen et al. (1997) and a chisel plough used by Lobb et al. (1999).

Although the plots in this experiment were paired and only a few meters apart, the distribution of landform elements among the plots is different for the two groups and in many cases there are only single representatives of some landform elements. The low sample numbers and uneven distribution do not allow for data analysis on a landform

basis, instead the results are simply grouped by the direction of tillage as shown in Figure 4.8. Figure 4.8 clearly shows the difference in soil displacement between upslope and downslope tillage in this experiment.

Tracer recovery, determined using the mean values from the combined samples, was highly variable, ranging from 0.4 to 1.3 times that initially applied. This is similar to the range of recovery noted by Lobb et al. (1999) (0.39 to 1.04) who suggest that the variability in tracer recovery has no net effect on the accuracy of the results, but that improvements are needed in the method used to measure translocation. Figure 4.9 shows the range of chloride recovery as grouped by tillage direction.

Figure 4.8 The mean tracer displacement for Tillage Experiment No.1, with data grouped by tillage direction.

4.3.7. Conclusions

The results support the general relationship between mean displacement distance and slope gradient that is reported in the literature, i.e., the greatest displacement occurs with downslope tillage on a steep slope, and the least displacement occurs with upslope tillage on a steep slope. In this experiment, reported slope gradient can account for 70%

of the variability in mean tracer displacement among the plots.

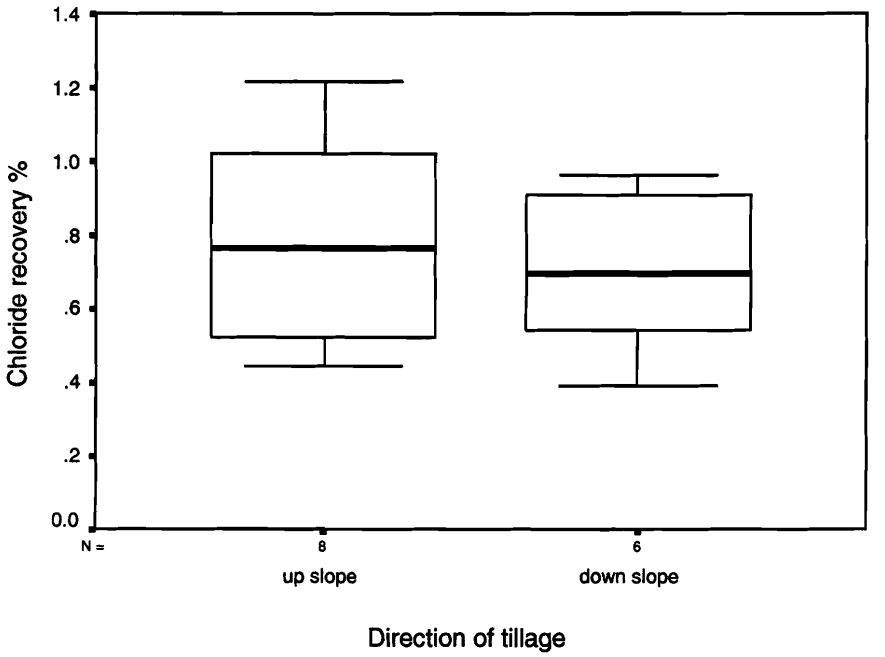

Figure 4.9 Chloride recovery (%) for Tillage Experiment No.1, with data grouped by tillage direction.

Variability about the trend line for tillage displacement versus tangent of the slope gradient (Figure 4.7) may be the result of interaction between complex topography and the tractor-tillage unit. Topography before or behind the plot may influence the alignment of the tillage unit, thus changing the depth of tillage and the potential for redistribution. The wide range in tracer recovery values may also be an artefact of topography-implement interaction as changes in tillage depth impact the amount of labelled soil that is taken off plot and the amount of non-labelled soil added to the plots.

Variability in tracer concentration across the width of the tillage path suggests that the lateral redistribution of the surface applied tracer is largely an artefact of the implement design and tillage speed. The averaging of the three sampling points across the sampling path may not provide an accurate mean of the chloride concentration. To overcome the limitations of the point sampling method, a unit area sampling approach may be considered (Quine et al., 1999).

Comparison of k values (the tillage transport coefficient) suggests that averaged over the entire landscape, this tillage operation is as erosive as others are that have twice the tillage depth (Table 4.3). As shown in equation 4.6, the value for k relies on the depth of tillage, the soil bulk density, and the relationship between the mean displacement distance and tangent of the slope gradient (B) to define it. Given that the depth of tillage in this experiment is approximately half that employed by other researchers, the similarity in k values must be due to the greater bulk density and the comparatively large B value. The comparatively large B value suggests that, given the type of tillage operation and landscape conditions found in this experiment, there can be considerable variation in local soil displacement in response to changes in slope gradient and tillage direction.

4.4. Tillage Experiment No. 2

4.4.1. Introduction

In Tillage Experiment No. 1 the investigative focus was on the translocation of materials at the soil surface. Crop residues, surface applied fertilizers and pesticides, and other materials at the soil surface may respond differently to tillage events than the bulk soil of the plough layer. To facilitate this investigation a fertilizer-like granular tracer was applied to the soil surface and its distribution monitored following tillage. In Tillage Experiment No. 2 the investigative focus is on the bulk soil materials that are an integral part of the plough layer. In this experiment, 3 L of potassium chloride solution were applied to the surface of twelve $1m^2$ plots, from which all surface litter had been removed, in order to label the upper portion of the plough layer. Again, the primary objective of this experiment was to assess the influence of topography on tillage-induced translocation in the study environment.

Unlike the work of earlier researchers, the tillage direction at each plot location in this experiment was not deliberately aligned with the maximum slope. Rather, the tillage direction across the field remained fixed and the aspect, gradient, profile and plan curvature varied at each plot. This approach was taken to reproduce the conditions

encountered in farming operations, when tillage direction is often determined by field boundaries and at any location within the field, tillage direction can vary from the maximum slope direction.

4.4.2. Experimental Design

In this experiment (Tillage-2), twelve $1m^2$ plots were arranged in two rows of six plots each (Figure 4.10). Each row was 125 m long and aligned north to south on a dominantly south facing slope with complex topography; within each row, the plots are 25 to 30 m apart. The two rows are separated by 15 m. The study site was in summerfallow and had been tilled once using the same tillage implement approximately one month earlier. The previous crop was wheat. This experiment was located in the same part of the study field (SE-24-37-2-W3) used for Tillage Experiment No. 1 (Tillage-1).

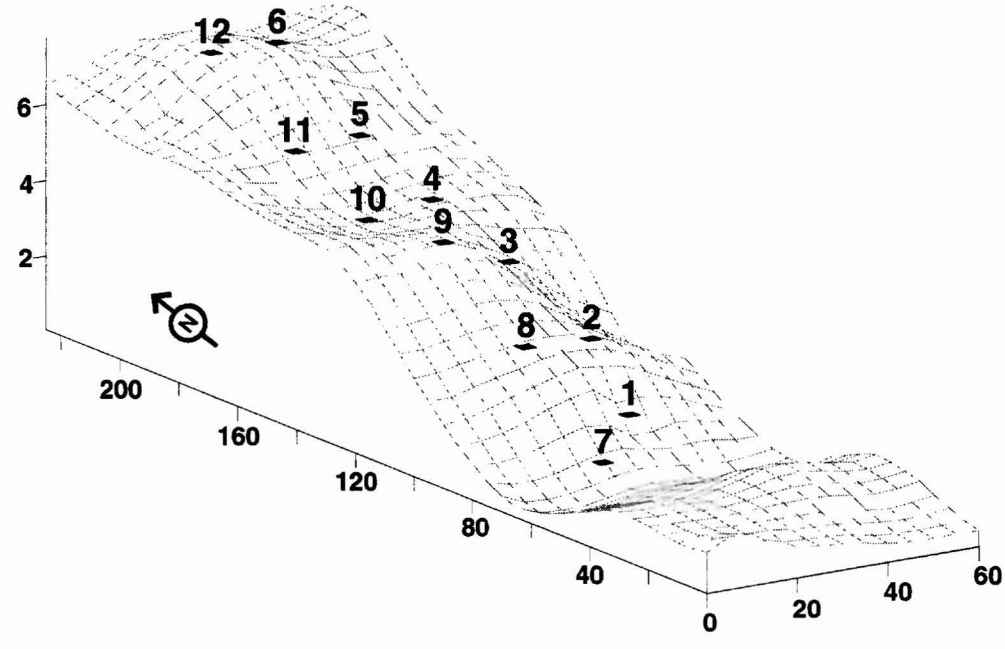

Figure 4.10 Wireframe image of the study area for Tillage Experiment No.2 showing the location of individual plots. Axes units are in meters.

Using a watering can, chloride was carefully applied to each plot (267 g m^{-2}) as three litres of potassium chloride aqueous solution. To sharply define the plot area and to prevent any solution from flowing off the plot before it could infiltrate the surface, a metal frame 100 x 100 x 15 cm was placed around the plot and forced below the soil surface to a depth of approximately 2 cm.

Two hours after the KCl solution was applied the plots were tilled using a 15.2 m wide cultivator with 0.40-m wide V-shaped shovels on 0.35-m centres and a spring loaded tine harrow with tines on 0.15-m centres. Tillage speed was estimated at 10.5 km h^{-1}. Tillage depth varied from 0.08- to 0.10-m. The westerly row was tilled from the north to the south (nominally in the downslope direction) and the easterly row of plots was tilled from the south to the north (nominally in the upslope direction).

4.4.3. Sampling Procedures

At each plot, post-tillage sampling was conducted as shown in Figure 4.11. Cores were taken of the 0- to 0.10-m plough depth using a hand held coring device of 0.02-m diameter. At set distances along the tillage pathway four individual samples were collected at 0.20 m intervals across the 1 m width of the plot. Each group of four samples was combined in the field. The Cl^- concentration in each bulked sample represents the mean tracer concentration at intervals along the tillage pathway and within the 1-m span defined by the plot width. This gave 10 combined samples collected at each plot.

To assess the amount of tracer that had been redistributed laterally (perpendicular to the tillage direction) beyond the 1-m plot width represented by the combined samples, additional sampling was conducted at plots 5, 6 and 10. Sampling design is shown in Figure 4.11. For this sampling, a core of 0.047-m diameter was used.

4.4.4. Laboratory Procedures

Soil samples were air dried, weighed and ground to pass through a 2-mm sieve. Chloride content was determined colormetrically using a Technicon® AutoAnalyzer®. Following the method of Janzen (1993) a 2:1 solution of de-ionized water:soil was mixed and shaken for 1 h. The mixture was filtered to remove solids and the extract

compared against known standards for chloride content using the AutoAnalyzer®.

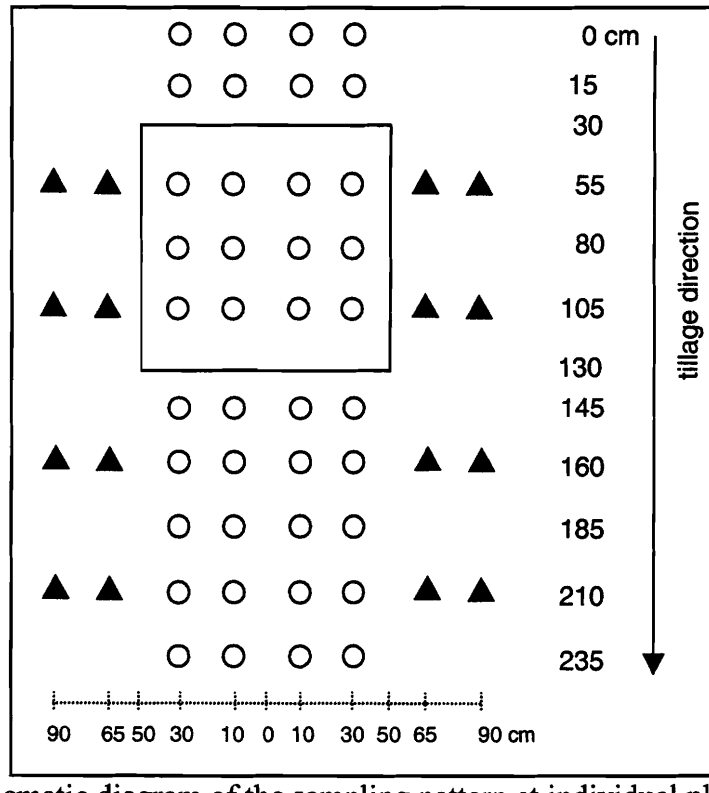

Figure 4.11 Schematic diagram of the sampling pattern at individual plots in the Tillage-2 experiment, showing the 1.0-m^2 plot and the sampling points. Circles indicate points sampled at all plot locations. The four samples (O) collected at each set distance along the tillage pathway were combined in the field and treated as one. Triangles indicate sampling points at selected plots to assess lateral movement of the chloride tracer.

4.4.5. Data Analysis

The measured chloride concentration (ug g^{-1}) for each sample was reduced by the background threshold value of 25 ug g^{-1}. The results were converted to a mass per area basis using the soil bulk density and 0.10-m sampling depth. The data from the combined cores for each plot are presented in Table 4.4 .

Mean translocation distance was determined as the difference between the centre of the chloride mass before tillage and after tillage. To establish the chloride centre of mass following tillage, the mean chloride concentration from the combined samples

Table 4.4 Chloride concentration for combined samples at set positions along the tillage pathway, Tillage Experiment No.2.

Plot	Distance Along Sampling Pathway	Chloride ($g\ m^{-2}$)	Plot	Distance Along Sampling Pathway	Chloride ($g\ m^{-2}$)	Plot	Distance Along Sampling Pathway	Chloride ($g\ m^{-2}$)
1 u*	0	0.0	5 u	0	0.0	9 d	0	0.0
	15	11.5		15	4.8		15	0.0
	55	183.9		55	126.2		55	79.3
	80	189.5		80	140.8		80	152.0
	105	72.5		105	121.2		105	60.9
	145	29.6		145	45.8		145	30.7
	160	35.8		160	22.8		160	53.0
	185	6.3		185	41.6		185	20.5
	210	1.2		210	5.7		210	7.3
	235	1.3		235	3.5		235	1.4
2 u	0	0.0	6 u	0	0.0	10 d	0	0.0
	15	0.0		15	0.0		15	0.0
	55	83.8		55	46.6		55	109.1
	80	239.3		80	86.3		80	161.2
	105	136.6		105	126.0		105	139.2
	145	86.1		145	62.0		145	138.9
	160	34.5		160	28.5		160	60.9
	185	44.3		185	16.8		185	48.4
	210	22.2		210	17.0		210	16.0
	235	15.1		235	5.0		235	24.3
3 u	0	0.0	7 d*	0	0.0	11 d	0	0.0
	15	0.0		15	0.0		15	0.0
	55	131.6		55	97.4		55	78.3
	80	210.0		80	221.8		80	178.3
	105	74.1		105	180.8		105	160.6
	145	23.9		145	94.8		145	53.1
	160	42.2		160	80.9		160	40.2
	185	15.5		185	32.6		185	35.1
	210	12.4		210	4.7		210	25.6
	235	2.1		235	10.3		235	8.3
4 u	0	0.0	8 d	0	0.0	12 d	0	0.0
	15	0.0		15	0.0		15	0.0
	55	167.8		55	107.5		55	155.3
	80	185.3		80	73.4		80	145.4
	105	103.5		105	147.2		105	131.5
	145	212.8		145	103.6		145	42.6
	160	36.2		160	77.2		160	16.1
	185	54.8		185	15.0		185	16.1
	210	13.6		210	25.8		210	16.9
	235	13.3		235	15.5		235	13.9

* u indicates tillage direction is upslope, d indicates tillage direction is downslope.

(Table 4.4) was graphed against distance along the tillage path and a function fit to these points using the computer program Mathcad® 8 Professional. A spline function was used to predict the continuous chloride concentration between the sampling points. The

area under the spline function was integrated, allowing for the chloride recovery and centre of mass to be determined.

In Table 4.5, the results from the lateral sampling at plots 5, 6, and 10 are presented in conjunction with the matching data from the combined samples at the same distance along the tillage pathway (see Figure 4.11). The approach used to estimate the proportion of chloride tracer moved laterally, beyond the 1 m width of the plot, is illustrated in Figure 4.12. The estimate is made by linearly interpolating the tracer concentration from the value determined for the bulked samples (central value) to the lateral points, and then assuming the area affected by this concentration is equal to the lateral distance between points multiplied by one half the distance to the next sampling point both in the direction of tillage and opposite to the direction of tillage. The volume of each lateral section is calculated giving a result in grams of chloride. This value is then divided by the mass of chloride originally applied to give the proportion recovered.

Table 4.5 Chloride tracer concentrations at lateral sampling points and from combined samples along central tillage pathway.

		Chloride Tracer ($g\ m^{-2}$)				
Plot	Distance Along Sampling Transect (cm)	West 40 cm	West 15 cm	Central	East 15 cm	East 40 cm
5 u*	55	0	0	25.2	0	0
	105	0	0	121.2	6.9	0
	160	0	0	22.8	0	0
	210	1.6	0	5.8	0	0
6 u	55	0	0	17.3	0	0
	105	0	0	126.0	0	0
	160	0	0	28.5	40.0	0
	210	0	0	17.0	37.2	4.5
10 d	55	0	0	31.9	0	0
	105	0	26.6	139.2	2.6	0
	160	0	50.4	60.9	0	0
	210	0	13.2	16.0	0	0

* u indicates tillage upslope, d indicates tillage downslope

Topographic properties were extracted from a digital elevation model constructed with a 5x5 meter grid size. Plots are assigned the topographic properties that are averaged over the 5x5 meter cell in which they are found. Landform classification into landform elements and landform element complexes was done

following Pennock et al. (1994b) and Pennock et al. (1987).

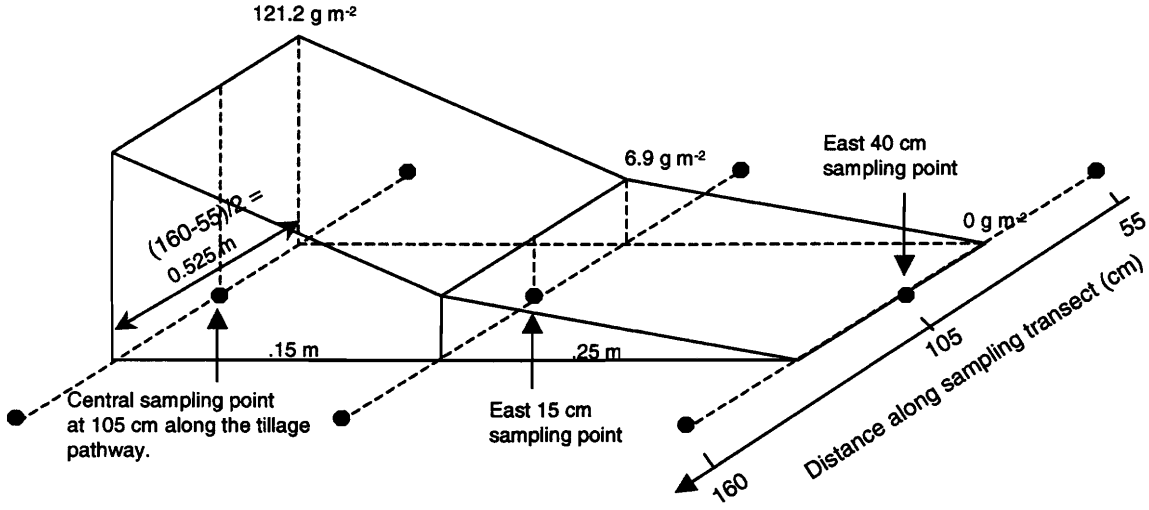

Figure 4.12 An example of the conceptual approach used to estimate the proportion of chloride tracer transported perpendicular to tillage direction in Tillage Experiment No. 2 (Plot 5). The volume calculated for each segment has units in grams. Dividing this number by the total mass of chloride initially applied gives the proportion of chloride recovered.

4.4.6. Results and Discussion

Mean recovery of the chloride tracer in the Tillage Experiment No.2 (59%, Table 4.6) was lower than that found in Tillage Experiment No.1 (80%, Table 4.2). The lower recovery probably reflects the smaller plot size used in the second experiment. The smaller plot would be expected to have greater off-plot translocation of the tracer, and a greater dilution within the plot from material moved on. The results support these expectations; Tillage-1 has 65% of the applied Cl^- recovered on plot with 15% recovered off the plot, a ratio of 4.3:1. Tillage-2 has 34% of the applied Cl^- recovered on plot with 25% recovered off the plot, a ratio of 1.4:1. The values for chloride recovery off plot do not include any estimates of laterally redistributed chloride.

Table 4.6 Topographic characteristics and tracer translocation results for Tillage Experiment No.2.

Location	Nominal Tillage Direction	Tangent of the Slope Gradient	Profile Curvature ($^{O}m^{-1}$)	Plan Curvature ($^{O}m^{-1}$)	Aspect (^{O})	Landform Element	Chloride Recovery Total (%)	Chloride On Plot (%)	Chloride Off Plot (%)	Mean Displacement* (m)	Bulk Density (g cm^{-3})	T_M (kg m^{-1})
1	upslope	0.14	0.14	-4.64	167.7	CSH	55.0	40.5	14.5	-0.01	1.23	-1.3
2	upslope	0.05	0.04	6.15	128.7	DBS	65.2	39.2	26.1	0.28	1.19	26.2
3	upslope	0.10	0.13	-0.91	121.4	CSH	49.6	33.0	16.6	0.10	1.20	9.3
4	upslope	0.02	-0.01	9.45	191.9	LEV	84.5	50.9	33.6	0.25	1.29	26.2
5	upslope	0.08	-0.08	1.01	182.9	DBS	55.1	33.3	21.8	0.16	1.21	15.4
6	upslope	0.03	0.07	8.66	92.0	LEV	41.9	13.7	28.2	0.32	1.22	30.8
7	downslope	-0.10	-0.10	2.90	191.0	DBS	72.1	46.5	25.7	0.25	1.29	26.2
8	downslope	-0.07	0.01	2.04	189.2	DBS	60.8	27.0	33.9	0.30	1.31	31.9
9	downslope	-0.04	0.19	11.17	141.1	DSH	38.2	14.2	24.0	0.19	1.30	19.4
10	downslope	-0.01	-0.03	-21.56	255.4	LEV	71.8	38.3	33.5	0.31	1.19	29.2
11	downslope	-0.09	-0.06	1.85	189.4	DBS	59.2	34.4	24.7	0.28	1.26	28.0
12	downslope	-0.03	0.23	4.73	233.3	DSH	58.5	40.7	17.8	0.13	1.22	12.5
mean							59.3	34.3	25.0	0.21	1.24	21.1
std dev							13.0	11.4	6.6	0.10	0.04	10.2

* A negative sign on mean displacement distance indicates displacement behind the direction of travel.

The lateral redistribution of Cl^-, i.e., perpendicular to the direction of tillage, is shown in Table 4.5. Although the data set is limited, it appears to show two different patterns of lateral displacement. The data for plot 5 suggest a pattern of random lateral movement, possibly the result of a non-uniform mixing process. The data for plots 6 and 10 show the displaced Cl^- to be dominantly skewed towards one side of the tillage pathway. This pattern may be explained to some extent by looking at the dominant slope aspect for each plot. At plot 5 slope aspect is 182°, suggesting that tillage is dominantly straight up and down the slope, not across the slope. However, at plot 6, slope aspect is 92°, and at plot 10 it is 255° indicating that tillage is largely across the slope in both cases. For both plots 6 and 10, the pattern of laterally dispersed Cl^- is skewed towards the downslope side of the tillage path.

For plots 5, 6 and 10 there is no lateral displacement of Cl^- at the 55 cm position. However, as the implement moves forward we observe relatively higher concentrations of laterally moved tracer and the occurrence of tracer at greater lateral distance. This pattern is consistent with field observations, and reports in the literature, of a mixing action just ahead of the cultivator shovel and a lateral movement of soil over the shovel wings as the implement continues to drag the soil forward (Poesen et al., 1997; Sharifat and Kushwaha, 1997). The estimated amount of tracer moved laterally to the tillage pathway at plots 5, 6, and 10 was 5, 8, and 11 %, respectively, or 8% on average.

In Figure 4.13, translocation distance is graphed against slope gradient; in Figure 4.13A the data points are labelled with the plot number, and in Figure 4.13B the points are labelled with the landform element. In these images, the plots tilled in the upslope direction show a distinct linear pattern with greater displacement as slope gradient decreases. For those plots tilled in the downslope direction the pattern is much less clear. Downslope tillage does not show the clear linear pattern observed in the literature or the Tillage Experiment No.1.

If we examine the results by landform element, we see that level and backslope plots, have a relatively constant displacement distance, showing little response to slope tangent regardless of tillage direction (Figure 4.14). Shoulder sites, in contrast, have overall smaller displacement distances, and are impacted by tillage direction. These

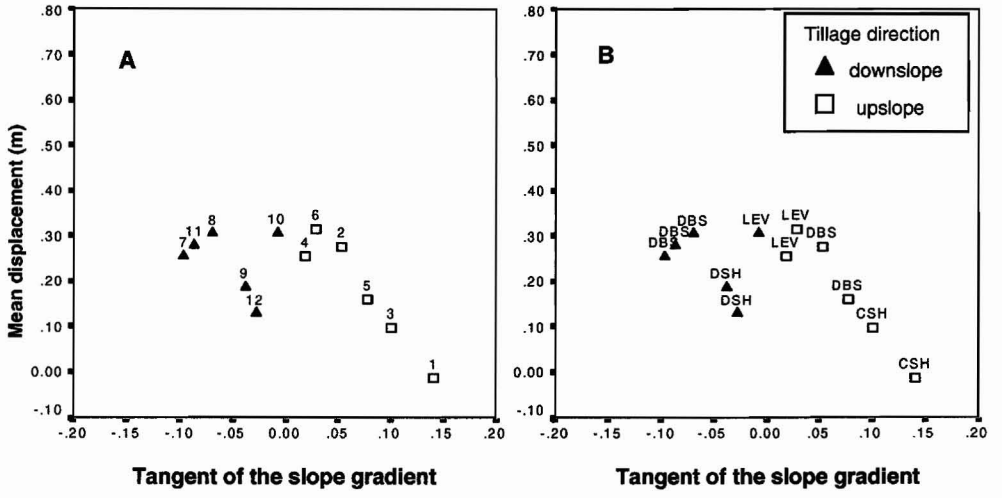

Figure 4.13. Mean tracer displacement (m) versus the tangent of the slope gradient for Tillage Experiment No. 2. Figure A has plots labelled by plot number; B has plots labelled by landform element. Positive slope tangents indicate tillage upslope, negative slope tangents indicate tillage downslope.

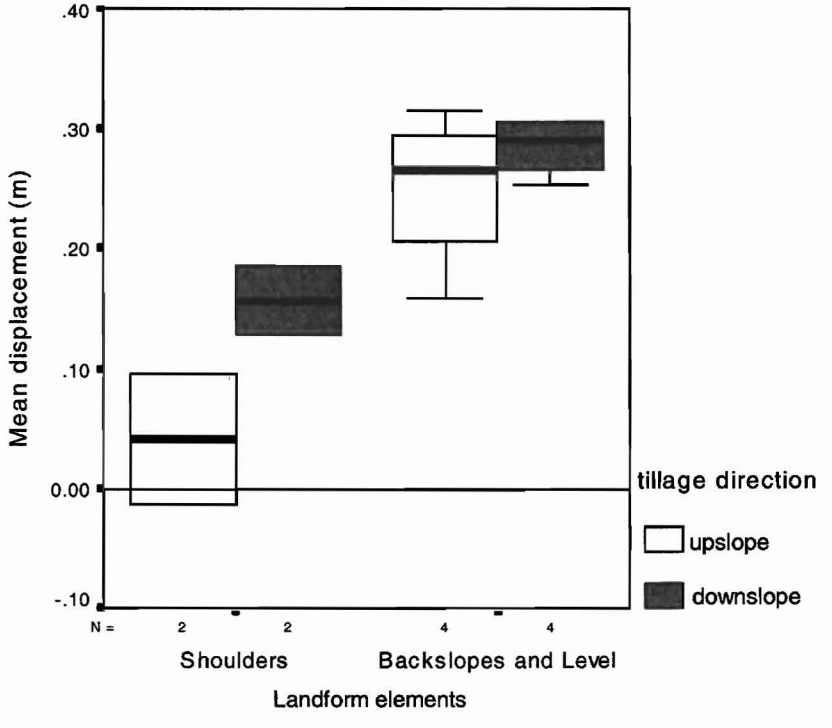

Figure 4.14 Mean displacement distance for Tillage Experiment No. 2, with data grouped by landform element and tillage direction. Negative values indicate back translocation of the tracer.

results suggest that if we have tillage events equally in the up and downslope directions, then the linear slopes – backslope and level landform elements – will experience only minor net erosion given that downslope displacement is nearly equal to upslope displacement. Shoulder elements, are considered to be non-linear slopes and are defined as having a profile curvature (i.e., the rate of change in the slope) greater than 0.10 $^{o}m^{-1}$. They will experience greater net erosion, because downslope displacement is significantly greater than the upslope displacement. This difference in tracer displacement between groups of landform elements is shown more clearly in Figure 4.15.

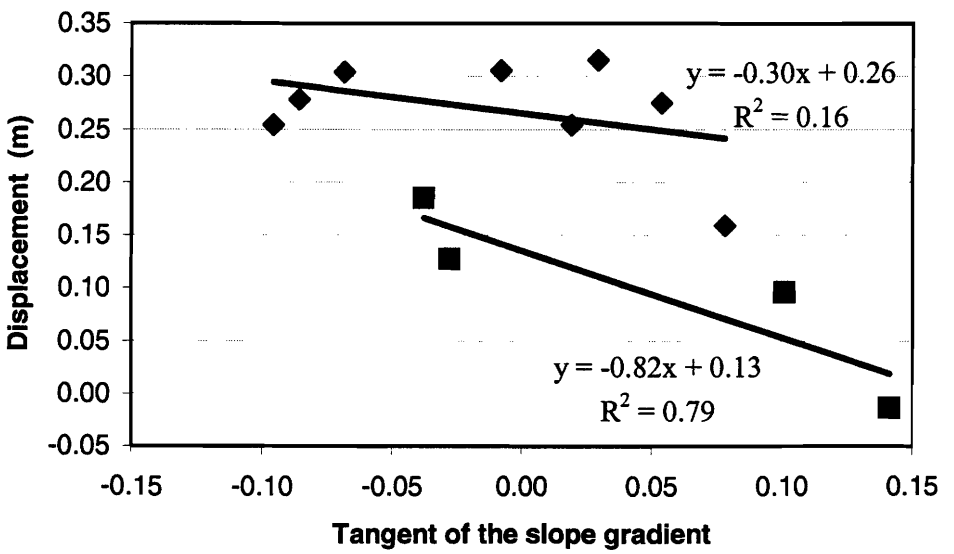

Figure 4.15 Displacement distance versus the tangent of the slope gradient for Tillage-2 plots grouped by landform element into shoulders (squares) and backslopes and levels (diamonds).

In Figure 4.15, the plots are grouped by landform element as proposed above, and then graphed with displacement distance versus slope tangent. Using the resulting linear equations in Figure 4.15 to estimate upslope and downslope displacement, we are able to calculate the expected net soil translocation for given slope gradients using equation 4.8 (Poesen et al., 1997):

$$Q_{snet} = \frac{\left(\overline{d}_{down} - \overline{d}_{up}\right)}{2} \cdot D \cdot \rho_b \qquad (4.8)$$

where,

Q_{snet} = the net soil flux per meter width of implement following one tillage operation upslope and one downslope (kg m^{-1})

$\overline{d}_{down}$ = the mean tracer displacement following one tillage operation downslope (m)

$\overline{d}_{up}$ = the mean tracer displacement following one tillage operation upslope (m)

D = the tillage depth (m)

ρ_b = soil bulk density (kg m^{-3})

The expected values for net soil translocation presented in Figure 4.16 show clearly that shoulder landform elements will experience greater translocation of soil than backslope or level elements following tillage in both the up and downslope directions.

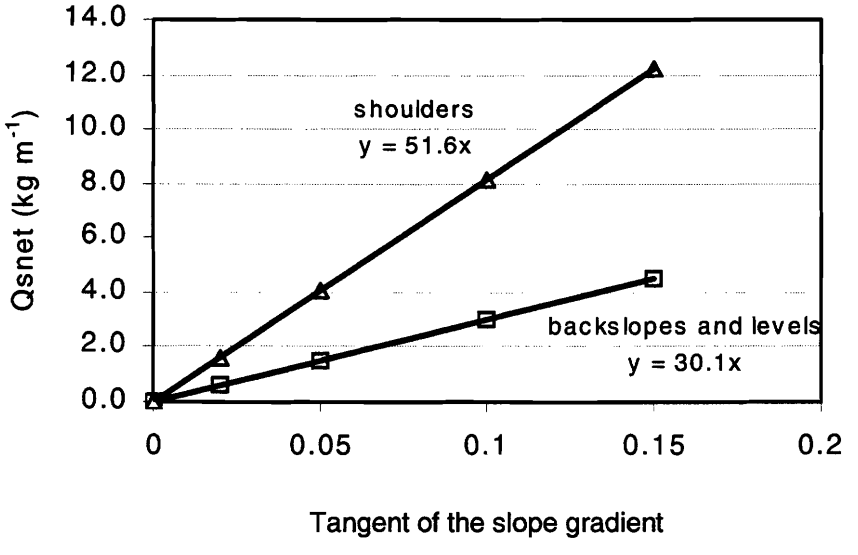

Figure 4.16 Expected net soil translocation (kg per meter of tillage width) for different groups of landforms following one upslope and one downslope tillage operation.

The data from both Tillage Experiment No.1 and No.2 are graphed together in Figure 4.17. In this figure the similarity in upslope tillage is clearly apparent. When tillage is upslope, the least movement of the tracer occurs on the steepest slope; and the greatest translocation of the tracer occurs where the slope gradient is least, dominantly among the backslope and level landforms.

However, as noted above, the plots tilled downslope in Tillage Experiment No.2 do not show the same pattern as that observed for those tilled downslope in Tillage Experiment No.1 Instead of displacement distance continuing to increase as downslope gradient increases (as in Tillage Experiment No.1), the plots in Tillage Experiment No.2 tilled in the downslope direction appear to show little response to slope tangent and displacement remains relatively constant even as downslope gradient increases (Figure 4.17). Although the bulk of the literature suggests that with downhill tillage the displacement distance should continue to increase as slope gradient increases, this is not always the case. For example, Lobb et al. (1999) observed virtually no influence of slope tangent on displacement distance (B = 0.09) when using a C-tine cultivator with harrows. For Tillage Experiment No.2, it appears that there is a similar result for tillage in the downslope direction.

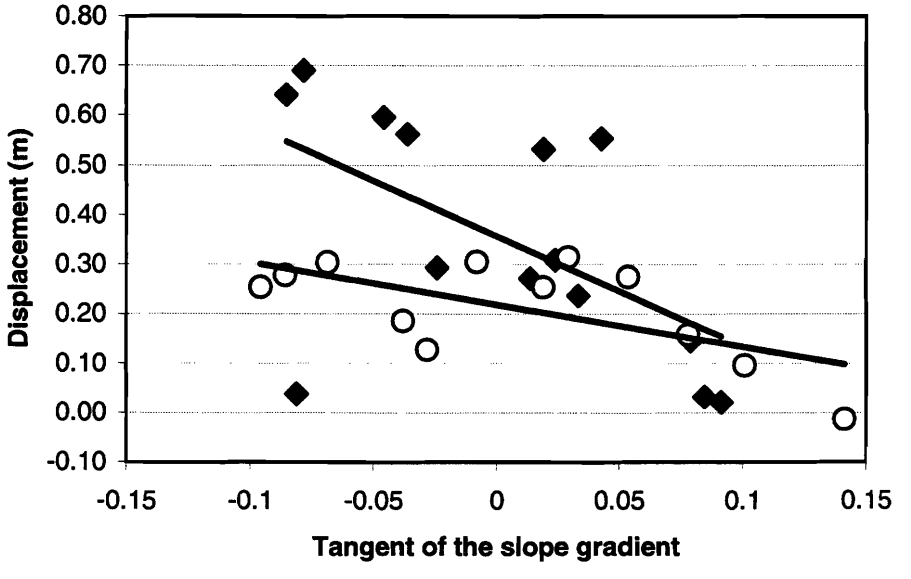

Figure 4.17 Graph of the combined results from Tillage Experiment No.1 (diamonds) and Tillage Experiment No.2 (circles), showing the mean translocation distance versus slope tangent. For Tillage-1, y = -2.22x + 0.36, R^2 = 0.33. For Tillage-2, y = -0.85x + 0.22, R^2 = 0.40.

Fitting a linear function to the full data set from the Tillage Experiment No.2 (Figure 4.17) gives a B value (equation 4.3) of 0.85. Multiplying this by the depth of

tillage and the mean bulk density produces a tillage transport coefficient, k, of 84.7 kg m^{-1}. This value is approximately three times smaller than that determined for Tillage Experiment No.1. The two tillage experiments were conducted on the same part of the same field and have the same soil, same range of topography and similar tillage implements. The difference in k values probably lies with the difference in surface condition of the plots and the mode of tracer application.

The plots used for Tillage Experiment No.2 had been pre-tilled one month before the tillage trial. The Tillage Experiment No.1 experiment was conducted on plots of standing wheat stubble. As would be expected, the Tillage Experiment No.2 had a lower mean bulk density (1.24 g cm^{-3}), whereas the Tillage Experiment No.1 had a higher mean bulk density (1.49 g cm^{-3}). However, contrary to the results of van Muysen et al. (2000), the pre-tilled experiment did not show the greatest tracer displacement. In fact, Tillage Experiment No.1, while having a greater mean bulk density, had six plots with displacement distance >0.50 m and nearly double that observed for similar slope tangents in the Tillage Experiment No.2 (Figure 4.14).

In Tillage Experiment No.1 the granular tracer was broadcast on the surface and left untouched until the plots were tilled. In Tillage Experiment No.2 the 3 L of Cl^- solution would be expected to penetrate the top 2 cm of soil, given a mean volumetric water content of 15% prior to application and assuming a field capacity of 30% by volume. It has been shown that a tracer initially placed shallowly will move further than one initially placed deeper in the soil (Sharifat and Kushwaha, 1997; Sharifat, 1999; van Muysen et al., 2000). However, in both experiments, the tracer was effectively at the soil surface and the effect of differences in depth of application are expected to be minor. It may be that the large displacement distances observed for plots tilled on the level or downslope in Tillage Experiment No.1 result from the surface application of granular tracer to a well consolidated surface which facilitates the movement of the tracer over the surface, perhaps in association with the stubble litter, rather than incorporation. In the second experiment, the tracer was within the soil matrix, and is not as free to move forward with the surface litter as in Tillage Experiment No.1.

4.4.7. Conclusions

It is apparent that tillage in an upslope direction shows the same pattern of displacement in Tillage Experiment No.2 as in Tillage Experiment No.1. It is equally apparent that tillage in the downslope direction shows different patterns for the two experiments.

The difference in downslope tillage behaviour may be due to differences in experimental method. In Tillage Experiment No.1 discrete granules of KCl were applied to the surface of a stubble field. In Tillage Experiment No.2, the KCl tracer was applied as a solution to the surface of a tilled summerfallow field. The very large displacement distances observed in Tillage Experiment No.1 might be the result of the granular tracer rolling along a firm surface with the loose surface materials present at a stubble site.

From the literature, it is apparent that the magnitude of the erosion at any individual site will vary with gradient and to some degree with profile and plan curvature. The data from Tillage Experiment No.2 suggest that shoulder landforms will experience greater erosion than either backslope or level elements. Thus, given the field conditions identified in this experiment, differences in potential tillage translocation can be identified based on landform. In the landform classification system applied, shoulder elements have a profile curvature greater than 0.1 $^{\circ}$ m^{-1} while linear slopes have a profile curvature <0.1 and >-0.1 $^{\circ}$ m^{-1}. This criterion appears to provide a good distinction between different tillage erosion regimes within the field.

5. SYNTHESIS AND CONCLUSIONS

The research undertaken was based on the well-accepted model that the nature of soils (horizons and profiles) within the landscape is strongly related to the redistribution of water and the redistribution of soil by erosion. The redistribution of water affects the nature and intensity of pedological processes occurring at a point in the landscape; the redistribution of soil through erosional processes modifies the attributes of the solum. The soil taxa, and the horizons associated with them, are the best field indicator of the interaction of soil formation and soil erosion processes. In turn, the distribution of soil taxa, and the redistribution processes that control them, can be related to readily mappable topographical attributes, either as single attributes (e.g., gradient) or as three-dimensional landform elements. The use of topographic attributes as surrogates for the soil taxa and the main processes that control them enables us to use digital elevation models to predict the distribution of soils and processes in the landscape.

This chapter is designed to summarize the major findings of the process-focused chapters and to examine the interaction of these processes and their effects on soil taxa distribution.

5.1. Moisture Redistribution and Soil Formation

The conceptual model of soil development and distribution in Saskatchewan that has been in place since the 1920s (Ellis, 1938) suggests that differences in soil profile characteristics within a landscape (of uniform parent material) occur in response to different hydrological regimes. These different hydrological regimes occur due to water flowing on and within the soil. Research carried out in the 1980's (Martz and de Jong, 1987; Pennock et al., 1987; Zebarth and de Jong, 1989a) established that the different hydrological regimes in hummocky landscapes were associated with distinct topographical units. Surface and subsurface flows will converge at positions where slope curvature is concave, and will diverge from positions where slope curvature is

convex. Where moisture converges there is an increased potential for lateral and vertical redistribution of soil materials and enhanced development of the soil profile. Thus, differences in profile development are considered to reflect differences in soil moisture regime. Given that the redistribution of soil moisture in the landscape is in response to the three dimensional form of the topography, it follows that where the topographic form is different, differences in moisture redistribution and consequently differences in profile development may be expected.

Although there has been strong secondary evidence, and a sound theoretical basis, to support the conceptual model of moisture redistribution/soil development, the differences in the direction and magnitude of within-soil water flow across the landscape have not been directly documented for cultivated Saskatchewan landscapes. In order to directly identify differences in the water flow patterns within a cultivated Saskatchewan landscape, and thus quantify the conceptual model, this study monitored the redistribution of a chloride tracer at multiple locations within the study landscape over a fifteen-month period. The chloride redistribution was used as a surrogate for moisture redistribution. The chloride observations were then analyzed by topographic form and by differences in soil profile development to explore the possibility of using readily mappable topographic and pedogenic properties as surrogate indicators of the flow redistribution regime.

The emphasis in this study has been on the use of topographic attributes as surrogate indicators of moisture redistribution because topographic data are presumed to be easier to collect and map than soil profile data. Topographic data collection does not require specialized soil survey knowledge, and is not subject to the interpretation of the surveyor as is soil profile data. For example, in cultivated landscapes tillage introduces a degree of uncertainty into the measurement of the depth of the A- and B-horizons. In addition, a map of moisture redistribution patterns based on topographic form could be easily produced from a digital elevation model, whereas a map based on soil profile description would require a more detailed initial field survey to establish the spatial extent of each relevant soil profile type.

Utilizing a digital elevation model, the study landscape was grouped into seven

three-dimensional units based on plan curvature, profile curvature and slope gradient to facilitate the identification of patterns of moisture redistribution. The distribution of soil profile characteristics by landform element conforms to the expected model of soil development based on published sources. The initial split between landscape elements is based on profile curvature, and soil thickness generally increases in the sequence from shoulders < backslopes < footslopes. Differences within the profile groups are largely due to the secondary effect of plan curvature. Convergent locations, those with a concave plan curvature, are dominated by soil profiles in which the calcium carbonate has been leached from the A- and B-horizons (mainly Orthic Chernozemic profiles) and which have a greater depth of B-horizon and depth to the C-horizon (parent material) than observed at divergent positions. Divergent locations, those with a convex plan curvature, are dominated by soil profiles from which the calcium carbonate has not been removed, and which have a shallower depth of B-horizon and depth to C-horizon than at convergent locations. Level locations occupy a middle position between the two groups.

Ten soil subgroups were identified in the study landscape. These were re-grouped into five soil profile classes that were selected to reflect major differences in the degree of profile development (Table 5.1). Soil subgroups were regrouped because subtle differences in the interpretation of profile characteristics can place profiles into different subgroups when in fact there is no real difference in the major soil-forming processes. The soil profile classes represent different soil moisture regimes and degrees of profile development.

Table 5.1 The distribution of the soil profile classes by landform element.

		Landform element							
Soil Profile Class	Associated Soil Moisture Regime	DSH	CSH	DBS	CBS	DFS	CFS	LEV	*Total*
REGO	upland	11		8	1	2			22
CALC	upland	3		6	3	1	2	5	20
ORTHIC	upland		1	4	21		5	7	38
GLEYED-REGO	depression					2		2	4
GLEYED	depression					1	10	1	12
Total		14	1	18	25	6	17	15	96

Profiles were initially grouped by the presence or absence of gley characteristics. Gleyed profiles are associated with soil moisture regimes that have periods of temporary

or permanent saturation. These conditions will develop at convergent locations that have an upslope contributing area large enough to maintain saturation over time (Bedard-Haughn and Pennock, 2002; O'Loughlin, 1981). In the study landscape, gleyed profiles where found to occur at CFS, DFS and LEV landform elements. The GLEYED group was primarily associated with the CFS elements, and the discharge-related GLEYED-REGO group was found at DFS and Level elements.

Non-gleyed soil profiles are found in association with upland or up-slope soil moisture regimes that do not experience extended periods of saturation. Non-gleyed soil profiles were found among all landform elements. Calcareous Dark Brown soils have the widest distribution at the site and are not clearly associated with any particular element, whereas the Orthic Dark Brown soils are dominantly associated with the CBS elements. The REGO group is associated primarily with the DSH elements. Overall this pattern of soil distribution is typical of many of the published hummocky glacial till sites from the northern Great Plains and indicates the comparability of this site with the other published sites.

5.2. Water Redistribution Patterns

Chloride redistribution was used in this study to assess the direction and magnitude of water flow in the landscape. The focus was on the landscape or meso-scale variability in redistribution patterns, rather than a more detailed examination of redistribution at only a few locations. This required that tracer redistribution be monitored at multiple locations across the study site, which largely dictated the sample spacing and the depth of sampling. Total sampling depth was restricted to 0.50 m, and the number of sample cores at each location was restricted to a minimum (generally ten cores) in order to restrict total sample numbers. Thus the results presented here are based on the chloride remaining in the upper 0.50 m and show only broad trends in redistribution. Future researchers may want to employ finer sampling grids and a greater depth of sampling at fewer sites, in order to further our detailed understanding of variability in the pattern of redistribution.

The tracer was applied in June 1997 and the first sampling in the Fall of 1997

was conducted to assess redistribution over a summer period with no tillage. Sampling in the Spring of 1998 was conducted to assess the influence of the spring melt on the redistribution pattern before tillage. The final sampling time in the Fall of 1998 was conducted to assess the redistribution in a second growing season in which the field was planted in the spring and then tilled following the fall harvest, and to assess the net redistribution over the fifteen months.

In general, the observations collected in late September 1997 indicate only minor differences in chloride redistribution between landform elements and soil profile classes during the mid-summer. There was 178 mm of rainfall at the site from June 24 to October 22, 1997, approximately 1.2x the long-term normal amount for this period (Environment Canada, 1992). Recovery of the chloride tracer in the fall was high for all plots. Soils in the GLEYED profile class, and to some extent the soils in the GLEYED-REGO class, had more chloride retained in the 0- to 0.10-m depth than other soil profile classes. The GLEYED profile class shows the shallowest chloride centre of mass, and the least downslope lateral movement. There is little difference in the redistribution of chloride between the soils of the GLEYED-REGO, REGO, CALC and ORTHIC classes during this summer period (Figure 5.1).

Given that the GLEYED class has the deepest profile development (depth of A-horizon, depth to C-horizon, depth to carbonates) the shallow depth to the chloride centre of mass was unexpected for these soils. The shallow depth to the chloride centre of mass may largely be explained by their location within the landscape. All the soil profiles included in the GLEYED class were found at positions in or adjacent to the depression-centred tillage pond; all were characterized as CFS landform elements. The shallow depth to the chloride centre of mass may be due to net upward movement of soil moisture (evaporative discharge) from the water table beneath the depression.

Alternatively, the shallow depth to the chloride centre of mass in the GLEYED profile class may be due to localized differences in soil texture. The cesium-137 redistribution pattern identifies CFS landform elements as sites of deposition. Soil redistribution in hummocky prairie landscapes can result in the preferential redistribution of finer particles towards the depressions rather than onto the surrounding

adjacent uplands (Bedard-Haughn and Pennock, 2002). These finer textured soils can retard downward movement of soil water thus keeping the chloride pulse near the surface. The CFS elements at this site had 5 to 10% less sand and correspondingly more silt in the 0- to 0.10-m depth than other landform elements.

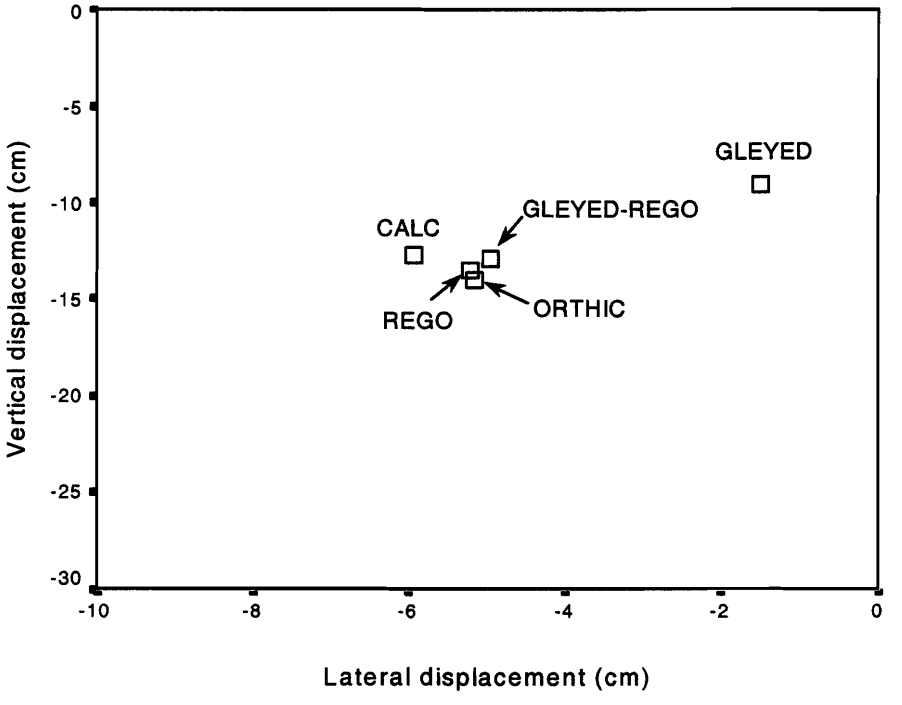

Figure 5.1 Fall 1997 median vertical and lateral displacement of the chloride centre of mass (cm) for soil profile groups. Negative lateral movement indicates a downslope orientation, positive lateral movement an upslope orientation.

When the fall 1997 results are grouped by landform element (Figure 5.2), the footslope elements, have a median depth to the chloride centre of mass that is only a few centimetres shallower than other landform elements. DSH, DBS and CBS landform elements were similar to each other, with the chloride tracer moving marginally deeper into the soil than the footslopes and with little lateral movement (Figure 5.2). Level landform elements had the greatest median lateral displacement of the chloride centre of mass.

The landform elements and profile groups were clearly separated into two response groups after tracer redistribution by snow melt in the spring of 1998. Large

losses of chloride mass and substantial lateral movement of the remaining chloride centre of mass were observed at the footslope locations that were subject to temporary flooding.. The positions sampled following flooding retained less than 20% of the initial chloride tracer in the 0- to 0.50-m depth. The remaining upslope positions show some minor redistribution of chloride within the profile but continue to retain greater than 80% of the chloride tracer.

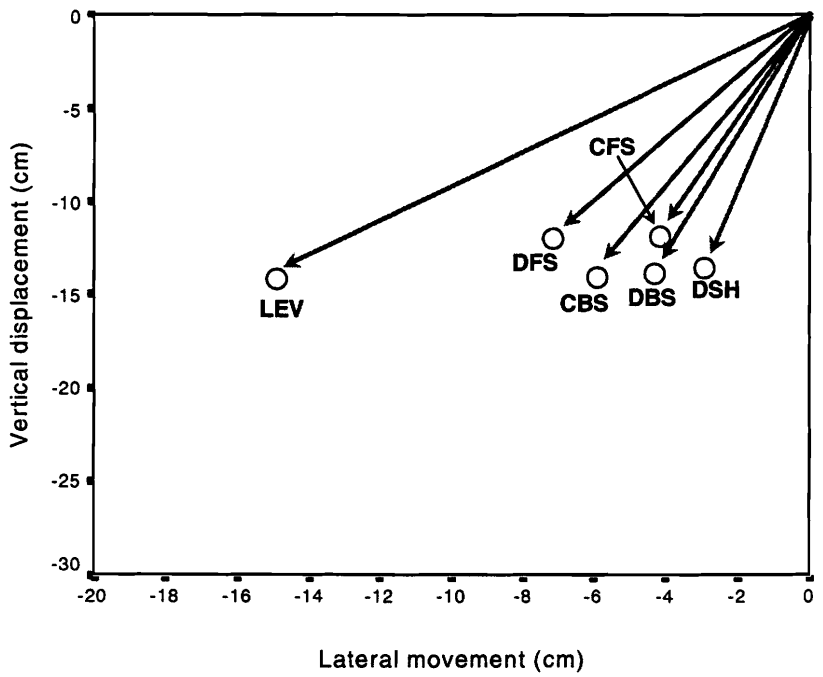

Figure 5.2 Fall 1997 median vertical and lateral displacement of the chloride centre of mass (cm) for landform elements. The arrows highlight the net direction of movement of the chloride centre of mass from the centre of the 1-m^2 plot at the soil surface. Negative lateral movement indicates a downslope orientation, positive lateral movement an upslope orientation.

By the Fall of 1998 the relationship between landform elements and the percentage of chloride tracer remaining in the upper 0.50 m takes on a pattern consistent with the long term pattern of soil moisture distribution. Chloride recovery decreases in the order DSH>DBS>CBS>LEV≥DFS>CFS (Figure 3.15), which is the same sequence that soil moisture has been presumed to increase in literature from the region (e.g. Pennock et al., 1994b; Zebarth and de Jong, 1989a). Total displacement of chloride tracer among the landform elements increases in the order DSH≤DBS<CBS<LEV. The

DFS and CFS landform elements subjected to spring flooding lost approximately 80% of the chloride tracer at that time, and the observed displacement of the centre of mass for these locations in the fall of 1998 is an underestimation of the true displacement distance.

When the median vertical and lateral displacement of the chloride centre of mass are displayed for landform elements using data from Fall 1998 and Fall 1997 (combining Figures 3.22 and Figure 5.2) the differences in the magnitude and direction of tracer movement over time are clearly shown (Figure 5.3). All landform elements show an increase in vertical displacement of the tracer by Fall 1998. The comparatively shallow depth to the chloride centre of mass among the footslope elements in the Fall of 1998 largely reflects the impact of spring flooding on these landscape positions that are dominantly associated with the depression-centred tillage pond. Nearly 80% of the chloride mass appears to have been removed by the saturated conditions in the Spring of 1998. The Fall 1998 chloride centre of mass in the footslope positions is defined only by this tighltly held remnant of the tracer. It may also reflect some reversal of flow direction over the summer that restricts the net movement of the tightly held soil water.

DFS elements are a mixture of carbonated and rego profiles with a shallow depth to the C-horizon. The DFS landform elements exhibit significant lateral redistribution with an upslope orientation. This is consistent with the outward flow of soil moisture from a discharge slough to the surrounding uplands as discussed above. The comparatively shallow centre of chloride mass suggests upward flow. The observed redistribution of the chloride centre of mass in the Fall 1998 data is in keeping with the supposition that the profile development at these positions is the result of upward flow, originating in the adjacent tillage pond. As discussed in Section 2.2.1, these soils appear to have secondary carbonate accumulation in the C-horizon, which is consistent with upward flow. Secondary accumulation of carbonates in this horizon is designated as Cca in the Canadian System of Soil Classification. Within the Canadian System of Soil Classification a C-horizon is defined as parent material essentially unaltered by pedogenic processes. This is inconsistent with the acknowledgement of pedogenic deposit of secondary carbonates within this horizon. American soil taxonomists

explicitly acknowledge the pedogenic nature of these "calcic" horizons identifying them as B horizons with carbonate accumulation, i.e., Bk.

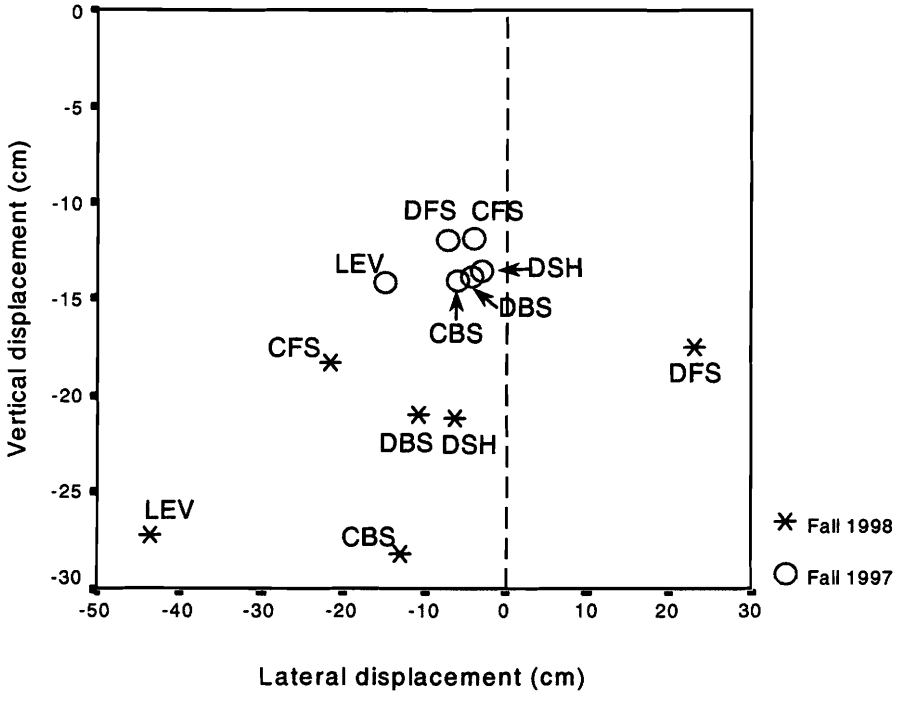

Figure 5.3 Median vertical and lateral displacement of the chloride centre of mass (cm) for landform elements, Fall 1997 and Fall 1998. Negative lateral displacement indicates a downslope movement, positive lateral displacement an upslope movement.

By the Fall of 1998, among those landscape positions not associated with the tillage pond, the chloride centre of mass has moved the deepest in the LEV and CBS landform elements, and retains a shallower position among the DSH and DBS landform elements.

The comparatively deep chloride centre of mass for soils of the ORTHIC soil profile class (Figure 5.4) is consistent with their degree of profile development. Similarly the shallow depth to the chloride centre of mass for the CALC and REGO soil profile classes corresponds with their minimal profile development. The soils within the GLEYED class are found in association with the tillage pond, as with the footslope elements discussed above, the shallow centre of mass is among the GLEYED soils is

determined largely by the small amount of the tracer mass retained following spring flooding and evaporative discharge to the soil surface.

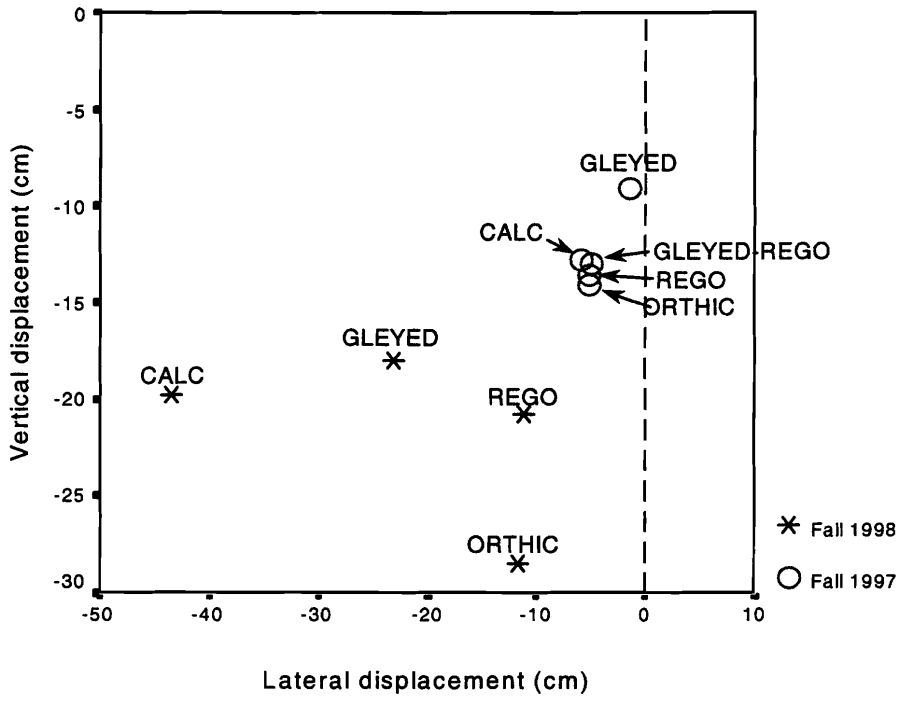

Figure 5.4 Median vertical and lateral displacement of the chloride centre of mass (cm) for soil profile groups, Fall 1997 and Fall 1998.

5.2.1. Tillage impact on tracer redistribution in the moisture study

The results of Tillage Experiments No.1 and No.2 clearly demonstrate that tillage during the 1998 growing season has the potential to impact the tracer redistribution on the small plots used in the moisture redistribution study. The results of Tillage Experiment No. 2, using a 1-m^2 plot similar to those in the moisture study, show that a single pass of the field cultivator will move an average 66% of the tracer off the plot. Tracer is recovered at least as far as 1 m from the plot edge, with only a minor amount (approximately 6%) recovered within the first 0.2 m off the plot. Thus the majority of the tracer is moved beyond the extent of the sampling design used in the moisture study (Figure 3.3).

In the fall of 1997 mean tracer recovery for all locations in the 0- to 0.10-m sampling increment was 41%. A similar mean of 47% was found in the spring of 1998

for the DSH, DBS, CBS, and LEV landform elements, i.e. those locations that were not subject to flooding. By the fall of 1998 mean chloride recovery, across all locations, in the 0- to 0.10-m sampling increment has dropped to 4% from approximately 45% the previous spring and fall. The large loss of tracer from the surface increment and the uniform low level of chloride recovery across all locations in the Fall 1998 sampling strongly suggest that tillage has contributed to the redistribution of the tracer.

Tracer redistribution in the 0- to 0.10-m sampling increment, over the 1998 growing season, is influenced by spring seeding, summer rainfall and soil moisture redistribution, and by the fall tillage operation. Assuming an initial 45% of tracer in the surface increment in the spring of 1998, and that 66 % is then removed from the upper 0.03 cm by the seeder, this suggests that 31% of the original tracer remains on the plot. Assuming then, in the extreme, that there is no redistribution by moisture, the fall tillage operation will remove 66% of the remaining tracer, leaving 11% of the tracer in the surface increment. Alternatively, if we assume that the summer rains remove 60% of the 31% from the surface increment (as occurred over the summer of 1997) this leaves 12% of the chloride prior to the fall tillage. Fall tillage will then leave only 4% of the tracer mass in the surface increment. Clearly, tillage redistribution alone can result in levels of chloride, in the surface increment, that approach the results observed in the fall of 1998. However, when we couple tillage redistribution with moisture driven redistribution our estimate of tracer loss from the surface increment more closely matches the field observation from the Fall 1998 sampling.

While approximately 36 % of the original chloride mass is lost from the surface increment during the 1998 growing season there has been relatively little change to the chloride levels in the deeper sampling increments. This further suggests that moisture redistribution accounts for a minor portion of the total chloride loss from the surface increment. A tillage controlled loss of chloride mass from the surface increment will result in the centre of mass and subsequent displacement values being affected more strongly by the chloride contained in the deeper increments, notably the 0.10- to 0.20-m and 0.20- to 0.35-m increments. Thus, attributing the results solely to moisture redistribution should be done with caution.

5.2.2. Moisture Redistribution Summary

The chloride tracer study provided clear evidence for the direction and magnitude of water flow during the study period.

An initial distinction can be drawn between the depression-influenced soils and those outside the zone of influence of the depression (i.e., the upland soils) Depression-influenced soils were dominated by gleyed profiles in convergent footslope locations. The main control on the movement of the tracer at these positions was spring flooding in early 1998 and leaching of the majority of the tracer at this time. Redistribution of the tracer at divergent footslope landform elements was more complex, and the remaining tracer after flooding clearly showed a net lateral upslope movement. This net upslope movement of the soluble tracer is consistent with observations that net lateral and upslope movement in soils adjacent to depressions is a major hydrological pathway in these landscapes (Hayashi et al., 1998).

Water flow in the upland soils is distinctly anisotropic, as indicated by the difference between the lateral and vertical redistribution of the chloride tracer. In the fall of 1997 the median displacement of the chloride centre of mass was approximately 13 cm vertically and 5 cm downslope. By the fall of 1998 the tracer in CBS and Level elements exhibited vertical displacement of approximately 27 cm and lateral displacement downslope of 12 to 19 cm, respectively. These elements were dominated by Orthic Dark Brown and Calcareous Dark Brown soils, neither of which have a pronounced textural B-horizon. DBS elements had less vertical and lateral displacement of the tracer compared to the CBS elements, indicating a difference in hydrological response that is consistent with water concentration in the convergent elements. DSH elements as a whole show almost no net lateral displacement, and vertical displacement values comparable to that of the DBS elements.

Pennock et al. (1987) postulate that Level elements are dominated by vertical infiltration of water with little or no lateral displacement. This is clearly not the case in this study – the Level elements with mainly O.DBC soils exhibit the greatest net displacement over the course of the study. The criterion selected by Pennock et al. (1987) to separate Level from backslope elements was a gradient threshold of 3°, which

was drawn from the literature on water erosion. The wide lateral displacement that was observed for Level elements in this study suggests that their hydrological behaviour is similar to the backslope elements and that the existing landform element classification may have to be revised.

The occurrence of anisotropic lateral flow had not been previously documented in these hummocky, glacial till landscapes. Indeed, since the work of McCord and Stephens (1987) and McCord et al. (1991) there has been little evidence published on the existence of anisotropic within-soil flow. The evidence presented in this dissertation establishes the existence of these flows in the hummocky till landscapes and provides process-based evidence for the linkage between topography and intra-soil water flows that has been proposed by many authors.

5.3. Tillage redistribution

Until the 1990s research into tillage as an erosion mechanism had largely been ignored. The prevailing focus of erosion-based research was dominated by the concept of erosion as a water driven phenomenon (Govers et al., 1999), with a contribution of wind erosion in arid and semi-arid regions. However, the processes of water or wind erosion could not explain the observed field-scale pattern of net erosion and deposition that was being found by early users of the cesium-137 technique both in Saskatchewan (Kiss et al., 1986, Martz and de Jong, 1987, Pennock and de Jong, 1987; Pennock and de Jong, 1990b), and in Europe (Quine et al., 1994; Govers et al., 1996). Recent research into the spatial pattern of long-term net erosion (Govers et al., 1993; Govers et al., 1994; Quine et al., 1994; Govers et al., 1996) and the impact of topography on the magnitude of tillage translocation (Lindstrom et al., 1990; Lindstrom et al., 1992; Lobb and Kachanoski, 1994; Poesen et al., 1997; Lobb et al., 1999; Quine et al., 1999) has established that tillage is the dominant mechanism of erosion on many cultivated sites.

Govers et al. (1994) have shown that in theory the long-term field-scale pattern characteristic of soil redistribution by tillage should have erosion at convex landscape positions and deposition at concave positions. This pattern is different to that expected for water-dominated erosion. Erosion by water would be highest along steep slopes and

in concavities where the contributing area is large.

In this study, the long-term net soil redistribution as determined from cesium-137 measurements conforms to the predicted spatial pattern for tillage redistribution, i.e., topographic positions with convex curvature have greater net loss of soil than positions with concave curvature. The DSH, DBS, DFS and the LEV landform elements with a convex (divergent) plan curvature behave similarly and have a combined mean net soil erosion of 36.9 Mg ha^{-1} y^{-1} (standard deviation 14.3 Mg ha^{-1} y^{-1}). CBS elements have a lower mean net soil loss of 8.1 Mg ha^{-1} y^{-1} (std. dev. 10.2 Mg ha^{-1} y^{-1}). Convergent footslope landform elements are sites of soil deposition, with a mean net gain of 2.4 Mg ha^{-1} y^{-1} (std. dev. 20.0 Mg ha^{-1} y^{-1}).

A poor correlation between long-term erosion rates and slope curvature, in either the plan or profile dimension, was found in this study and that by Pennock and de Jong (1987). However, the strong relationship between erosion rates and three-dimensionally defined landform elements observed in this study and others (e.g., Martz and de Jong, 1987; Pennock and de Jong, 1987; Pennock and de Jong, 1990b; Pennock et al., 1994b) suggests that under field-scale conditions it is necessary to consider the three-dimensional form of the topography when attempting to predict the spatial pattern of soil redistribution.

Tillage experiments conducted under Saskatchewan field conditions demonstrated the dominant influence of slope gradient and the direction of tillage on soil displacement by tillage. In slope segments with a constant gradient, we expect that the soil mass moved away from one point will be replaced with an equal mass of soil, resulting in no net soil loss or gain (Figures 5.5 and 5.6). In slope segments where the slope gradient changes from one edge of the segment to the other the net balance of deposition and removal will be changed. When tillage is in an upslope direction, the displacement will decrease as the gradient increases, i.e. when moving from the footslope to a midslope position. As the implement crosses the peak of the shoulder position, the gradient begins to decrease and greater displacement can be expected. When tillage is in a downslope direction the displacement will increase as gradient increases. Thus at the top of the knoll where the gradient is low, displacement will be

small. As the implement moves down the slope, the displacement increases with the gradient and then decreases again near the foot of the slope as the gradient is reduced.

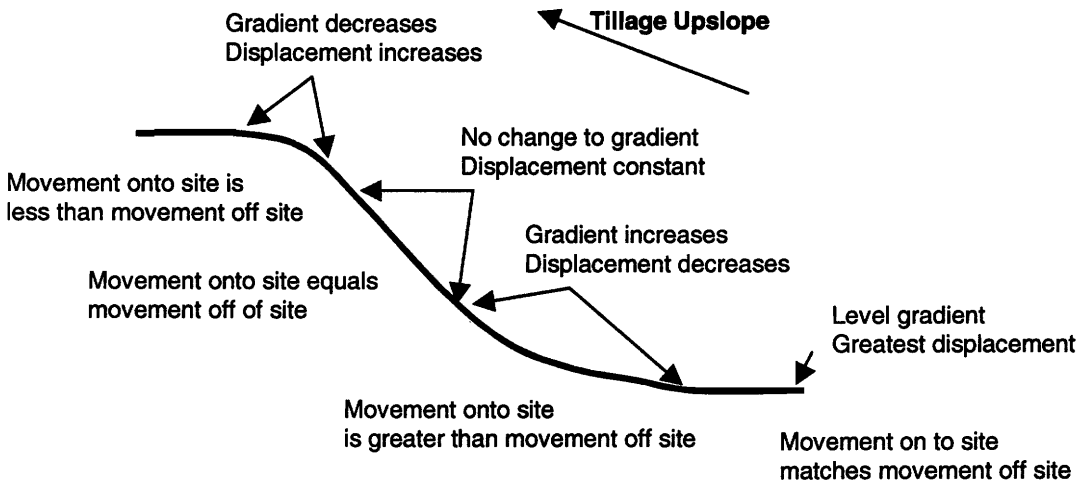

Figure 5.5 Conceptual diagram of soil displacement with tillage in the upslope direction

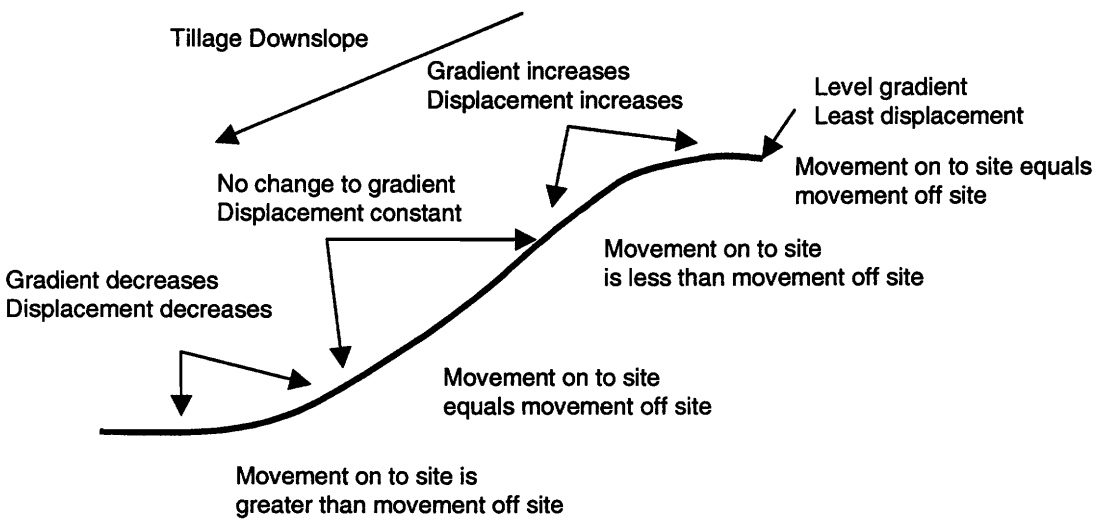

Figure 5.6 Conceptual diagram of soil displacement with tillage in the downslope direction.

Slope gradient is the dominant control on soil displacement for the short slope segments used in the tracer studies. Slope curvature, i.e., the change in slope gradient, is, however, the topographic control on the long-term field-scale pattern of erosion and deposition by tillage (Govers et al., 1994; Quine et al., 1999). Over the long-term, the tillage translocation processes will result in net erosion of the shoulder elements and net deposition in the footslope positions. The convex curvature associated with shoulder elements will cause them to be eroded during upslope and downslope tillage, i.e., soil displaced from the shoulder is always greater than the amount of soil moving onto the shoulder. Along linear backslopes, the amount of soil displaced during a tillage operation does not vary from point to point and erosion along such a slope results from the greater net displacement following downslope tillage than following upslope tillage. Thus we expect the backslopes will be eroded but at a slower rate than shoulder elements.

Estimates of the erosion rate over a unit area (hectare) can be derived from the results of the tillage experiments by dividing the unit soil transport flux (T_M, kg m^{-1}) by the slope length (Lobb et al., 1995; Poesen et al., 1997) (Table 5.2). Conceptually the slope length has no additional inputs of soil at the top, and all soil losses are from the lower end of the slope. For this estimate a slope length of 5 m was selected because it matches the length of the grid cell used to define the landform elements. The expected soil transport flux (T_M) was calculated by multiplying $\bar{d}_{NET}$ by tillage depth and soil bulk density. Net tillage displacement ($\bar{d}_{NET}$) was determined as the difference between one upslope and one downslope tillage operation for the median slope gradient of each landform element category. Tillage depth was taken as 0.1 m, and bulk density estimated at 1300 kg m^{-3}. The erosion estimates based on Tillage Experiment No.1 were found to match or exceed the long-term erosion rates determined by the cesium-137 technique. The erosion estimates based on Tillage Experiment No.2 were similar to or exceeded erosion rates determined by the cesium-137 technique for the backslopes. The estimated erosion rate for DSH (Tillage Experiment No.2) appeared to be significantly below cesium-137 measured erosion rate. The tillage implements used in these experiments, and typically used in Saskatchewan farm practice, clearly have the

potential to produce the localized erosion rates that are observed in these landscapes.

In the conceptual model of soil development in uncultivated hummocky Saskatchewan landscapes, profile development and thickness of the Ah-horizon increases from the knoll to the footslope (King et al., 1983; Pennock and de Jong, 1990b; St. Arnaud, 1976). Several investigators have noted that in cultivated Saskatchewan landscapes the majority of slope positions are eroded and have unnaturally thin A-horizons; the concave depressions are sites of soil deposition and have over-thickened A-horizons (Martz and de Jong, 1987; Pennock and de Jong, 1987; Pennock and de Jong, 1990b).

Table 5.2 Estimated tillage erosion rates (Mg ha^{-1} y^{-1}) for three landform elements based on the experimental tillage displacement results.

Landform Element	Median Slope Gradient (°)	Tangent of the Slope Gradient	Selected Slope Length (m)	Tillage-1 Estimated Net Erosion	Tillage-2 Estimated Net Erosion	^{137}Cs Derived Erosion
				Mg ha^{-1} y^{-1}		
DSH	2.2	0.038	5	44	16	42.3
DBS	3.6	0.064	5	74	28	32.4
CBS	4.2	0.074	5	86	32	10.8

This site clearly shows the influence of cultivation on A-horizon thickness. At most ridge and shoulder positions the carbonate-rich subsoil has been mixed with the remaining topsoil, indicating that the plough layer now extends below the depth of the original Ah-horizon. Pennock et al. (1994b) and Slobodian (2001) report the mean depth of the Ah-horizon at uncultivated sites with similar topography and parent material as being 0.14 to 0.18 m. Median depth of the A-horizon on the heavily eroded DSH and DBS elements after nearly 40 years of tillage approximates the depth of tillage at 0.08 and 0.09 m respectively. Any original remaining Ah has now been mixed with carbonated subsoil from the Bk-horizon or the carbonated parent material of the C-horizon.

The median cesium-137 determined soil erosion rate on DSH was found to be 42.3 Mg ha^{-1} y^{-1}. Assuming a bulk density of 1300 kg m^{-3} this is equivalent to an annual

topsoil loss of 0.0032 m. After 40 years of tillage, topsoil loss approaches 0.13 m or almost the entire original A-horizon. These projections indicate that total soil loss is of sufficient magnitude to expose the carbonated subsoil in localized convex positions.

In summary, this study has shown that the field- or landscape-scale pattern of erosion at this Saskatchewan site clearly corresponds to the characteristic pattern for tillage erosion. The magnitude of erosion using commonly employed tillage implements is similar to the long-term erosion rates determined using the cesium-137 technique. The magnitude of erosion is sufficient to account for the observed loss of the A-horizon at localized convex slope positions.

There is surprisingly little difference in the median depth of the A-horizon among DSH, DBS, CBS and DFS following almost 40 years of tillage. The cesium-137 data suggest that nearly all landform positions, with the exception of the CFS landform elements, have undergone net soil erosion. As in other studies, only the depressions or convergent footslopes are sites of deposition. At divergent positions the original thin A-horizon has been fully eroded; remnants of this horizon are now mixed in the plough layer with soil from the B- or C-horizons. Some convergent positions have undergone net erosion yet the current A-depth may still exceed the depth of cultivation, reflecting the interplay between historic soil depth and the net erosion rate. The net erosion rate is in turn controlled by topographic curvature.

Clearly, measurements of horizon depth will not be a good measure of net erosion because of the confounding effects of the plough layer and the lack of initial pre-tillage data. The mapping of potential soil erosion would best be achieved by mapping topographic units that can be defined by slope attributes known to control soil redistribution by tillage.

5.4. Conclusions

This study has provided direct evidence of the variable redistribution of soil moisture in a cultivated Saskatchewan landscape. The redistribution of the chloride tracer has confirmed the existence of lateral flows within this environment, supporting

our conceptual model of moisture redistribution, soil genesis and the distribution of soil taxa across the landscape. Variations in the chloride recovery and the displacement of the chloride centre of mass are readily explained with reference to landform position and pedological attributes.

Among the well-drained upland soils which dominate the shoulder, backslope and level landscape positions chloride recovery and the displacement of the centre of mass varied as would be expected along a hillslope or catenary sequence. Chloride recovery was found to vary in the sequence DSH>DBS>CBS>LEV and displacement of the chloride centre of mass varied in the reverse sequence. Moisture redistribution among shoulder and backslope elements is dominated by vertical flows. The greatest vertical displacement was observed among the convergent backslope elements (median 0.28 m), and the least vertical displacement was found among the divergent shoulder and divergent backslope landform elements (median 0.21 m). Level landform elements have a greater lateral (median 0.43 m) than vertical (median 0.27 m) displacement of the tracer centre of mass.

The recovery and movement of the chloride tracer within the convergent and divergent footslope elements was dominated by the moisture regime associated with the depression-centred tillage pond at the study site. Chloride retained in these landform elements following the 1998 spring flooding showed a greater lateral rather than vertical redistribution. However, because recovery was low, this study cannot determine whether the predominant redistribution pathway was vertical or lateral flow. Divergent footslopes are dominated by soil profiles indicative of soil moisture discharge. The results strongly suggest that lateral redistribution among the divergent footslopes is associated with this discharge phenomenon. Median lateral redistribution among the convergent and divergent footslope elements was 0.23 m and 0.22 m respectively. Median vertical displacement was 0.18 m for both the convergent and divergent footslope elements.

The cesium-137 investigation has shown that this study site is heavily eroded (soil losses of up to 70 Mg ha^{-1} y^{-1}) compared with other studies in the region. The field-scale pattern of erosion matches that attributed to tillage by other researchers. Net soil

loss is maximized at convex positions and net soil gain occurs at concave positions. Small plot tillage trials conducted in this study confirm that the tillage implements employed here clearly have the potential to account for the localized erosion rates observed in these landscapes. The median soil loss (based on ^{137}Cs data) on divergent shoulder elements (42 Mg ha^{-1} y^{-1}) is equivalent to the loss of the entire pre-cultivation A-horizon (0.13 m). This loss of the surface horizon and subsequent mixing of the plough layer with deeper horizons may be great enough to cause the soil to be reclassified into a different soil subgroup thereby altering our perception of the distribution of soil taxa across this landscape.

In summary this research has been able to confirm the topographic control on moisture redistribution in this landscape. The pattern of soil moisture redistribution in lower slope positions associated with depression-centred tillage ponds is complicated by spring flooding and soil moisture discharge phenomenon. Tillage dominated erosion over the medium term (30 to 40 years) has been sufficient to change the vertical distribution of soil profile attributes across the field.

6. BIBLIOGRAPHY

Acton, D.F. and Ellis, J.G., 1978. The soils of the Saskatoon map area, 73-B Saskatchewan. Saskatchewan Institute of Pedology Publication S4. Extension Division University of Saskatchewan, 146 pp.

Afyuni, M.M., Cassel, D.K. and Robarge, W.P., 1994. Lateral and vertical bromide ion transport in a Piedmont landscape. Soil Science Society of America Journal, 58: 967-974.

Allison, G.B., Gee, G.W. and Tyler, S.W., 1994. Vadose-zone techniques for estimating groundwater recharge in arid and semiarid regions. Soil Science Society of America Journal, 58: 6-14.

Andreini, M.S. and Steenhuis, T.S., 1990. Preferential paths of flow under conventional and conservation tillage. Geoderma, 46: 85-102.

Angulo-Jaramillo, R., Gaudet, J., Thony, J. and Vauclin, M., 1996. Measurement of hydraulic properties and mobile water content of a field soil. Soil Science Society of America Journal, 60: 710-715.

Ballantyne, A.K., 1974. The movement of salts, and the effects on cereal yields resulting from the application of potassium refinery dust to the soil surface. Canadian Journal of Soil Science, 54: 45-51.

Bedard-Haughn, A.K. and Pennock, D.J., 2002. Terrain controls on depressional soil distribution in a hummocky morainal landscape. Geoderma, in press.

Beven, K. and Germann, P., 1982. Macropores and water flow in soils. Water Resources Research, 18: 1311-1325.

Bloschl, G. and Sivapalan, M., 1995. Scale issues in hydrological modelling: A review. Hydrological Processes, 9: 251-290.

Bowman, R.S., 1984. Evaluation of some new tracers for soil water studies. Soil Science Society of America Journal, 48: 987-993.

Burrough, P.A. and McDonnell, R.A., 1998. Principles of Geographical Information Systems. Oxford University Press, 333 pp.

Burt, T.P. and Butcher, D.P., 1985. Topographic controls on soil moisture distributions. Journal of Soil Science, 36: 469-486.

Burt, T.P. and Trudgill, S.T., 1985. Soil properties, slope hydrology and spatial patterns of chemical denudation. In: R.R. Arnett and S. Ellis (Editors), Geomorphology and Soils. Allen and Unwin, London, UK, pp. 13-36.

Butters, G.L. and Jury, W.A., 1989. Field scale transport of bromide in an unsaturated soil. 2. Dispersion modeling. Water Resources Research, 25: 1583-1589.

Butters, G.L., Jury, W.A. and Ernst, F.F., 1989. Field scale transport of bromide in an unsaturated soil: 1. Experimental methodology and results. Water Resources Research, 25: 1575-1581.

Chappell, N. and Ternan, L., 1992. Flow path dimensionality and hydrological modelling. Hydrological Processes, 6: 327-345.

Chen, S., Franklin, R.E., Quisenberry, V.L. and Dang, P., 1999. The effect of preferential flow on the short and long-term spatial distribution of surface applied solutes in a structured soil. Geoderma, 90: 229-241.

Costa-Cabral, M.C. and Burges, S.J., 1994. Digital elevation model networks (DEMON): A model of flow over hillslopes for computation of contributing and dispersal areas. Water Resources Research, 30: 1681-1692.

Davis, J.J., 1963. Cesium and its relationship to potassium in ecology. In: V. Schultz and J. Klement, A.W. (Editors), Radioecology. Reinhold, New York, pp. 539-556.

Davis, S.N., Thompson, G.M., Bentley, H.W. and Stiles, G., 1980. Groundwater tracers - a short review. Ground Water, 18: 14-23.

de Jong, E., Begg, C.B.M. and Kachanoski, R.G., 1983. Estimates of soil erosion and deposition for some Saskatchewan soils. Canadian Journal of Soil Science, 63: 607-617.

de Jong, E. and Kachanoski, R.G., 1987. The role of grasslands in hydrology. In: M.C. Healy and R.R. Wallace (Editors), Canadian Aquatic Resources. Department of Fisheries and Oceans, Canadian Government Publishing Centre, Ottawa, pp. 213-241.

de Jong, E. and Kachanoski, R.G., 1988. The importance of erosion in the carbon balance of prairie soils. Canadian Journal of Soil Science, 68: 111-119.

Dyck, M.F., 2001. Long-term solute transport under transient, semi-arid conditions. M.Sc. Thesis, University of Saskatchewan, Saskatoon.

Eghball, B., Binford, G.D. and Baltensperger, D.D., 1996. Phosphorus movement and adsorption in a soil receiving long-term manure and fertilizer application. Journal of Environmental Quality, 25: 1339-1343.

Ellis, J.G., 1938. The Soils of Manitoba. Manitoba Economic Survey Board., Winnipeg, Manitoba, 111 pp.

Ellsworth, T.R. and Jury, W.A., 1991. A three-dimensional field study of solute transport through unsaturated, layered, porous media. 2.Characterization of vertical dispersion. Water Resources Research, 27: 967-981.

Environment Canada, 1992. Canadian Climate Normals 1961-1990, Prairie Provinces., Atmospheric Environment Service, Environment Canada, Ottawa.

Espeby, B., 1990. Tracing the origins of natural waters on a glacial till slope during snowmelt. Journal of Hydrology, 118: 107-127.

Freeze, A., 1980. A stochastic-conceptual analysis of rainfall-runoff processes on a hillslope. Water Resources Research, 16: 391-408.

Fuller, D.O., Wang, D. and Anderson, D.W., 1999. Evidence for solum recarbonation following forest invasion of a grassland soil. Canadian Journal of Soil Science, 79: 443-448.

Gerontidis, D.V.S., Kosmas, C., Detsis, B., Marathianou, M., Zafirious, T. and Tsara, M., 2001. The effect of moldboard plow on tillage erosion along a hillslope. Journal of Soil and Water Conservation, 56: 147-152.

Golden Software Inc., 1999. Surfer 7.0 User's Guide. Golden Software, Inc., Golden, Colorado, 619 pp.

Govers, G., Lobb, D.A. and Quine, T.A., 1999. Tillage erosion and translocation: emergence of a new paradigm in soil erosion research. Soil & Tillage Research, 51: 167-174.

Govers, G., Quine, T.A., Desmet, P.J.J. and Walling, D.E., 1996. The relative contribution of soil tillage and overland flow erosion to soil redistribution on agricultural land. Earth Surface Processes and Landforms, 21: 929-946.

Govers, G., Quine, T.A. and Walling, D.E., 1993. The effect of water erosion and tillage movement on hillslope profile development: a comparison of field observations and model results. In: S. Wicherek (Editor), Farm Land Erosion: In Temperate Plains Environment and Hills. Elsevier Science Publishers B.V., pp. 285-300.

Govers, G., Vandaele, K., Desmet, P., Poesen, J. and Bunte, K., 1994. The role of tillage in soil redistribution on hillslopes. European Journal of Soil Science, 45: 469-478.

Guiresse, M. and Revel, J.C., 1995. Erosion due to cultivation of calcareous clay soils on hillsides in south-west France. II. Effect of ploughing down the steepest slope. Soil & Tillage Research, 35: 157-166.

Hall, G.F. and Olson, C.G., 1991. Predicting variability of soils from landscape models. In: SSSA (Editor), Spatial Variabilities of Soils and Landforms, SSSA Special Publication no. 28. Soil Science Society of America, pp. 9-24.

Hayashi, M., van der Kamp, G. and Rudolph, D.L., 1998. Water and solute transfer between a prairie wetland and adjacent uplands. 1. Water balance. Journal of Hydrology, 207: 42-55.

Hillel, D., 1998. Environmental Soil Physics. Academic Press, Toronto, 771 pp.

Hudson, B.D., 1992. The soil survey as paradigm-based science. Soil Science Society of America Journal, 56: 836-841.

Huggett, R.J., 1975. Soil landscape system: a model of soil genesis. Geoderma, 13: 1-22.

Hutchinson, M.F. and Gessler, P.E., 1994. Splines - more than just a smooth interpolator. Geoderma, 62: 45-67.

Jackson, C.R., 1992. Hillslope infiltration and lateral downslope unsaturated flow. Water Resources Research, 28: 2533-2539.

Janzen, H.H., 1993. Soluble salts. In: M.R. Carter (Editor), Soil sampling and methods of analysis. Lewis Publishers, Boca Raton, pp. 162-166.

Kachanoski, R.G., 1993. Estimating soil loss from changes in soil cesium-137. Canadian Journal of Soil Science, 73: 629-632.

Kachanoski, R.G., Hamlin, C. and van Wesenbeeck, I.J., 1990. Spatial variability of water and solute flux in a layered soil. In: K. Roth, H. Fluhler, W.A. Jury and J.C. Parker (Editors), Field-scale Water and Solute Flux in Soils. Birkhauser Verlag, Boston, pp. 31-40.

King, G.J., Acton, D.F. and St. Arnaud, R.J., 1983. Soil-landscape analysis in relation to soil distribution and mapping at a site within the Weyburn association. Canadian Journal of Soil Science, 63: 657-670.

Kiss, J.J., de Jong, E. and Rostad, H.P.W., 1986. An assessment of soil erosion in West-Central Saskatchewan using cesium-137. Canadian Journal of Soil Science, 66: 591-600.

Knuteson, J.A., Richardson, J.L., Patterson, D.D. and Prunty, L., 1989. Pedogenic carbonates in a Calciaquoll associated with a recharge wetland. Soil Science Society of America Journal, 53: 495-499.

Laslett, G.M., McBratney, A.B., Pahl, P.J. and Hutchinson, M.F., 1987. Comparison of several spatial prediction methods for soil pH. Journal of Soil Science, 38: 325-341.

Lin, H.S., McInnes, K.J., Wilding, L.P. and Hallmark, C.T., 1999. Effects of soil morphology on hydraulic properties: II. Hydraulic pedotransfer functions. Soil Science Society of America Journal, 63: 955-961.

Lindstrom, M.J., Nelson, W.W. and Schumacher, T.E., 1992. Quantifying tillage erosion rates due to moldboard plowing. Soil & Tillage Research, 24: 243-255.

Lindstrom, M.J., Nelson, W.W., Schumacher, T.E. and Lemme, G.D., 1990. Soil movement by tillage as affected by slope. Soil & Tillage Research, 17: 255-264.

Lissey, A., 1968. Surficial mapping of groundwater flow systems with application to the Oak River Basin, Manitoba. Ph.D. Thesis, University of Saskatchewan, Saskatoon.

Lobb, D.A. and Kachanoski, R.G., 1994. Quantification of tillage translocation and tillage erosion. Canadian Journal of Soil Science, 74: 353-.

Lobb, D.A. and Kachanoski, R.G., 1999. Modelling tillage translocation using step, linear-plateau and exponential functions. Soil & Tillage Research, 51: 317-330.

Lobb, D.A., Kachanoski, R.G. and Miller, M.H., 1995. Tillage translocation and tillage erosion on shoulder slope landscape positions measured using ^{137}Cs as a tracer. Canadian Journal of Soil Science, 75: 211-218.

Lobb, D.A., Kachanoski, R.G. and Miller, M.H., 1999. Tillage translocation and tillage erosion in the complex upland landscapes of southwestern Ontario, Canada. Soil & Tillage Research, 51: 189-209.

Lobb, D.A., Quine, T.A., Govers, G. and Hecrath, G., 2001. Comparison of methods used to calculate tillage translocation using plot-tracers. Journal of Soil and Water Conservation, in press.

Martz, L.W. and de Jong, E., 1987. Using cesium-137 to assess the variability of net soil erosion and its association with topography in a Canadian prairie landscape. Catena, 14: 439-451.

McCauley, J.D. and Engel, B.A., 1997. Approximation of noisy bivariate traverse data for precision mapping. Transactions of the American Society of Agricultural Engineers, 40: 237-245.

McCord, J.T. and Stephens, D.B., 1987. Lateral moisture flow beneath a sandy hillslope without an apparent impeding layer. Hydrol. Proc., 1: 225-238.

McCord, J.T., Stephens, D.B. and Wilson, J.L., 1991. Toward validating state-dependent macroscopic anisotropy in unsaturated media: Field experiments and modeling considerations. Journal of Contaminant Hydrology, 7: 145-175.

McKyes, E., 1985. Soil cutting and tillage. Developments in Agricultural Engineering, 7. Elsevier Science Publishing Company Inc., New York, 217 pp.

Mech, S.J. and Free, G.A., 1942. Movement of soil during tillage operations. Agricultural Engineering, 23: 379-382.

Meyboom, P., 1963. Patterns of ground-water flow in the prairie profile., Proceedings of the Hydrology Symposium, No.3 Groundwater. Queen's Printer, Ottawa.

Meyboom, P., 1966. Unsteady groundwater flow near a willow ring in hummocky moraine. Journal of Hydrology, 4: 38-62.

Miller, J.J., 1983. Hydrology of a morainic landscape near St. Denis, Saskatchewan, in relation to the genesis, classification and distribution of soils. M.Sc. Thesis, University of Saskatchewan, Saskatoon, 233 pp.

Miller, J.J., Acton, D.F. and St. Arnaud, R.J., 1985. The effect of groundwater on soil formation in a morainal landscape in Saskatchewan. Canadian Journal of Soil Science, 65: 293-307.

Mills, J.G. and Zwarich, M.A., 1986. Transient groundwater flow surrounding a recharge slough in a till plain. Canadian Journal of Soil Science, 66: 121-134.

Milne, G., 1936. A provisional soil map of East Africa. Eastern African Agricultural Research Station, Tanganyika Territory.

Miyazaki, T., 1993. Water Flow in Soils. Marcel Dekker, Inc., New York, 296 pp.

Moore, I.D., Gessler, P.E., Nielsen, G.A. and Petersen, G.A., 1993. Soil attribute prediction using terrain analysis. Soil Science Society of America Journal, 57: 443-452.

Moore, I.D., O'Loughlin, E.M. and Burch, G.J., 1988. A contour-based topographic model for hydrological and ecological applications. Earth Surface Processes and Landforms, 13: 305-320.

Nicholaichuk, W., 1967. Comparative watershed studies in southern Saskatchewan. Transactions of the American Society of Agricultural Engineers, 10: 502-504.

O'Loughlin, E.M., 1981. Saturation regions in catchments and their relations to soil and topographic properties. Journal of Hydrology, 53: 229-246.

O'Loughlin, E.M., 1986. Prediction of surface saturation zones in natural catchments by topographic analysis. Water Resources Research, 22: 794-804.

Olson, G.L. and Cassel, D.K., 1999. Bromide leaching on a piedmont toposequence. Soil Science Society of America Journal, 63: 1319-1326.

Padbury, G.A. and Acton, D.F., 1994. Ecoregions of Saskatchewan. Centre for Land and Biological Resources Research, Research Branch, Agriculture and Agri-Food Canada, Ottawa.

Park, S.J. and Burt, T.P., 1999. Identification of throughflow using the distribution of secondary iron oxides in soils. Geoderma, 93: 61-84.

Pennock, D.J., Anderson, D.W. and de Jong, E., 1994a. Distribution of cesium-137 in uncultivated Black Chernozemic landscapes. Canadian Journal of Soil Science, 74: 115-117.

Pennock, D.J., Anderson, D.W. and de Jong, E., 1994b. Landscape-scale changes in indicators of soil quality due to cultivation in Saskatchewan, Canada. Geoderma, 64: 1-19.

Pennock, D.J. and de Jong, E., 1987. The influence of slope curvature on soil erosion and deposition in hummock terrain. Soil Science, 144: 209-217.

Pennock, D.J. and de Jong, E., 1990a. Regional and catenary variations in properties of Borolls of Southern Saskatchewan, Canada. Soil Science Society of America Journal, 54: 1697-1701.

Pennock, D.J. and de Jong, E., 1990b. Spatial pattern of soil redistribution in Boroll landscapes, Southern Saskatchewan, Canada. Soil Science, 150: 867-873.

Pennock, D.J., Zebarth, B.J. and de Jong, E., 1987. Landform classification and soil distribution in hummocky terrain, Saskatchewan, Canada. Geoderma, 40: 297-315.

Phillip, J.R., 1980. Field heterogeneity: Some basic issues. Water Resources Research, 16: 443-448.

Poesen, J., van Wesemael, B., Govers, G., Martinez-Fernandez, J., Desmet, P., Vandaele, K., Quine, T.A. and Degraer, G., 1997. Patterns of rock fragment cover generated by tillage erosion. Geomorphology, 18: 183-197.

Pomeroy, J.W. and Gray, D.M., 1995. Snowcover: Accumulation, Relocation and Management., NHRI Report No. 7. National Hydrology Research Institute, Saskatoon, 144 pp.

Quine, T.A., 1999. Use of caesium-137 data for validation of spatially distributed erosion models: the implications of tillage erosion. Catena, 37: 415-430.

Quine, T.A., Desmet, P.J.J., Govers, G., Vandaele, K. and Walling, D.E., 1994. A comparison of the roles of tillage and water erosion in landform development and sediment export on agricultural land near Leuven, Belgium. In: L.J. Olive, R.J. Loughran and J.A. Kesby (Editors), Variability in stream erosion and sediment transport. International Association of Hydrological Sciences, Publication No. 224, Canberra, Australia, pp. 77-86.

Quine, T.A., Govers, G., Poesen, J., Walling, D.E., van Wesemael, B. and Martinez-Fernandez, J., 1999. Fine earth translocation by tillage in stony soils in the Guadalentin, south-east Spain: an investigation using caesium-134. Soil & Tillage Research, 51: 279-301.

Quisenberry, V.L., Smith, B.R., Phillips, R.E., Scott, H.D. and Nortcliff, S., 1993. A soil classification system for describing water and chemical transport. Soil Science, 156: 306-315.

Reuter, R.J., McDaniel, P.A., Hammel, J.E. and Falen, A.L., 1998. Solute transport in seasonal perched water tables in loess-derived soilscapes. Soil Science Society of America Journal, 63: 977-983.

Richardson, J.L., Arndt, J.L. and Montgomery, J.A., 2001. Hydrology of wetland and related soils. In: J.L. Richardson and M.J. Vepraskas (Editors), Wetland Soils: Genesis, Hydrology, Landscapes, and Classification. Lewis Publishers, Boca Raton, FL., pp. 35-84.

Richardson, J.L., Wilding, L.P. and Daniels, R.B., 1992. Recharge and discharge of groundwater in aquic conditions illustrated with flownet analysis. Geoderma, 53: 65-78.

Ritchie, J.C. and McHenry, J.R., 1973. Vertical distribution of fallout cesium-137 in cultivated soils. Radiation Data and Reports, 14: 727-728.

Ritchie, J.C. and McHenry, J.R., 1990. Application of radioactive fallout cesium-137 for measuring soil erosion and sediment accumulation rates and patterns: a review. Journal of Environmental Quality, 19: 215-233.

Ritchie, J.C., Sprayberry, J.A. and McHenry, J.R., 1974. Estimating soil erosion from the redistribution of fallout ^{137}Cs. Soil Science Society of America Proceedings, 38: 137-139.

Rogowski, A.S. and Tamura, T., 1965. Movement of ^{137}Cs by runoff, erosion and infiltration on the alluvial Captina silt loam. Health Physics, 11: 1333-1340.

Rogowski, A.S. and Tamura, T., 1970. Erosional behaviour of cesium-137. Health Physics, 18: 467-477.

Roth, K., Jury, W.A., Fluhler, H. and Attinger, W., 1991. Transport of chloride through an unsaturated field soil. Water Resources Research, 27: 2533-2541.

St. Arnaud, R.J., 1976. Pedological aspects of glacial till. In: R.F. Legget (Editor), Glacial Till: An inter-disciplinary study. The Royal Society of Canada, Ottawa, pp. 133-155.

Schulin, R., van Genuchten, M.T., Fluhler, H. and Ferlin, P., 1987. An experimental study of solute transport in a stony field soil. Water Resources Research, 23: 1785-1794.

Seyfried, M.S. and Wilcox, B.P., 1995. Scale and the nature of spatial variability: Field examples having implications for hydrologic modeling. Water Resources Research, 31: 173-184.

Sharifat, K., 1999. Soil translocation with tillage tools. Ph.D. Thesis, University of Saskatchewan, Saskatoon, Saskatchewan, 133 pp.

Sharifat, K. and Kushwaha, R.L., 1997. Soil translocation by two tillage tools. Canadian Agricultural Engineering, 39: 77-84.

Sikora, F.J. and Stevenson, F.J., 1987. Interference of humic substances on chloride analysis using the chloride ion-selective electrode. Soil Science Society of America Journal, 51: 924-926.

Slobodian, N., 2001. The landscape-scale distribution of below ground plant biomass in a fescue prairie and a wheat field. M.Sc. Thesis, University of Saskatchewan, Saskatoon, 120 pp.

Soil Classification Working Group, 1998. The Canadian System of Soil Classification, Publ. 1646 (Revised 3rd edition). Agriculture and Agri-Food Canada, 187 pp.

Speight, J.G., 1974. A parametric approach to landform regions. Special Publication Institute of British Geographers, 7: 213-230.

Steinwand, A.L. and Richardson, J.L., 1989. Gypsum occurrence in soils on the margin of semipermanent prairie pothole wetlands. Soil Science Society of America Journal, 53: 838-842.

Stewart, J., 1987. Single Variable Calculus. Brooks/Cole Co., California, 640 pp.

Stewart, J., 1995. Multivariable Calculus. Brooks/Cole Publishing Co., Toronto, 1015 pp.

Toth, J., 1963. A theoretical analysis of groundwater flow in small drainage basins. Journal of Geophysical Research, 68: 4795-4812.

Utset, A., Lopez, T. and Diaz, M., 2000. A comparison of soil maps, kriging and a combined method for spatially predicting bulk density and field capacity of ferralsols in the Havanna-Matanzas Plain. Geoderma, 96: 199-213.

Van de Pol, R.M., Wierenga, P.J. and Nielsen, D.R., 1977. Solute movement in a field soil. Soil Science Society of America Journal, 41: 10-13.

van Muysen, W., Govers, G., van Oost, K. and van Rompaey, A., 2000. The effect of tillage depth, tillage speed, and soil condition on chisel tillage erosivity. Journal of Soil and Water Conservation, 55: 355-364.

van Oost, K., Govers, G., van Muysen, W. and Quine, T.A., 2000. Modeling translocation and dispersion of soil constituents by tillage on sloping land. Soil Science Society of America Journal, 64: 1733-1739.

van Wesenbeeck, I.J. and Kachanoski, R.G., 1991. Spatial scale dependence of in situ solute transport. Soil Science Society of America Journal, 55: 3-7.

van Wesenbeeck, I.J. and Kachanoski, R.G., 1994. Effect of variable horizon thickness on solute transport. Soil Science Society of America Journal, 58: 1307-1316.

Walling, D.E. and He, Q., 1999. Improved models for estimating soil erosion rates from cesium-137 measurements. Journal of Environmental Quality, 28: 611-622.

Western, A.W., Grayson, R.B., Bloschl, G., Willgoose, G.R. and McMahon, T.A., 1999. Observed spatial organization of soil moisture and its relation to terrain indices. Water Resources Research, 35: 797-810.

Winter, T.C., 1992. A physiographic and climatic framework for hydrologic studies of wetlands. In: R.D. Roberts and M.L. Bothwell (Editors), Aquatic Ecosystems in Semi-arid Regions: Implications for Resource Management. Environment Canada, Saskatoon, pp. 127-148.

Young, A., 1972. Slopes. Oliver and Boyd, Edinburgh, 288 pp.

Zaslavsky, D. and Rogowski, A., 1969. Hydrologic and morphologic implications of anisotropy and infiltration in soil profile development. Soil Science Society of America Proceedings, 33: 594-599.

Zaslavsky, D. and Sinai, G., 1981. Surface hydrology: III - Causes of lateral flow. Journal of the Hydraulics Division, Proceedings of the American Society of Civil Engineers, 107: 37-52.

Zebarth, B.J., 1988. Saturated and unsaturated flow in a hummocky landscape in relation to topography and soil morphology. Ph.D. Thesis, University of Saskatchewan, Saskatoon, 256 pp.

Zebarth, B.J. and de Jong, E., 1989a. Water flow in a hummocky landscape in central Saskatchewan, Canada, I. Distribution of water and soils. Journal of Hydrology, 107: 309-327.

Zebarth, B.J. and de Jong, E., 1989b. Water flow in a hummocky landscape in central Saskatchewan, Canada, III. Unsaturated flow in relation to topography and land use. Journal of Hydrology, 110: 199-218.

7. APPENDICES

Appendix A

The sum of chloride found in all cores at each depth for each location.Fall 1997.

			sum of chloride (mg cm^{-2})				
			---------- sampling increments (cm) ----------				
landform element	location	soil profile	0-10	10-20	20-35	35-50	0-50
DSH	6	O.DBC	23.60	57.00	80.55	0.75	161.83
	26	O.R	47.70	69.20	17.70	0.00	134.72
	43	O.R	55.90	60.40	30.60	0.60	147.59
	52	CA.DBC	70.80	35.70	3.30	0.00	109.80
DBS	8	CA.DBC	60.50	41.10	7.20	0.15	108.99
	14	O.DBC	61.20	81.50	21.45	0.00	164.13
	15	O.DBC	42.90	61.00	51.30	7.95	163.07
	38	O.R	20.90	51.20	60.30	2.55	135.02
	40	CA.DBC	28.50	44.50	20.10	0.30	93.52
	50	CA.DBC	60.20	58.20	24.15	0.00	142.61
CBS	2	O.DBC	39.80	65.40	42.75	9.75	157.84
	12	O.DBC	37.60	48.10	20.85	0.30	106.92
	22	CA.DBC	59.40	69.80	19.65	0.00	148.93
	24	O.DBC	39.60	43.00	17.10	0.00	99.73
	28	O.DBC	38.00	65.20	20.55	12.75	136.60
	30	O.DBC	53.60	56.40	15.75	0.00	125.76
	32	O.DBC	39.60	55.00	18.75	5.70	119.05
DFS	19	R.DBC	48.80	52.00	10.95	0.00	111.83
	35	R.HG	49.80	36.10	10.20	0.15	96.26
	46	GLR.DBC	83.40	64.40	29.55	3.15	181.06
CFS	11	GL.DBC	101.70	37.20	7.65	1.50	147.88
	17	O.DBC	65.60	79.40	21.00	0.00	166.11
	20	HU.LG	111.60	26.70	7.50	1.65	147.50
	34	R.HG	65.30	41.20	27.75	28.50	162.58
	44	O.HG	49.70	29.10	9.90	1.65	90.28
	49	O.DBC	62.00	65.30	11.85	2.85	141.93
LEV	4	CA.DBC	14.70	39.80	40.20	28.50	122.40
	13	CA.DBC	55.20	62.20	13.20	0.00	112.54
	37	O.DBC	49.00	47.50	22.05	3.75	122.43

Appendix B

The sum of the chloride measured in all cores at each sampling depth, Spring 1998.

			chloride sum (mg cm^{-2})				
			sampling increments (cm)				
landform element	location	soil subgroup	0-10	10-20	20-35	35-50	0-50
DSH	26	O.R	41.87	49.88	31.20	14.78	126.36
	43	CA.DBC	119.87	24.20	10.63	2.59	155.18
DBS	14	O.R	85.18	26.63	13.65	1.13	126.17
	50	O.R	88.34	32.94	5.16	0.00	126.44
CBS	2	O.DBC	28.31	34.17	42.31	1.35	109.30
	12	O.DBC	39.12	22.84	2.10	0.71	64.06
	22	O.DBC	33.68	22.67	31.76	0.40	91.21
	24	O.DBC	43.39	34.41	27.48	3.41	105.68
	30	O.DBC	11.31	25.12	53.79	0.72	105.01
DFS	46	CA.DBC	4.83	7.26	5.99	0.00	20.67
CFS	11	HU.LG	4.53	15.20	8.22	0.00	28.36
	17	CA.DBC	12.84	14.28	0.44	3.10	28.69
	49	O.DBC	75.13	32.10	12.84	0.00	120.07
LEV	4	CA.DBC	56.27	30.85	27.68	0.40	116.14
	37	O.DBC	38.94	55.42	16.28	0.48	111.36

Appendix C

The sum of chloride recovered from all cores in each sampling depth for each location, Fall 1998.

			chloride sum (mg cm^{-2})				
			---------- sampling increments (cm) ----------				
landform element	location	soil subgroup	0-10	10-20	20-35	35-50	0-50
DSH	6	R.DBC	7.80	54.10	55.39	3.03	120.40
	26	O.R	2.00	31.10	33.94	2.06	69.14
	43	R.DBC	11.00	59.80	10.90	0.00	81.70
	52	O.R	12.50	43.00	33.02	14.21	102.80
DBS	8	CA.DBC	8.40	58.50	21.70	0.58	89.26
	14	O.R	2.80	41.70	32.16	0.00	76.62
	15	O.R	4.00	23.40	29.64	3.26	60.34
	38	O.DBC	2.60	16.30	38.47	25.09	82.47
	40	O.R	9.60	45.60	21.65	0.23	76.47
	50	O.R	1.80	30.50	34.61	2.12	67.55
CBS	2	O.DBC	1.60	14.60	31.03	32.89	80.07
	12	CA.DBC	1.20	22.20	13.50	0.00	36.83
	22	O.DBC	1.80	12.50	26.95	26.09	67.24
	24	O.DBC	3.10	21.40	37.63	26.50	88.62
	28	O.DBC	2.20	15.00	31.73	14.38	63.28
	30	O.DBC	9.60	22.30	27.14	27.42	97.92
	32	E.DBC	2.70	15.60	18.22	0.65	37.11
DFS	19	O.R	15.30	28.10	12.73	0.53	56.59
	35	O.HG	13.40	32.10	25.01	0.16	70.31
	46	CA.DBC	4.90	5.30	8.94	1.30	20.45
CFS	11	HU.LG	7.10	14.40	14.49	0.67	36.72
	17	O.DBC	10.20	7.90	1.47	0.00	19.61
	20	O.HG	5.00	6.85	4.28	2.10	37.28
	34	O.HG	19.50	21.00	3.17	0.29	39.52
	44	HU.LG	1.80	5.40	4.99	0.82	13.01
	49	CA.DBC	1.50	12.10	29.81	12.94	56.35
LEV	4	CA.DBC	0.30	11.90	42.51	9.22	63.92
	13	O.DBC	1.50	5.10	11.79	6.75	26.24
	37	E.DBC	5.60	20.90	24.60	9.78	60.96

Appendix D

The coordinate values for the chloride center of mass in the 0- to 0.50-m increment, and the displacement distance from the axis origin to the center of mass, Fall 1998.

			center of mass coordinates			displacement distances (cm)	
landform element	location	soil subgroup	x	y	z	xy	xyz
DSH	6	R.DBC	12.9	3.4	-20.8	13.4	24.7
	26	O.R	-6.3	0.6	-21.7	6.4	22.6
	43	R.DBC	-0.4	-6.2	-15.3	6.2	16.5
	52	O.R	-1.3	-0.8	-21.6	1.5	21.7
DBS	8	CA.DBC	-3.5	-9.5	-17.3	10.1	20.0
	14	O.R	5.8	-14.6	-19.9	15.7	25.3
	15	O.R	10.6	-3.5	-22.0	11.1	24.6
	38	O.DBC	-10.1	2.8	-28.9	10.5	30.7
	40	O.R	11.6	-5.7	-17.4	12.9	21.7
	50	O.R	7.5	1.7	-22.0	7.7	23.3
CBS	2	O.DBC	-6.1	-11.5	-30.9	13.0	33.6
	12	CA.DBC	7.5	-50.7	-19.3	51.2	54.7
	22	O.DBC	-4.0	-4.5	-30.4	6.0	31.0
	24	O.DBC	-6.4	-1.5	-28.2	6.5	28.9
	28	O.DBC	3.8	-9.4	-27.2	10.2	29.0
	30	O.DBC	9.7	-11.4	-30.1	14.9	33.6
	32	E.DBC	5.3	-31.1	-20.9	31.6	37.9
DFS	19	O.R	-16.3	11.5	-15.4	20.0	25.2
	35	O.HG	-23.0	2.9	-17.5	23.1	29.0
	46	CA.DBC	51.3	-50.7	-19.8	72.1	74.8
CFS	11	HU.LG	-9.1	-48.2	-18.5	49.1	52.5
	17	O.DBC	11.5	-36.5	-10.7	38.3	39.7
	20	O.HG	16.5	-28.4	-18.0	32.8	37.4
	34	O.HG	4.3	-1.4	-11.9	4.5	12.8
	44	HU.LG	-6.4	8.1	-20.1	10.3	22.6
	49	CA.DBC	4.8	-0.5	-27.7	4.8	28.1
LEV	4	CA.DBC	41.4	-13.6	-27.2	43.6	51.4
	13	O.DBC	12.9	-54.6	-29.0	56.1	63.1
	37	E.DBC	8.4	1.0	-23.5	8.4	25.0

*Note: Displacement distances are calculated as $(x^2+y^2)^{1/2}$ and $(x^2+y^2+z^2)^{1/2}$ respectively.

Appendix E

Lateral and total displacement of the chloride center of mass, Fall 1998. Displacement distances are in centimeters. The initial position of the center of mass in all cases is considered to be at the soil surface and in the center of the 1-m^2 micro-plot.

			total displacement (cm) xyz				lateral displacement (cm) xy			
			----sampling increment (cm)----				-------sampling increment (cm)--			
landform element	location	soil subgroup	0-10	10-20	20-35	35-50	0-10	10-20	20-35	35-50
DSH	6	R.DBC	24.3	25.6	29.3	53.3	23.8	20.7	10.0	32.1
	26	O.R	27.7	19.4	27.9	49.7	27.2	12.3	4.6	25.7
	43	R.DBC	28.3	15.5	29.9	.	27.9	4.1	11.7	.
	52	O.R	8.6	17.0	29.3	52.0	7.1	7.9	10.2	29.9
DBS	8	CA.DBC	7.4	19.6	30.5	55.3	5.4	12.6	13.2	35.4
	14	O.R	34.7	24.4	29.2	.	34.4	19.3	9.9	.
	15	O.R	19.8	22.7	30.6	49.6	19.2	17.1	13.3	25.5
	38	O.DBC	30.1	21.4	29.5	42.9	29.7	15.3	10.7	5.6
	40	O.R	6.1	20.0	32.3	107.7	3.5	13.2	16.9	99.0
	50	O.R	26.2	15.7	31.3	54.7	25.8	4.8	15.0	34.5
CBS	2	O.DBC	9.3	16.6	30.1	46.1	7.8	7.1	12.1	17.8
	12	CA.DBC	62.1	48.8	70.8	.	61.9	46.5	65.2	.
	22	O.DBC	28.1	32.4	28.7	42.7	27.7	28.7	8.1	4.5
	24	O.DBC	11.7	15.8	29.8	43.2	10.6	5.1	11.6	7.7
	28	O.DBC	47.7	24.4	29.0	43.3	47.4	19.3	9.2	8.5
	30	O.DBC	19.6	22.0	33.4	43.5	18.9	16.1	19.0	9.4
	32	E.DBC	7.5	38.1	42.3	59.6	5.6	35.0	32.2	41.8
DFS	19	O.R	19.1	24.2	36.6	81.9	18.5	19.0	24.1	70.0
	35	O.HG	32.7	23.5	39.8	101.5	32.3	18.1	28.8	92.2
	46	CA.DBC	47.3	56.4	103.0	102.1	47.0	54.4	99.2	92.8
CFS	11	HU.LG	50.5	42.8	63.0	82.5	50.2	40.1	56.7	70.7
	17	O.DBC	28.9	49.2	70.6	.	28.4	46.9	65.1	.
	20	O.HG	9.5	44.0	58.8	67.1	8.0	41.3	51.9	51.9
	34	O.HG	8.4	16.8	34.3	50.3	6.7	7.5	20.6	26.9
	44	HU.LG	9.0	20.4	35.0	43.8	7.4	13.9	21.6	10.6
	49	CA.DBC	73.5	16.5	28.1	43.2	73.3	6.9	5.7	8.0
LEV	4	CA.DBC	99.1	32.8	52.5	70.8	99.0	29.2	44.8	56.7
	13	O.DBC	24.2	44.6	65.4	80.7	23.7	42.0	59.4	68.7
	37	E.DBC	16.2	23.8	27.6	43.4	15.4	18.5	2.8	8.8

Note: Missing values indicate that no chloride was recovered at this depth.